COMPARATIVE STUDY OF AMMONIA-BASED CLEAN RAIL TRANSPORTATION SYSTEMS FOR GREATER TORONTO AREA

by

Janette Hogerwaard

A Thesis Submitted in Partial Fulfillment
of the Requirements for the Degree of

Master of Applied Science in Mechanical Engineering

Faculty of Engineering and Applied Science
University of Ontario Institute of Technology
April 2014

Abstract

Ammonia as a transportation fuel offers a carbon-free, hydrogen rich energy source that emits no greenhouse gases in combustion, and has no global warming potential. Furthermore, it may be produced from any renewable energy resource, and is a strong option for long term sustainability. Ammonia also provides a pathway towards a hydrogen economy, which is the long term goal for environmental sustainability.

This thesis investigates the feasibility of integrating ammonia as a combustion fuel, hydrogen carrier, heat recovery and working fluid, and for indirect engine cooling, within locomotive propulsion systems for nine novel ammonia-based configurations. Thermodynamic, environmental, and economic analyses are conducted for a typical modern diesel-fueled locomotive and the proposed ammonia configurations. The study comparatively assesses potential long term solutions for sustainable, clean rail transportation.

From the modeled results, the proposed systems operating with 50% of required fuel energy replaced by ammonia have a reduction in diesel fuel consumption from 0.211 kg/s to less than 0.10 kg/s. This is associated with a reduction in GHG emissions of more than 8 tonnes CO_{2eq} for a typical daily locomotive duty cycle for commuter operation. Criteria air contaminants are reduced to below upcoming Tier 3 emission levels for NO_x and HC emissions, and meet current levels for PM emissions. In total, ten locomotive propulsion systems are investigated including the diesel-fueled locomotive baseline, and the performance gains are considered against economic factors for fuel and equipment costs in a comparative assessment.

Keywords: Ammonia, locomotive, environmental impact, sustainability.

Acknowledgements

First and foremost, I would like to express my deepest gratitude to my supervisor, Dr. Ibrahim Dincer. The years spent as his student have been some of the most challenging and rewarding times in my life so far, and I couldn't ask for a better mentor. I look forward to continuing to learn from him as my academic journey continues.

I also sincerely thank Dr. Calin Zamfirescu, for always being so generous with his wealth of knowledge. It has been my pleasure to work with him, and I am a better student for it.

I am truly grateful to my dear friend Canan Acar, for her endless humour, advice, and company on this journey. As well, I would like to thank Sadi Hamut, Rami El-Emam, Jason Huang, Eric Kool, and Robert Maillet for their support and friendship for these years spent together as students, and friends.

I also thank my friends Nadia Pizzimenti, Meagan Montpetit, Eva Filomena, and Natalie Pistillo, who are like my family. I especially thank Scott Appleton for always supporting me, and the Appleton family for all of their kind encouragement and interest in my work.

Of course, I thank my family—my mother, Tessa Hogerwaard, for being such a strong role model, and my sister Erika, for always being beside me. I am always happy to live our parallel lives.

Finally, I would like to dedicate this work to my father, Ernst Hogerwaard, who I wish was here to share this with me. So much of this is because of him, and I hope this would make him proud.

Table of Contents

List of Figures

List of Table Captions

Nomenclature

a	Molar air-fuel ratio
AF	Mass-based air-fuel ratio
C_o	Reference cost, $
D_p	Depletion factor
$\dot{E}$	Energy rate, kW
EF	Emission factor
ex	Specific exergy, kJ/kg
$\dot{E}x$	Exergy rate, kW
$ExDR$	Exergy destruction
f_c	Conversion factor
GF	Greenization factor
h	Specific enthalpy, kJ/kg
$\dot{H}$	Enthalpy rate, kW
M	Molar mass, kg/kmol
$\dot{m}$	Mass flow rate, kg/s
P	Pressure, kPa
pr	Pressure ratio
Q	Heat rate, kW
s	Specific entropy, kJ/kg·K
SI	Sustainability Index
T	Temperature, °C or K
v	Specific volume, m^3/kg
V	Volume, m^3 or L
$\dot{V}$	Volume flow rate, m^3/s
$\dot{W}$	Work rate, kW
x	Vapour quality
x_d	Dissociation fraction

Greek Letters

Δ	Difference
η	Energy efficiency
ρ	Density, kg/m^3
φ	Equivalence ratio
ψ	Exergy efficiency

Subscripts

1,2,…,*i*	State points
a	Air
ac	After-cooler
b	Brake
c	Cooling
C	Compressor
cc	Combustion chamber
d	Destruction
e	Exit
ec	Engine cooling
el	Electric
eq	Equivalent
eqp	Equipment
exh	Exhaust
i	Inlet
P	Pump
PC	Purchase cost
rec	Recovery
s	Isentropic
sh	Shaft
SM	Starter motor
st	Stoichiometric

T	Turbine
TM	Traction motor
TP	Traction power
u	Utilization
wjc	Water jacket cooling

Superscripts

ch	Chemical
ph	Physical

Acronyms

BATT	Battery
BHP	Brake horsepower
BSFE*i*	Brake specific fuel emissions of species i
$C_{12}H_{23}$	Diesel fuel
CAC	Criteria air contaminant
CH_4	Methane
CI	Compression ignition
CN	Canadian National
CNG	Compressed natural gas
CO	Carbon monoxide
CO_2	Carbon dioxide
COP	Coefficient of performance
DSU	Decomposition and separation unit
EMD	Electro-motive Diesel
EPA	Environmental Protection Agency
EXP	Expansion valve
FFE	Feed-plus-fuel energy
GOV	Engine governor
GEN	Generator

GHG	Greenhouse gas
GTA	Greater Toronto Area
GWP	Global warming potential
H_2	Hydrogen
HC	Hydrocarbon
HCCI	Homogeneous charge compression ignition
HEP	Head end power
HHV	Higher heating value
HPDI	High pressure direct injection
HRR	Heat recovery rate
HX-ac	After–cooler
HX	Heat exchanger
ICE	Internal combustion engine
IPCC	Intergovernmental Panel on Climate Change
LEM	Locomotive Emissions Monitoring
LHV	Lower heating value
LNG	Liquefied natural gas
LPG	Liquefied petroleum gas
LPI	Low pressure injection
MOU	Memorandum of Understanding
MSDS	Material Safety Data Sheet
NG	Natural gas
N_2	Nitrogen
N_2O	Nitrous oxide
NH_3	Ammonia
NO_x	Nitrous oxide
O_2	Oxygen
ORC	Organic Rankine cycle
PAX	Passenger
PM	Particulate matter
RAC	Railway Association of Canada

RES	Reservoir/storage tank
RTK	Revenue Tonne-kilometre
RC	Rankine cycle
S	Sulfur
SCR	Selective catalytic reducer
SM	Starter motor
SO_x	Sulfur oxide(s)
TC	Turbocharger
THP	Traction horsepower
TM	Traction motor
ULSD	Ultra low sulfur diesel
US	United States
WHO	World Health Organization

CHAPTER 1: INTRODUCTION

The environmental impacts of fossil fuel consumption are a global concern; in particular, greenhouse gas (GHG) and harmful criteria air contaminant (CAC) emissions associated with fossil fuel combustion. Continuing in the objectives of the Kyoto Protocol to reduce climate change, Canada has committed to a 17% GHG reduction from 2005 levels by 2020, a target limit of 612 Mt CO_{2eq}, under the Copenhagen Accord [1]. Current measures to reduce emissions have resulted in a 5% reduction from 2005 levels, totaling 699 Mt $CO_{2,eq}$ in 2012 [2]; however, projected emission trends presented in [2] indicate 2020 totals of 714 Mt $CO_{2,eq,}$ suggesting that investigations of more aggressive measures is necessary in order to meet the Canadian Copenhagen target.

The Transportation Sector is the largest contributor to GHG emissions by economic sector in Canada, representing ~25% of the national total in 2012 [2]. This is due to combustion of fossil fuels in vehicles; primarily heavy duty freight trucks, light duty trucks, and light vehicles (passenger cars). Improved fuel efficiency, fuel production/refining methods, and combustion technologies have reduced total fossil fuel consumption and emissions from vehicles; however, the issue of the sheer volume of light duty vehicles on the roads limits the improvement potential of technology and combustion efficiencies alone. In order to significantly reduce the impact of the Transportation Sector, two primary issues must be addressed in parallel with current fuel consumption and emission reduction measures:

- implementation of sustainable, more environmentally benign energy alternatives to traditional high carbon content fuels,
- on-road traffic density, particularly passenger cars in population-dense urban regions,

Alternative fuels and energy resources play a key role in both the short and long-term sustainable development of transportation. As a carbon-free chemical energy carrier, hydrogen (H_2) is widely recognized as the ideal synthetic fuel for sustainable

development [3,4,5]; however, significant challenges with respect to production methods, transport infrastructure, onboard storage, and safety standards require further development before it can be considered practical as a transportation fuel. Natural gas (NG) is currently in use as a transportation fuel, applying compressed and liquid natural gas (CNG, LNG) technologies. The higher H/C ratio of NG (considered as methane, or CH_4) reduces GHG and certain CAC emissions compared to diesel fuel, and is suitable for fuel cell and hydrogen synthesis applications (i.e. steam–CH_4 reforming). While the NG option makes significant strides in reducing environmental impact—and continues to improve with NG technology development—it is primarily obtained from fossil fuel reserves, making this ultimately a short-term solution with respect to environmental sustainability as a transportation fuel. Biomass derived hydrocarbons (i.e. CH_4, biodiesel) offer a more sustainable fuel source, with promising results in demonstration projects.

Ammonia (NH_3) is the only carbon-free chemical energy carrier (other than hydrogen) suitable for use as a transportation fuel [6]. Furthermore, NH_3 has a high octane rating (110–130), can be thermally cracked to produce H_2 fuel using only ~12% of the higher heating value [7], presents no explosion danger when properly transported and stored, has a well-established production and distribution infrastructure, and has zero global warming potential (GWP). In addition to its attractive qualities as a fuel, NH_3 is widely used as a NO_x reducing agent for combustion exhaust gases using selective catalytic reduction (SCR), and its capacity as a refrigerant can be applied to recover and further utilize engine heat that would otherwise be lost. In terms of environmental sustainability, NH_3 can be produced using either fossil fuels, or any renewable energy source, using heat and/or electricity [3], which allows for evolution of NH_3 production methods and technologies in parallel with sustainable development.

With respect to high density of on-road traffic, one long term solution is to strongly promote the use of public transit to reduce passenger vehicle traffic density; developing mass transit infrastructures that provide a convenient alternative to personal vehicles to a wider range of locations and passengers. There is a caveat to this—fossil fuels are the

primary resource for transportation fuels, which limits the long term sustainability of this solution.

1.1 Potential Solutions for Sustainable Rail Transportation

With established infrastructures in place for passenger and freight operations, rail transportation is well positioned to reduce environmental impacts throughout the Transportation Sector. Infrastructure improvements and expansion of passenger rail transit networks can help to increase the number of rail commuters. The benefits of such improvements include reduction of urban transportation congestion due to passenger car traffic—with an associated reduction in fuel combustion emissions—and the use of rail for freight transport over long distances can lower the number of on-road freight trucks.

Beginning in 1995, in response to national and international environmental initiatives to reduce GHG's and CAC's, the Railway Association of Canada (RAC), its member organizations, and Environment and Transport Canada, developed a voluntary agreement outlined in a Memorandum of Understanding (MOU) to manage environmental effects associated with diesel fuel combustion. Under the terms of the MOU agreement, member organizations provide detailed emission and operation information to the RAC, who then compiles and publishes this information annually as part of the Locomotive Emissions Monitoring (LEM) program. These data are used to assess the overall performance of rail operations and to determine future emission reduction targets. To meet these targets, strict limitations are imposed on diesel fuel standards, particularly with respect to sulfur content—limited to 15 ppm as of 2012—and locomotive technologies are being updated or replaced with more efficient models and or retrofits. In addition to technology improvements and diesel emission reduction initiatives, rail and locomotive industries are continuously investigating and implementing alternative fuels and fueling technologies to reduce harmful emissions, with multiple projects throughout North America and internationally since the mid–1980's [8], including natural gas, biodiesel, and various diesel hybrid technologies.

Ammonia has significant potential as an alternative fuel to further the sustainable development of rail transportation. Rail is already a part of the NH_3 transport infrastructure, therefore onboard storage and transport requirements are already well understood. As well, locomotive upgrades and retrofits to meet upcoming CAC reduction targets include SCR technology, which can be used with either urea or NH_3, further supporting the integration of NH_3 by offering immediate multi-use options for both fuel and emission-control.

1.2 Motivation and Objectives

This thesis investigates the feasibility of ammonia-based dual-fueling for modern two-stroke diesel locomotives, integrating NH_3 with major propulsion systems as a combustion fuel, H_2 carrier, NO_x emission reducer, and heat transfer fluid. Alternative system configurations are proposed for a locomotive prime mover, applying the novel ammonia-powered technology and methods outlined by Dincer and Zamfirescu in [7], with the aim of effectively and efficiently applying NH_3 to improve fuel energy utilization and reduce the environmental impact of rail transportation.

The following points outline the specific objectives of the thesis:

- To develop conceptual designs of an ammonia-fueled locomotive for reducing environmental impact and emissions
- To investigate the integration of on-board hydrogen fuel production by thermal decomposition of ammonia using recovered heat from the exhaust of the locomotive prime mover to improve performance and further reduce diesel fuel demand
- To explore conceptual designs for further utilization of ammonia, such as:
    - Working fluid for additional power generation by converting recovered waste heat to mechanical power,
    - Provide cooling effect for the locomotive systems, to reduce the power demand of current air-cooled radiator systems,
    - Heat transfer fluid for locomotive cab heating/cooling systems

- To assess the energy, exergy, environmental, and economic sustainability and feasibility of the conceptual systems using life cycle considerations.

System configurations integrating various auxiliary ammonia subsystems are analyzed and compared against a modern Tier 2 diesel locomotive at rated operation, and a best approach is selected based on locomotive performance and impact assessment results.

CHAPTER 2: BACKGROUND

2.1 Rail Transportation in Canada

The relationship between levels of GHG emissions and transportation emissions is well-established in the Canadian example, with contributions from the Transportation Sector representing the largest portion of GHG emissions by economic sector in Canada, at ~25% of the national total in 2012 [2]. With road vehicles such as, heavy duty freight trucks, light duty trucks, and light (passenger) vehicles, contributing the majority of GHG emissions within the transportation sector—primarily due to the combustion of fossil fuels—practical solutions for the integration of more environmentally benign options for passenger transit are an important and necessary area for exploration. However, solutions which aim to address the GHG-producing technology utilized in the operation of passenger vehicles, but which do not address the prevailing social, cultural and economic factors that contribute to the dominance of fossil fuels as the primary choice for personal transportation, do little to reduce the environmental impact of the high density on-road traffic that characterizes many of Canada's urban centres.

Rail transit presents a practical, efficient and realistic alternative to passenger vehicles, and is, in many cases, an existing, operational system utilized in urban and suburban centres across Canada. In the best case scenario, commuter trains provide a comfortable, predictable and affordable alternative to cars or other light vehicles, and on a broader scale, move large numbers of passengers quickly and efficiently with a considerably smaller environmental impact, at just at ~1% of total GHG emissions in 2012. Furthermore, as an attractive option for business and personal travel alike, commuter trains have the potential to reduce the number of passenger vehicles utilized for transportation, the related wear and tear on roads and other infrastructure required for car travel, and traffic congestion and density, particularly in densely populated urban centres—as is the case with the rail-based commuter transit system in the GTA, the case study which is discussed in this research.

2.1.1 Commuter Rail Transit in the GTA

As one of the most highly populated cities in North America, Toronto and the surrounding GTA has the most extensive diesel locomotive commuter rail network in Canada [9]. The GO Transit, a division of Metrolinx, provides regional public transit service to the GTA and Hamilton Area with passenger trains and buses across 11,000 square–kilometres [10]. The rail network details are shown in Figure 2.1. At full capacity, one locomotive is able to carry the same number of passengers as 1670 cars based on an average of 1.15 passengers per vehicle during rush hour [11], indicating the potential for commuter rail to reduce urban traffic congestion. As part of a continuous effort to reduce GHG's from locomotive exhaust in the GTA, Metrolinx is in the process of converting Tier-2 locomotives to meet Tier-4 limits by upgrading emission control technologies, with in-service testing of ten locomotives estimated to begin in 2015 [12].

Figure 2.1: GO Train Map [13].

2.1.2 GHG Emissions Outlook: Status of Rail Sector

While rail transit systems like the GO Rail commuter fleet provide attractive alternatives to personal vehicles, this system, and similar systems across Canada, continues to rely on fossil fuels and GHG-producing technology to function. Projections of Canada's GHG emissions for 2020 based on current emission reduction strategies exceed the Copenhagen target level by more than 100 megatonnes (Figure 2.2). Significant effort is necessary in order to close this gap. Fossil fuel combustion is the primary source of GHG emissions—approximately 75% of total GHG emissions [14]—mainly from stationary and transportation combustion sources.

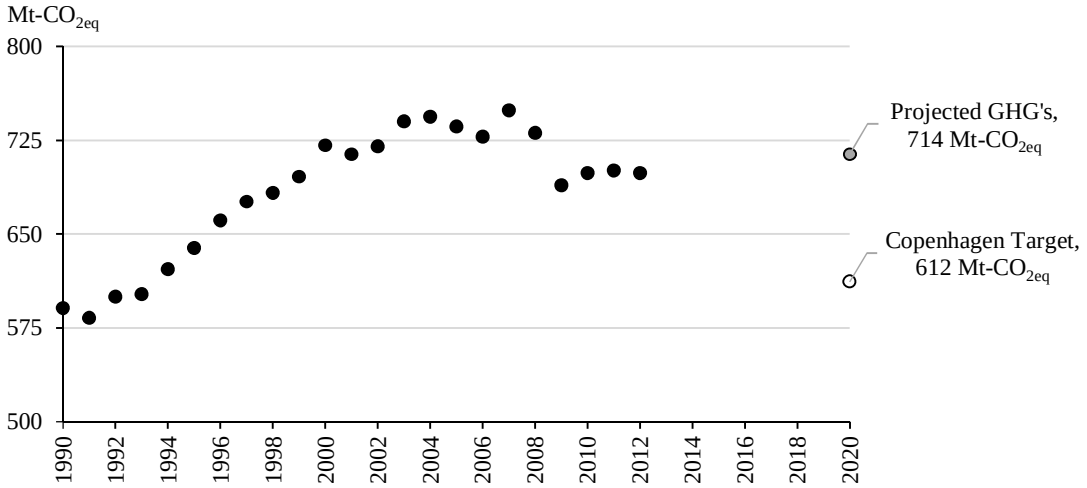

Figure 2.2: Total GHG emissions in Canada (data from [15]).

With the considerable role played by fuel in emission levels, commuter transit—which effectively addresses traffic congestion and reduces pressures on infrastructure—is still reliant on the use of fossil fuels, and stemming from this, GHG emissions. However, when placed in context with other forms of transportation (Figure 2.3), rail transit represents only a small percentage of the total GHG emissions in the Canadian landscape, making it a worthwhile endeavour to consider viable alternatives that are environmentally benign and or neutral.

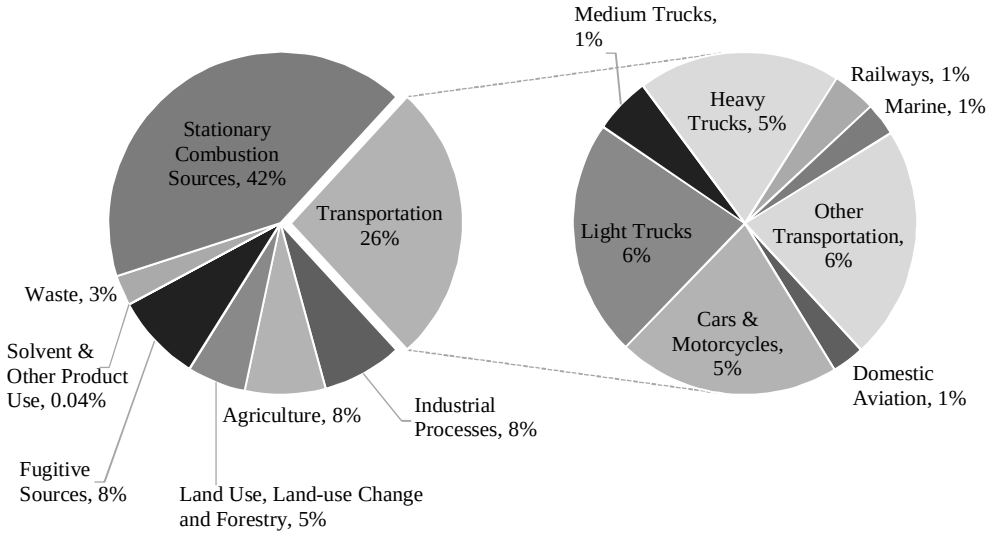

Figure 2.3: GHG distribution by IPCC sector and mode of transportation, 2012 (data from [16]).

2.1.3 Rail Emissions Intensity

Although the Rail Sector is not a significant contributor in terms of total Transportation Sector GHG emissions, the locomotive fleet is fueled almost entirely by diesel fuel. Between 2009 and 2010, diesel consumption by railway operations increased significantly, from 1.87 billion litres of fuel to over 2 billion, due to increased freight operations (Figure 2.4).

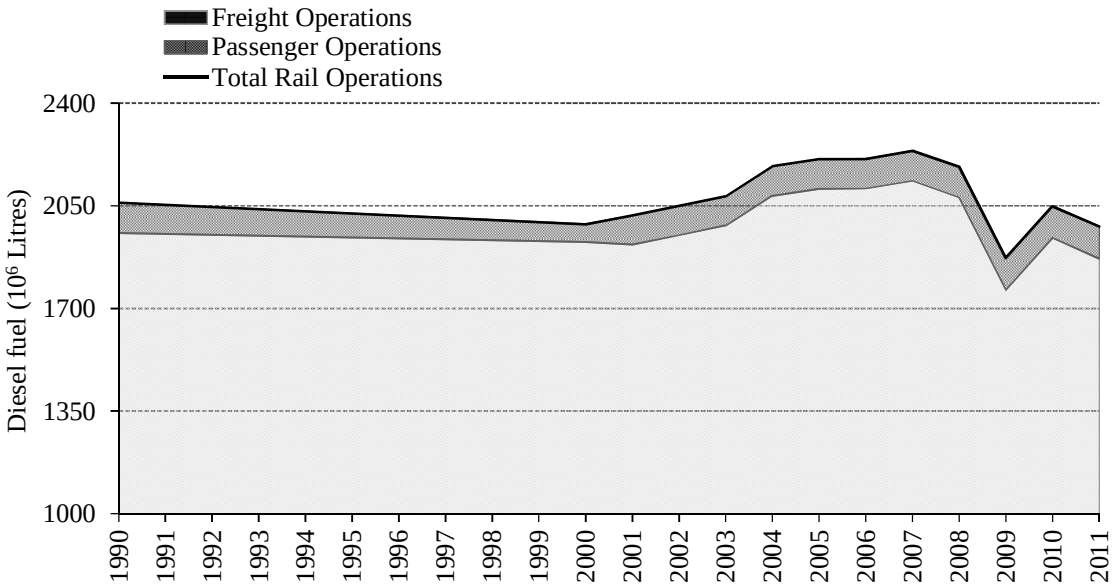

Figure 2.4: Diesel fuel consumption by rail operation (data from [12,17]).

To mitigate the effects of diesel combustion, emission reduction targets are set by the RAC and Canadian Government for all rail operations, imposing increasingly stringent GHG and CAC emission limits over time. Current limits, listed in Table 2.1 and Table 2.2, are in line with those established by the US EPA, and are given in terms of emission intensity standards using a tiered approach based on the year of manufacture, and specific mode of operation of a locomotive.

Table 2.1: Rail industry GHG emission intensities and MOU targets.

Rail Operation	Units[a]	2006	2007	2008	2009	2010	2011	%– Red. (2015)[b]	2015 Target
Class I Freight	kg/1,000 RTK	17.40	17.32	17.61	16.94	16.43	15.24	6%	15.44

Regional & Short Lines	kg/1,000RTK	14.77	15.22	15.80	14.20	15.21	14.88	3%	14.75
Intercity Passenger	kg/PAX-km	0.13	0.13	0.12	0.13	0.12	0.12	6%	0.11
Commuter Rail	kg/PAX	1.70	1.71	1.74	1.95	2.06	2.19	NA	1.46

a. Units are expressed in terms of kg CO_{2eq} per productivity unit; RTK = Revenue tonne kilometre, PAX = passenger
b. %-Reduction from 2010 levels.
Source: [12,18]

Table 2.2: EPA locomotive CAC exhaust emission standards (g/bhp·hr).

Duty-Cycle	Tier	Year	HC	NO_x	PM	CO
Line-haul	Tier 0	1973-1992	1.00	9.50	0.22	5.00
	Tier 1	1993-2004	0.55	7.40	0.22	2.20
	Tier 2	2005-2011	0.30	5.50	0.10	1.50
	Tier 3	2012-2014	0.30	5.50	0.10	1.50
	Tier 4	2015+	0.14	1.30	0.03	1.50
Switch	Tier 0	1973-2001	2.10	11.8	0.26	8.00
	Tier 1	2002-2004	1.20	11.0	0.26	2.50
	Tier 2	2005-2010	0.60	8.10	0.13	2.40
	Tier 3	2011-2014	0.60	5.00	0.10	2.40
	Tier 4	2015+	0.14	1.30	0.03	2.40

Source: [19]

2.1.4 Locomotive Prime Mover

The Canadian locomotive fleet is made up of nearly 3,000 locomotives servicing freight and passenger transportation operations (Table 2.3). Freight locomotives and operations make up the majority of rail operations, representing more than 90% of the Canadian locomotive fleet.

The vast majority of the locomotive fleet is made up of diesel-electric locomotives, operating with either two-stroke or four-stroke prime mover diesel engines that is coupled to an electric alternator/generator to convert shaft power to electric to power the traction motors and control systems. The focus of this particular work is with respect to the propulsion systems of two–stroke diesel-electric locomotive prime mover engines, which are commonly used in alternative fuel demonstration projects.

Table 2.3: Canadian locomotive fleet for 2011.

	Total
Locomotive Fleet	**2,978**
Freight Operations	2,731
Passenger Operations	247
Diesel fueled	**2,933**
EPA emission limit compliant	**1,433**
Tier 0 / 0+	517 / 170
Tier1 / 1+	111 / 94
Tier 2	541

Source: [12]

The basic arrangement of a modern diesel–electric locomotive is shown in Figure 2.5. During operation, shaft power produced by the diesel internal combustion engine (ICE) directly drives the engine governor, cooling water and oil pumps, radiator fans, and air compressor(s) of the locomotive, as well as electric generator(s) used to power the traction motors and various other cooling subsystems and locomotive controls. An auxiliary generator charges a set of batteries, which supply power to the engine starter motor.

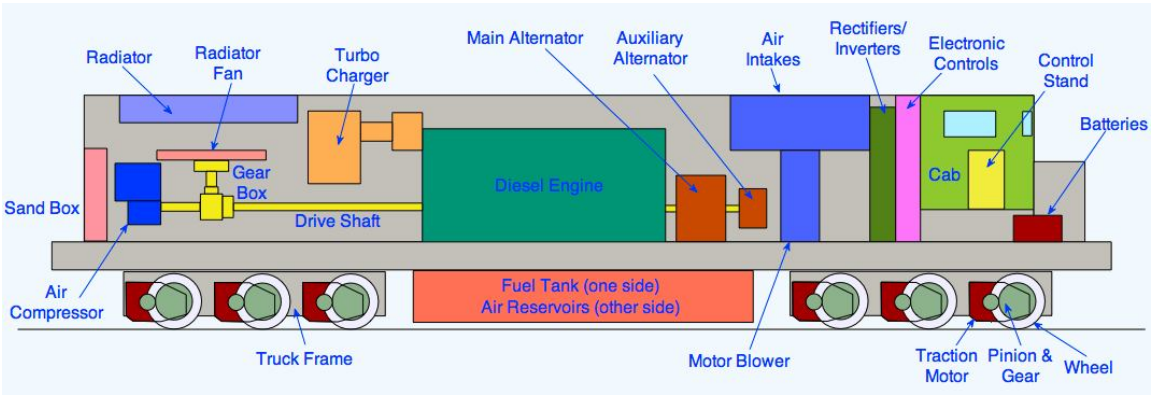

Figure 2.5: Diesel-electric locomotive arrangement [20].

A turbocharger system is used to raise the pressure of air at the intake manifold of the engine, which improves engine performance by recovering heat energy from the exhaust gases to drive the turbo-expander (turbine) and also by increasing the enthalpy of the intake air. The compressed fresh air is cooled in an aftercooler to raise its density—and therefore, the mass flow rate—of the air entering the cylinders.

Heat loss in the exhaust and engine cooling water are addressed as potential areas for locomotive performance improvement by integration with ammonia subsystems. In the proposed designs, additional work production and heat recovery processes are configured and analyzed.

A head end power (HEP) engine (not shown)—typically a smaller diesel ICE—is used for cooling/heating systems and other 'hotel power' operations within passenger occupied rail cars. Though not addressed in this work, the HEP-ICE is another locomotive application with excellent potential for ammonia fueling, since the engine operates constantly, regardless of the locomotive engine speed.

2.2 Ammonia as an Alternative Transportation Fuel

Ammonia has been considered for alternative fueling in transportation applications for more than 70 years [21], and is an important nitrogen source used in agricultural and industrial applications. There are two possible pathways for NH_3 as a transportation fuel: ICE engines, and fuel cell systems, with the subcategories for each application indicated in Figure 2.6. The main focus of this work is with respect to ICE application of NH_3 fuel, with the alternative locomotive configurations integrating direct feed, or a combination of direct feed and decomposition subcategory options for NH_3-fuel utilization.

Ammonia has many qualities that highlight it as a sustainable alternative to hydrocarbon fuels for transportation applications. Based on a review of multiple studies by [3] on the potential of ammonia as an alternative transportation fuel, the following are emphasized as particularly advantageous qualities of NH_3:

- High octane rating of NH_3 (110–130) make it suitable for ICE applications [22]
- With more than 150 Mt produced internationally each year, there is already a well-established production and distribution infrastructure in place for NH_3
- Can be thermally decomposed into hydrogen for fuel, and nitrogen gas

- NH_3 is safer than other fuels, including hydrogen, due to high rate of dissipation in air, strong (self-alarming) odour at very low concentration (~5 ppm in air), and is considered non–explosive due to its very narrow flammability range

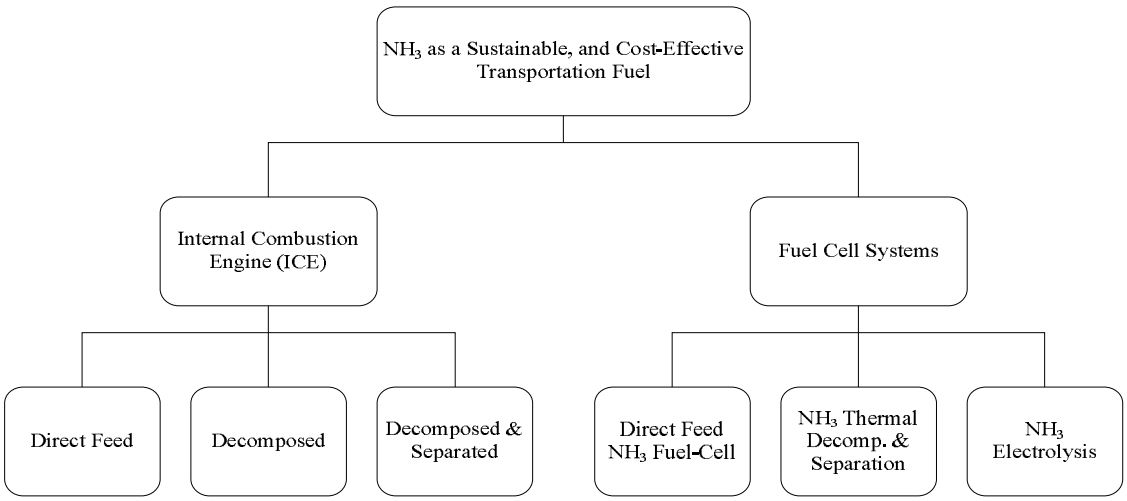

Figure 2.6: Ammonia fueling applications (reproduced from [3]).

2.2.1 Transportation Fuel Comparison

Compared to other fuels used in combustion applications, ammonia has the highest hydrogen energy density—higher even than pressurized and liquefied hydrogen fuel, based on current storage methods [21]—contains no carbon, has a global warming potential (GWP) of zero, and produces only nitrogen and water when combusted. Ammonia is compared to other traditional and alternative fuels in Figure 2.7, with density, ρ (kg/m^3), indicated for each fuel based on the fuel mass per storage volume.

While the comparatively low volumetric energy density of ammonia, relative to traditional hydrocarbons, presents a challenge to its introduction in passenger vehicles as a direct feed combustion fuel—requiring more than double the volume of diesel fuel or motor gasoline to provide the same amount of energy—large transportation vehicles such as rail and heavy duty trucks are well equipped to carry the additional fuel weight without significant performance penalties.

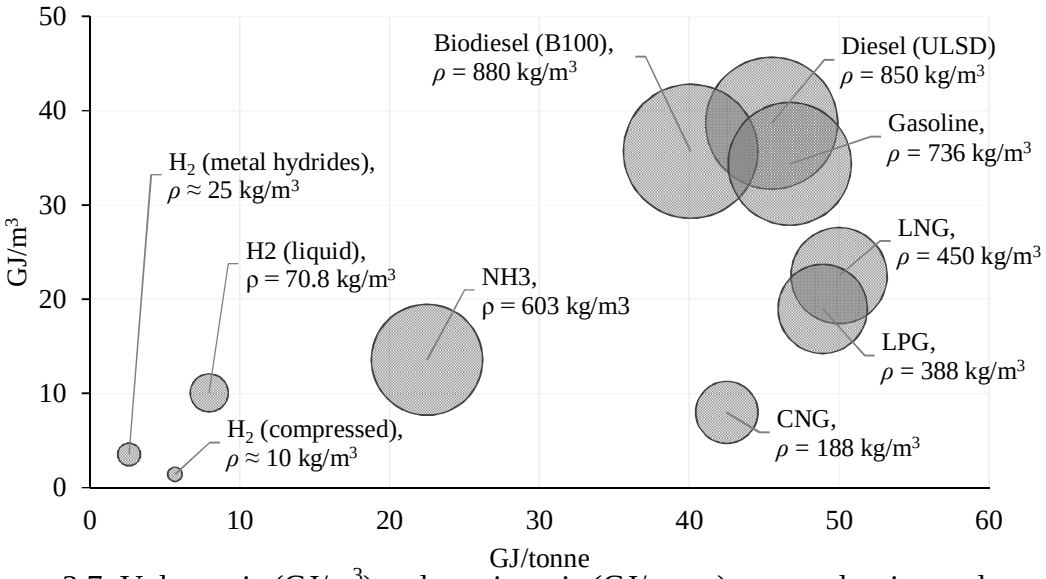

Figure 2.7: Volumetric (GJ/m^3) and gravimetric (GJ/tonne) energy density, and mass density (kg/m^3) of transportation fuels [3,23].

2.2.2 Ammonia Properties

The thermophysical properties of ammonia are listed in Table 2.4. The high latent heat of vaporization, in particular, make it a useful working fluid to provide indirect engine cooling, and can reduce the demand on the engine-driven cooling systems by providing indirect cooling of water coolant streams. Recovered heat may be utilized in various NH_3-based processes, producing additional power, and or heating and cooling applications (refrigeration, cabin air conditioning).

Table 2.4: Various thermophysical properties of NH_3.

Specification	Ammonia
Molecular formula	NH_3
Molecular weight, M_i (kg/kmol)	17.03
Liquid density, ρ (kg/m^3) (T = 25°C, P = 101.3 kPa)	603
Critical pressure, P_{cr} (MPa)	11.28
Critical temperature, T_{cr} (°C)	132.4
Latent heat of vaporization, h_{fg} (kJ/kg)	1370
Standard enthalpy of formation, h^o (T = 25°C), (kJ/kmol)	-46.22
Standard entropy, s^o (T = 25°C, P = 101.3 kPa), (kJ/kmol·K)	192.7
Lower heating value, *LHV* (MJ/kg)	18.57
Higher heating value, *HHV* (MJ/kg)	22.54
Chemical exergy, ex^{ch}	19.84

Source: [24]

Transport and On-Board Storage of NH_3

With one of the highest production rates of any chemical, there is a very well established transportation and delivery infrastructure in place for NH_3, both nationally and internationally, using rail, marine, truck, and pipeline transport methods. Storage of ammonia is similar to that of liquid propane, and is able to be stored as a liquid under mild pressure conditions (~1000 kPa).

Safety and Toxicity

Ammonia is classified as a toxic substance, with a low risk of flammability. Compared with the health and flammability ratings of other fuels in Figure 2.8, the flammability risk is significantly lower than NG fuels and hydrogen, which are considered explosive and are also stored at much higher pressures than NH_3.

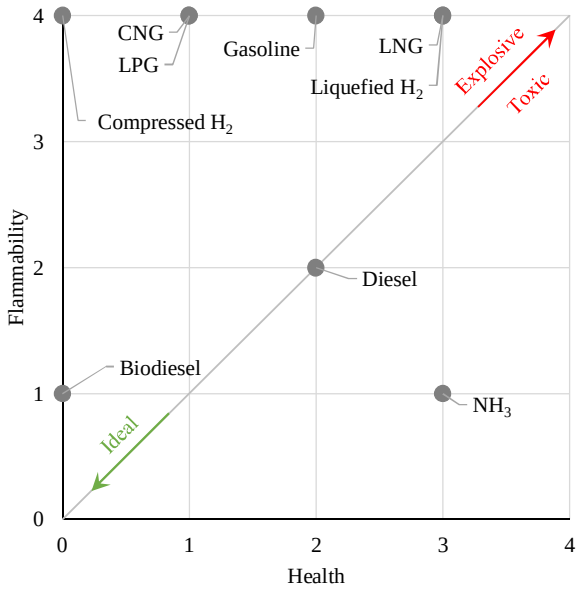

Figure 2.8: Toxicity and flammability of common transportation fuels (MSDS from [25]).

While NH_3 does have toxic properties, one must be exposed for an extended period of time at high local concentrations of NH_3 before it becomes a significant health risk. Furthermore, NH_3 has a very strong and pungent odour at very low concentrations, thus

providing ample warning to leave an area if a leak should occur. Furthermore, while hydrocarbons are not necessarily cancer causing in their fuel form, their combustion products are identified as a cause of lung cancer by health organizations such as the WHO and Canadian Cancer Society [26,27].

2.2.3 Ammonia Production

Ammonia is formed from two of the most abundant chemical elements in the universe—hydrogen and nitrogen—and is most commonly produced using the Haber-Bosch process, combining hydrogen and nitrogen in the reaction:

$$\frac{1}{2}N_2 + \frac{3}{2}H_2 \rightleftharpoons NH_3 \tag{2.1}$$

Hydrogen required for the reaction is obtained by electrolysis of water, or fuel reforming to generate synthesis gas. The most common NH_3 production methods are compared briefly in Table 2.5. GHG emissions from ammonia production with fuel reforming (natural gas, primarily) are associated with either fuel combustion or process-related CO_2 emissions; fuel related emissions result from combustion of CH_4 for steam/gas reforming and various heat requirements, and process related CO_2 emissions result from the conversion of natural gas (CH_4) to H_2 and CO_2 during synthesis. Many of the facilities producing ammonia recover a portion of CO_2 to produce urea; helping to reduce the overall GHG emissions and improve sustainability, while producing an additional valuable product.

Natural gas is the primary feedstock used for producing ammonia in Canada, and worldwide. There are 11 ammonia plants operating in Canada, producing an average of 4–5 million metric tonnes annually per plant [28]. Canadian ammonia plants recover a high percentage of process generated CO_2 (~40%) to produce urea, and have the highest feed-plus-fuel energy (FFE) plant efficiency internationally [28]—consuming an average of 33.8 GJ/tonne NH_3 for natural gas plants, compared to the international average of 38.6 GJ/tonne NH_3.

Table 2.5: NH_3 production method comparison[a,].

Production Method	Fuel	Energy (GJ/t NH_3)	Emissions (t CO_{2eq}/t NH_3)	$/t NH_3	Details
Steam-methane reforming	Natural gas (CH_4)	38.6 (33.8[b])	1.8	400 – >1000	- most common method - fossil fuel derived - highly unstable price
Gasification	Coal	54	4.6	150 - 425	- predominantly used in China - high energy and emission intensity
H_2O Electrolysis +Haber Bosch	electricity (hydro)	12 GWh	0	255 – 735	- electricity may be produced from any energy resource, including renewable
Solid state ammonia synthesis (SSAS)	electricity (hydro)	7.5 GWh	0-	140 – 440	- proton conducting membrane reactor - eliminates electrolysers and Haber-Bosch process - co-production of O_2 - direct steam to NH_3

a. Haber-Bosch process for NH3 synthesis for all except SSAS.
b. Canadian average
c. Electricity from 1 – 5 ¢/kWh
Sources: [29,30,31,32]

Given that the primary energy resource for NH_3 production is natural gas, it is certainly valid to propose to simply use natural gas instead for transportation fuel application – skipping the middle man, so to speak. But this doesn't take into account several key factors that make NH_3 such a valuable resource for sustainable development:

- NH_3 is naturally occurring in biological systems and doesn't do harm to the environment or human health in low quantities; in fact, it is necessary in agriculture to fertilize food crops
- NH_3 is not a fossil fuel, and therefore is not limited in its quantity and availability to fuel reserves, which will eventually be completely depleted
- NH_3 can be produced entirely from renewable resources, and does not require energy and environmentally taxing extraction processes to be made available
- NH_3 does not contain any carbon, and therefore does not produce and CO_2, CO, or soot (a primary constituent of particulate matter) during combustion

- Currently and historically used in a multitude of applications from nitrogen rich fertilizer, to household cleaner, refrigerant, NOx emission reduction agent, and fuel

It is possible to produce ammonia locally (relative to fueling points) from renewable sources, which can give further reductions in CO_2 emissions by minimizing the environmental and impact of transporting ammonia, and most significantly, can eliminate (or nearly eliminate) the feedstock related emissions.

Biofuel and biomass offer a sustainable option for ammonia production, for both syngas production and as a fuel for power plants to produce electricity for water electrolysis. Furthermore, biofuels may be produced locally from various agricultural feedstocks and waste, and municipal solid waste. Furthermore, the production of NH_3 can be a method of storing renewable energies such as solar or wind energy, which can be intermittent.

CHAPTER 3: LITERATURE REVIEW

3.1 Alternative Fueling of Locomotive Prime Mover Engines

Alternative fueling demonstration projects for locomotive engines are a long-standing area of investigation for the rail industry. Projects testing various locomotive powering methods aim to reduce emissions and further the development of more efficient technologies for mainstream use in passenger and freight transportation. Several different demonstration projects are discussed in the following, for the various fuels being tested.

3.1.1 Demonstration Projects and Case Studies

a) Natural gas (CNG or LNG)

Natural gas fueling has been demonstrated in several locomotive projects, as well as investigated in comprehensive reviews and studies [8,9] discussing the potential of CNG and LNG fueling. Natural gas (NG) offers a lower carbon content than diesel fuel (and therefore lower GHG emissions), and has a significant distribution network across Canada, making it an attractive option for locomotive fueling. Dual-fueling of NG and diesel is a common approach, using either low pressure injection (LPI), high pressure direct injection (HPDI), using diesel fuel to assist ignition of the NG. These technologies are installed into conventional diesel locomotives using conversion kits designed for both mono- and dual fueling applications.

Burlington Northern Railroad has been involved in various NG fueling demonstration projects. CNG-diesel fueling was tested in an operational locomotive on a 240 km line between Minneapolis and Wisconsin from 1985–1987. The CNG was stored in cylinders mounted on railway flat cars [9,33]. In a later project, Burlington Northern collaborated with Energy Conversions Inc. (ECI) to demonstrate ECI's LNG conversion technology in two SD40–2 locomotives, which operated successfully from 1990 to 1996 [34]. ECI has also installed a CNG spark–ignition conversion for Napa Valley Railroad in 2000, which is still operational. International CNG conversion projects with ECI include

road locomotives in Peru, Thailand, and Brazil, and recently commissioned for branch-line locomotive conversions for India passenger locomotives for 2012 operation [34].

Recently, CN launched two 3,000 hp Electro-Motive Diesel (EMD) SD40–2 locomotives installed with ECI conversion kits, operating with 90%/10% NG/diesel dual-fuel engines, stating ECI claims for potential emission reductions of 30% CO_2, and 70% NO_x for a locomotive duty cycle [35]. CN is also collaborating with EMD and Westport Innovations, with plans to launch two 4,300 hp EMD SD70–2 locomotives using LNG with Westport's HDPI technology in 2014 [35].

In a 2007 report prepared by BNSF Railway Company, Union Pacific Railroad Company, the Association of American Railroads, and California Environmental Associates [36], the feasibility of natural gas locomotives is evaluated. The study findings regarding CAC emissions state that except for a minor reduction in NO_x levels, higher levels of other CACs are present in exhaust emissions from natural gas-fueled locomotives than in modern Tier 2 diesel locomotives of the same size. Furthermore, the report addresses the recently high and unstable costs of natural gas in North America, stating that this makes it unfounded to consider natural gas as a cost effective option for locomotive fueling. To improve emissions performance, and better control fuel consumption of NG fueled locomotives, Motive Power manufactures LNG–fueled switcher locomotives using multiple engine (multi–genset) technology. According to Motive Power, the LNG multi–engine technology used in their line of switcher locomotives will meet Tier 2 emission levels for low horsepower and commuter locomotive operations [37].

b) Biofuel

In a dual-fueling demonstration project conducted by SwRI (2004), an EMD GP38–2 locomotive was tested with 20% (volume) biodiesel, blended with EPA locomotive diesel, and CARB diesel [38]. The results of the demonstration project found that the biodiesel blends were able to produce within 1–2% of the rated power without any operational issues, and without any significant increase in total fuel consumption. The

emissions produced by the biodiesel blends produced lower concentrations of CO, comparable emissions of HC, and showed an increase in NO_x production.

Norfolk Southern (NS) railroad launched the first 100% biodiesel (B100) locomotive in the US in 2012 [39]. The synthetic diesel fuel is made by Dynamic Fuels, LLC, in Geismar, LA, using locally–sourced waste animal fat and grease. Based on company sustainability reporting for 2013, lab tests of the biodiesel in a diesel-electric locomotive indicate lower NO_x, CO_2, and PM emissions than petroleum diesel, and required no engine modifications.

c) Hydrogen

Hydrogen fueling of locomotives is possible either by fuel cell or direct feed systems in a hydrogen ICE. The potential of these options for locomotives is investigated in [40], comparing H_2–ICE and H_2 proton exchange membrane fuel cell (PEM–FC) to conventional diesel ICE, and electrification. In the report, a case study is presented for GTA GO Transit, stating that by fueling the GO trains by H_2–ICE or PEM–FC it is possible to reduce annual CO_2 emissions by 2,260 tonnes, and 3,318 tonnes, respectively.

In 2010, French National Railways (SNCF) began demonstration of a hydrogen fuel cell hybrid locomotive by ALSTOM, built on a diesel-electric switcher platform [41]. The hybrid system incorporates a diesel-electric engine, hydrogen fuel cell, batteries, and a supercapacitor, which are managed by an energy optimization control system. The project results state significant reductions in fuel consumption and CO_2 emissions; 20% reduction for long distance travel, 40% reduction for switcher operation (85% reduction at idle), and 60–90% reduction of regulated exhaust emissions [41]. However, the advantages of the hybrid locomotive were less significant at peak power demand.

A hybrid PEM–FC locomotive developed and patented by BNSF in 2009 [42], and funded by the US Department of Defense [43], is being tested in switch operation. The

locomotive uses a set of batteries to drive electric traction motors, as well as a fuel cell power plant to supply additional power to traction motors, and recharge the batteries. The prototype unit began operation in Kansas in 2009, followed by testing in Colorado, and then in Los Angeles rail yards from 2010 to 2011.

d) Battery-Diesel Hybrid

Battery powered and battery–hybrid locomotives have been operated primarily in switcher operations. Railpower Technologies (now RJ Corman Railpower) manufactured 'Green Goat' diesel–battery hybrid switcher locomotives, on the recycled frames of retired locomotives [41]. In 2001, the 2000 hp 'Green Goat' prototype units entered service, followed by the smaller 1,000 hp 'Green Kid' prototype unit in 2003. Railpower manufactured production units from 2004 to 2006. The hybrid technology use diesel gen-set(s) to recharge batteries, and provide additional power as required, with overall fuel reduction of over 50–percent in operational units [41].

In 2009, Norfolk Southern, in collaboration with Penn State University and other industry partners began demonstration of a 1,500 hp EMD GP38 battery powered locomotive for switcher operations in the Altoona, PA switchyard [39]. The diesel prime mover and fuel tank were replaced with 1,080 12 V lead-acid batteries, which power the locomotive throughout the day, and are charged overnight [44]. The locomotive uses regenerative braking to recharge the batteries during operation. To address issues such as overheating and burning, the battery management system and structural design have been optimized to improve battery maintenance and maximize battery life [44], and more advanced lead-carbon batteries, produced by Axion Power International, are being used in the current (2013) generation model of the battery–powered locomotive [39].

In 2003, General Electric (GE) tested a diesel-battery hybrid prototype locomotive for line haul operation. The 4,400 hp locomotive was powered by the diesel engine, with large capacity batteries storing up to 2,000 hp equivalent, for up to 30 minutes [36]. The project is being evaluated for its practicality and commercial viability, – the large size of

the batteries make locomotive maintenance difficult, requiring an entire side of the locomotive for the battery bank.

3.1.2 Dual-Fuel Injection Technologies

For the possible ammonia-powering options discussed in this investigation, the fuel is either a supply of liquid fuels, or a combination of liquid and gas. In the case of liquid-only fueling, NH_3 and diesel fuel may be pre-mixed and injected together into the cylinder; however, for liquid–gas or gas–only mixtures, alternative fuel injection methods must be considered to mono-fuel direct injection system.

For various fuel mixtures, different dual injection systems are suitable depending on the mixture properties. To promote the ignition of secondary fuels, such as the NG–diesel injection indicated in Figure 3.1, a small amount of diesel fuel is piloted into the combustion chamber where it ignites, and initiates burning of the secondary fuel injection. This is an attractive option for NH_3 combustion when injected as a liquid fuel, due the high auto-ignition temperature, which typically requires high compression ratios to self-ignite in direct injection mono fuel engines.

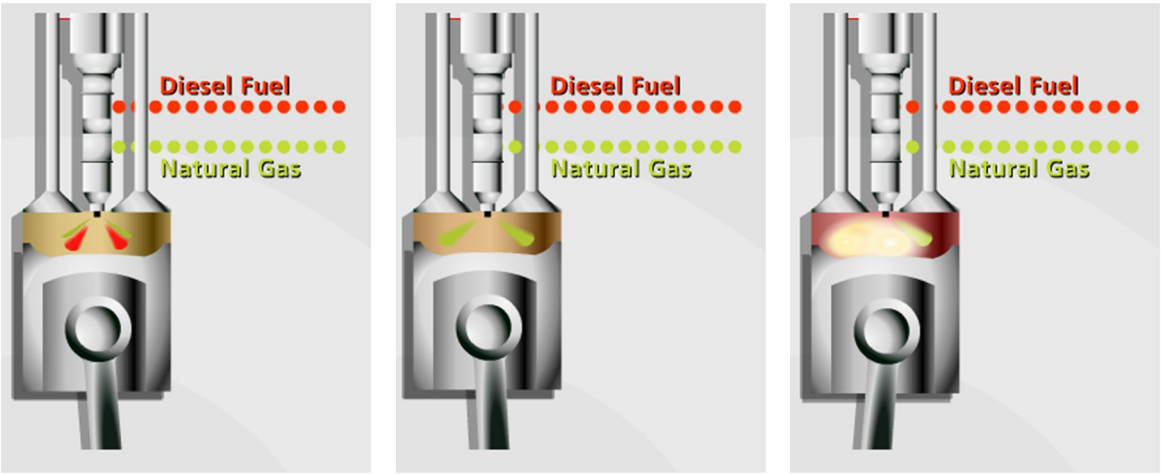

Figure 3.1: Dual-fuel injection [43].

Another arrangement of dual–fueling that uses pilot ignition of diesel is High Pressure Direct Injection (HPDI). Figure 3.2 shows the basic technology, developed by

Westport Power, in which diesel fuel is used to ignite high pressure gaseous fuel, injected at the end of the compression stroke.

Homogeneous Charge Compression Ignition (HCCI)

Suitable for either liquid or gas fuels, HCCI injection combines the advantages of spark-ignition and compression-ignition engines, by injecting fuel into the cylinder during compression (mixed with air), then using high compression ratio to promote auto-ignition of the fuel-air mixture. This method allows for higher diesel cycle efficiency levels and lower NO_x emissions, but problems may arise due to unpredictable auto-ignition conditions in the cylinder, which can cause significant damage to the engine [41].

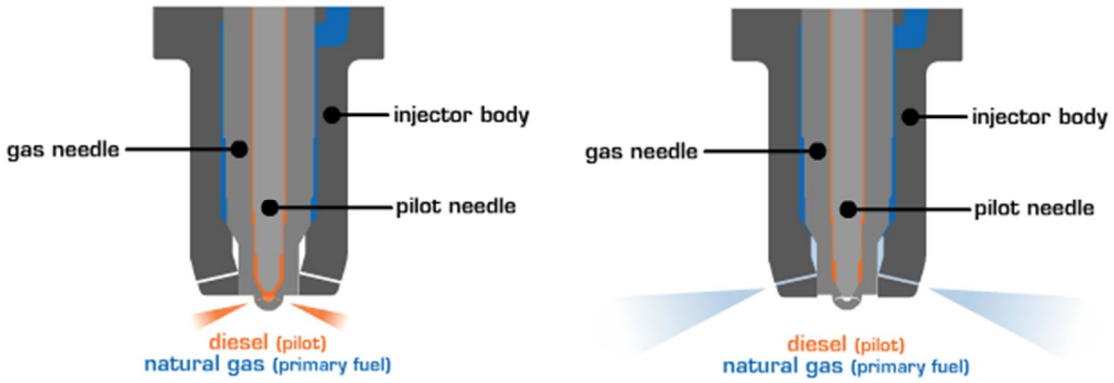

Figure 3.2: Westport HDPI Technology for natural gas application [42].

For gas-only injection, or for fuels which do not ignite as readily as diesel fuel (such as NH_3, or NG), a glow plug can be used to assist ignition instead of the diesel pilot-injection method, as shown in Figure 3.3, to maintain control of ignition timing.

Fuel injected into the cylinder contacts the hot surface of the glow plug, initiating combustion throughout the fuel-air mixture. This is a potential option for injection of partially decomposed ammonia, and would not require separation of hydrogen. With sufficient hydrogen production, the need for dual-fueling with diesel could potentially be eliminated.

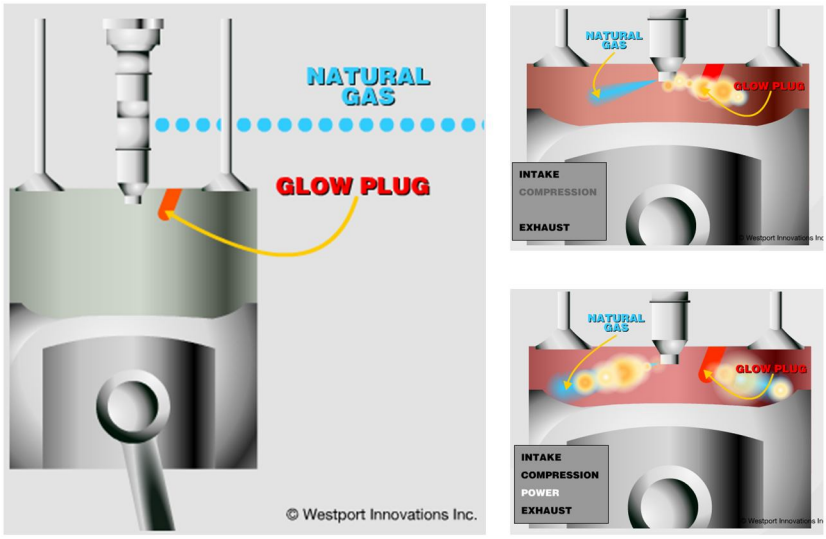

Figure 3.3: CNG-direct injection [43].

3.2 Ammonia Technologies for Transportation Applications

3.2.1 Selective Catalytic Reduction of NO_x Emissions

Selective catalytic reduction is a widely utilized method of reducing NO_x in combustion exhaust emissions in stationary engines. Ammonia is used as a reducing agent in SCR systems, supplied either directly or in a urea solution, to chemically react with NO_x present in combustion emissions, producing water vapour and nitrogen gas as products. The reactions and temperature range through the SCR are given in Table 3.1. The main reaction is dominant for the assumed operating temperature range of 250–450°C [44], and has a NH_3/NO_x ratio of 1:1, as described by its stoichiometric reaction. At temperatures above 500°C, NH_3 oxidation occurs, causing undesirable NO emissions, and at temperatures below 200°C the performance of the reaction is too low for NO_x reduction in diesel applications.

Table 3.1: SCR characteristics.

Chemical reaction equations	Main	$4NH_3 + 4NO + O_2 \rightarrow 4N_2 + 6H_2O$
	Fast	$8NH_3 + 6NO_2 + O_2 \rightarrow 7N_2 + 12H_2O$
	Oxidizing (T > 500°C)	$4NH_3 + 5O_2 \rightarrow 4NO + 6H_2O$
Operating temperature range, T_{SCR} (°C)		250–450
Average NOx reduction for temperature range		0.7–0.9

The process diagram is shown in Figure 3.4 for the main reaction. NH_3 vapour is injected into the exhaust upstream of the SCR catalyst. The mixing streams pass through the catalyst bed, where the reaction takes place. For the complete reaction, the products leave the catalyst as water vapour and nitrogen gas. Some ammonia slip is possible, which can cause formation of ammonium sulfates, and unwanted ammonia in exhaust emissions; the EPA permits an acceptable range of 2–10 ppm ammonia slip [45].

One of the challenges of installing SCR systems in vehicle applications is the generally large size of SCR units, and the vibrations affecting performance. The Compact SCR™ technology designed by [51] uses shock-mounting to damp vibrations, and has been installed in an operational 3,000 hp 12-cylinder EMD–710G3, a smaller model of the locomotive considered in the analysis with the same cylinder characteristics. The reported data indicate significant reductions for CAC emissions (not including SO_x) for line haul and switch locomotive operations, with almost complete elimination of HC emissions. Similar results are reported for commuter locomotives installed with SCR systems in Metrolink locomotives operating in California [52].

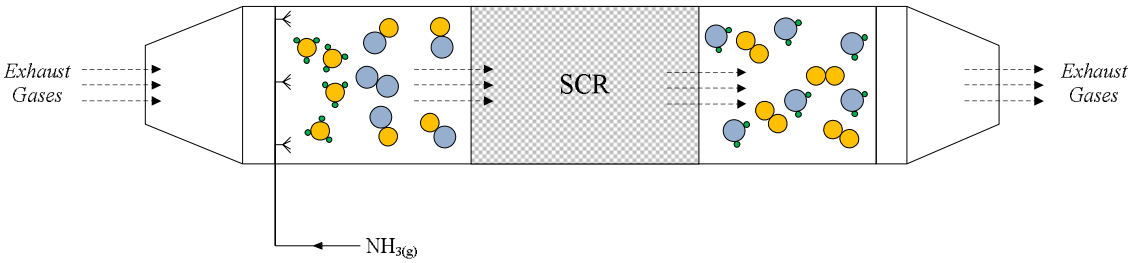

Figure 3.4: SCR process diagram for main reaction ($4NH_3 + 4NO + O_2 \rightarrow 4N_2 + 6H_2O$).

3.2.2 Onboard Hydrogen Fuel Production using Ammonia Decomposition

Ammonia is one of the most promising and least expensive methods of storing hydrogen [53]. As a hydrogen carrier, ammonia contains 1.5 mols of hydrogen per mol of ammonia, which amounts to 108 kg H_2/m^3 for liquid ammonia at 20°C and 8.6 bars [3]. Ammonia can be thermo-catalytically cracked to produce hydrogen using approximately 12% of the lower heating value of hydrogen [53]. The decomposition occurs according to the endothermic reaction, relative to the hydrogen energy content:

$$\frac{2}{3}NH_3 \rightarrow H_2 + \frac{1}{3}N_2 \qquad \Delta H=30.1 \text{ kJ/mol } H_2 \tag{3.1}$$

Three configurations of ammonia decomposition units are shown in Figure 3.5 are tube–type, plate–type, and catalytic membrane. The tube–type (Figure 3.5a) is the simplest of the options, using a tube filled with the catalytic bed material that is externally heated by passing flue gases. In this type, no separation occurs, and all three gas species are present in the product stream. Figure 3.5(b) shows a plate–type reactor, in which ammonia is fed from the bottom, and flue gas pass through cross-flow channels. Pure hydrogen is separated via selective membrane from the gas stream, and the remainder leaves the reactor as a mixture of nitrogen gas with traces of ammonia and hydrogen. The third type, shown in Figure 3.5(c), separates hydrogen via hydrogen–selective membrane, doped with ammonia cracking catalysts. A nitrogen-selective membrane placed at the outlet gas port is used to improve product separation by shifting the reaction further to the right [53].

There are a variety of catalyst materials that may be used for the decomposition process, but for the temperature range associated with diesel exhaust, ruthenium (Ru) catalysts have favourable performance for NH_3 decomposition for the temperature range considered, operating between 350–525°C [6,54]. At temperatures over 1000 K, this reaction occurs without any catalyst, however at lower temperatures, the reaction rate is too slow for the process to be practical for hydrogen production.

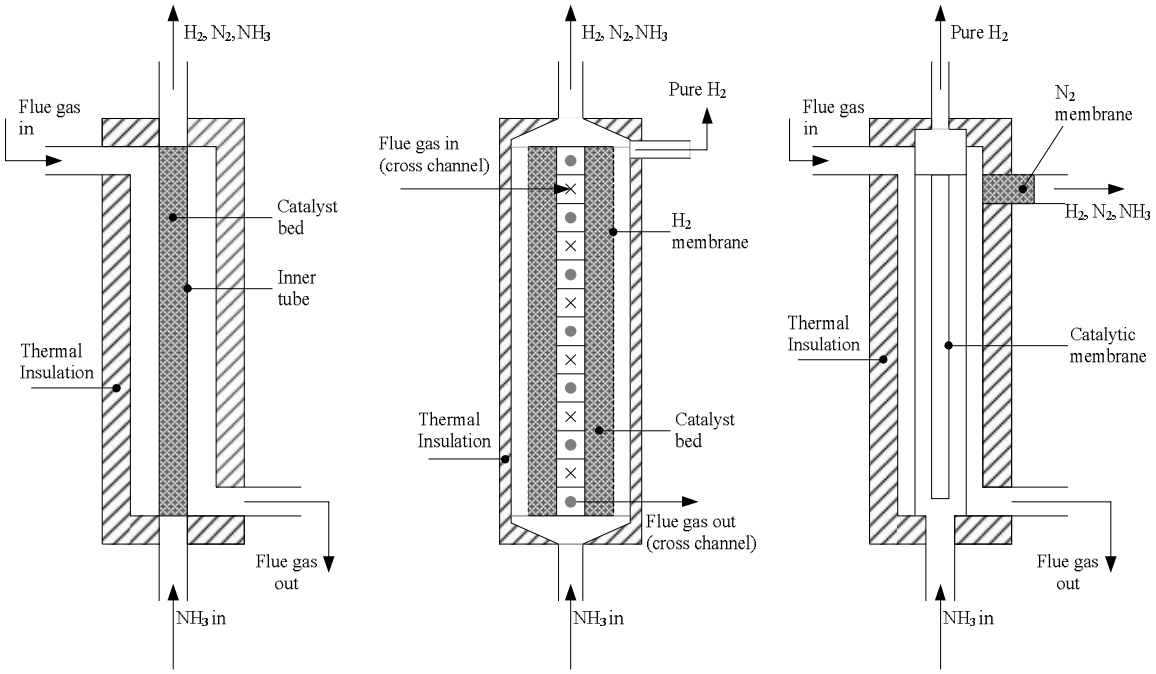

Figure 3.5: Thermo-catalytic NH3 DSU options: (a) tubular catalytic bed reactor, (b) plate catalytic bed reactor with H_2 membrane, (c) catalytic membrane reactor (reproduced from [53]).

CHAPTER 4: SYSTEM CONFIGURATIONS

4.1 System Design Approach: Sustainability and Green Engineering Principles

There are ten system configurations investigated in this study. The designs aim to improve overall performance of the locomotive propulsion systems using process integration and multigeneration to more efficiently utilize the energy supplied by fuel, and provide additional valuable outputs, thereby improving the overall system efficiency. Environmental sustainability and green engineering principles are outlined by [50] as guidelines toward the design approach, including:

- Reducing hazardous material and energy inputs/outputs – i.e., reducing diesel consumption and exhaust emissions;
- Prevention of waste formation instead of (or, as well as) waste treatment – i.e., heat recovery processes in place of large engine cooling systems;
- Maximize mass, energy, and space efficiency – i.e., using ammonia simultaneously as a fuel, coolant, working fluid, H_2 source, and NO_x reducing agent;
- Integrate interconnectivity with available material and energy flows in processes/systems – i.e., recovered heat is used as process heat to produce additional valuable outputs, such as, shaft work, cooling and/or heating;
- Material and energy should be renewable as opposed to depleting.

The proposed systems are introduced in Table 4.1. Included as System 1 is a typical diesel-electric locomotive unit fueled by ultra-low sulfur diesel (ULSD), used as a baseline for locomotive operation and performance assessments. In Systems 2 and 3, additional ammonia systems are integrated to supply required process heating for selective catalytic reduction of exhaust NO_x emissions, and hydrogen fuel production (in System 3), with heat supplied via waste heat recovery from exhaust gas. Systems 4–10 introduce additional options which further utilize the onboard ammonia for various heat recovery and power generation applications. The recovery processes reduce the energy requirements from diesel fuel by reducing temperature of hot streams to be cooled by

radiators, as well as heat energy lost in the exhaust stream, and by supplementing power requirements with work produced by ammonia sub–processes.

Table 4.1: Systems considered.

System	Brief Descriptions[a,b]
System 1	• Baseline diesel locomotive unit • Diesel-electric locomotive operation, fueled by ULSD • System diagram in Figure 4.1 (16 components, 23 state points)
System 2	• Diesel-ammonia (NH_3) locomotive fueling • Additional components: NH_3 storage tank (RES-2), NH_3 fuel pump (P2), expansion (throttle) valve (EXP), exhaust heat recovery heat exchanger (HX-1) and selective catalytic reducer (SCR) • System diagram in Figure 4.2 (21 components, 31 state points)
System 3	• Diesel-NH_3-H_2 (+N_2) locomotive fueling • Additional components: RES-2, P2, P8, EXP-1, EXP-2, HX-1, SCR, exhaust recovery heat exchangers (HX-2), decomposition and separation unit (DSU) • System diagram in Figure 4.3 (25 components, 37 state points)
System 4	• Diesel-NH_3-H_2 locomotive fueling with N_2 separation and expansion • Additional components: RES-2, P2, P8, EXP-1, EXP-2, HX-1, HX-2, SCR, DSU, N_2 Turbine (T2) • System diagram in • (26 components, 39 state points)
System 5	• Diesel-NH_3-H_2 locomotive fueling with NH_3 and N_2 turbines • Additional components: RES-2, P2, P8, EXP-2, HX-1, HX-2, SCR, DSU, T2, NH_3 turbine (T3), H_2 compressor (C2) • System diagram in Figure 4.5 (27 components, 40 state points)
System 6	• Diesel-NH_3-H_2 locomotive fueling with engine coolant heat recovery (indirect engine cooling) and NH_3 expansion • Additional components: RES-2, P2, EXP-2, EXP-3, HX-1, HX-2, SCR, DSU, T2, T3, C2, engine coolant (jacket water) heat exchanger (HX-3), NH_3 turbine (T4) • System diagram in Figure 4.6 (29 components, 42 state points)
System 7	• Integrated compressed N_2 gas storage • Additional components: RES-2, P2, P8, EXP-2, HX-1, HX-2, SCR, DSU, T2, T3, H_2-NH_3 compressor (C2), Exhaust heat recovery/NH_3 heating (HX-3), N_2 storage tank (RES-7) • System diagram in Figure 4.7 (29 components, 42 state points)
System 8	• Diesel-NH_3-H_2 locomotive fueling with combined heat recovery and fan powering (radiator cooling) • Additional components: RES-2, P2, EXP-2, EXP-3, HX-1, HX-2, HX-3, SCR, DSU, T2, T3, C2; NH_3 turbine with fan (T4) • System diagram in Figure 4.8 (29 components, 43 state points)
System 9	• Diesel-NH_3-H_2 locomotive fueling with NH_3 cab cooling (*CAB-C*) COP_C = 2.0 • Additional components: RES-2, P2, EXP-2, EXP-3, HX-1, HX-2, HX-3, SCR, DSU, T3, C2; *CAB-C* chilled water tank (CH), CAB-C air-cooling heat exchanger (HX-4) • System diagram in Figure 4.9 (28 components, 42 state points)
System 10	• Diesel-NH_3-H_2 locomotive fueling with exhaust heat recovery NH_3-RC • Additional components: RES-2, P2, EXP-2, EXP-3, HX-1, HX-2, SCR, DSU, T2, T3,T4, C2; NH_3-RC boiler (HX-4), NH_3-RC condenser (HX-5), NH_3-RC turbine (T5) • System diagram in Figure 4.10 (32 components, 45 state points)

a. Figure elements (components/connections) shown in grey are not included in component listing.
b. Split flows shown in system diagrams (*i*', *i*") are not included in state point count.

4.2 System Descriptions

System 1: Baseline Locomotive System

The operating characteristics of the locomotive prime mover are given in Table 4.2, including engine and cooling system details. These values are applied for each of the system analyses. The baseline system is shown schematically in Figure 4.1, for a typical diesel-electric locomotive powered by a two-stroke compression ignition diesel engine fueled by ULSD. During operation, air entering the system is compressed to higher pressure by a given factor, pr_{TC}, in the turbocharger compressor (C1). The air passes through an aftercooler (HX-ac), increasing the density (and therefore, mass) of the stream entering the intake manifold, and then is drawn into the engine cylinders. Following internal combustion and expansion stroke, exhaust gases pass through the turbine (T1) of the turbocharger unit, driving the rotor for C1. The combustion gases are exhausted following expansion.

Table 4.2: Prime mover sizing details and locomotive operating conditions.

Engine Sizing		
Engine Model (EMD)		16V-710G3
Traction Horsepower, THP (hp)		4,000
Traction Power, $\dot{W}_{TP}$ (kW)		2,983
Engine Speed, N_{ICE1} (rpm)		900
Brake mean effective pressure, bmep (kPa)		1,069
Displacement Volume per cylinder, V_d (L)		11.635
Compression Ratio, r		16:1
Bore (m)		0.23019
Stroke (m)		0.2794
Number of Cylinders, n_{cyl}		16
Fuel Tank Volume, V_{RES1} (L)		8,410
Baseline Operating Conditions		
Turbocharger Pressure Boost, p_{TC} (~)		1.25
Cooling water reservoir temperature, T_{RES3} (°C)		49
Engine jacket cooling water outlet temp. T_{12} (°C)		85
Heat Removal Rate[a]	Water Jacket Cooling, HRR_{wjc} (kJ/kW$_{TP}$·h)	2,377
	After Cooler, HRR_{ac} (kJ/kW$_{TP}$·h)	908
Maximum cylinder pressure, P_{max} (kPa)		10,800

a. Based on heat removal rates given by [51] for EMD-710 locomotive (converted from Btu/min·bhp).
Sources: [56,57,58]

System 2: ULSD-NH_3 Locomotive Fueling with NH_3-SCR

Ammonia for locomotive fueling and exhaust NO_x emission control is integrated System 2, shown in Figure 4.2. The ammonia is stored in RES-2 at 10 bar (1,000 kPa), and is assumed to be a saturated liquid. Fueling is supplied as an NH_3–ULSD liquid mixture, varying the ratio of fuel-energy input between NH_3 and ULSD. Ammonia supply for combustion is pumped by P2 from the storage tank and sent with the diesel fuel supply to the cylinder injectors. If a dual–injection system is considered, allowing liquid–gas injection, preheating of the liquid NH_3 fuel may also be included to increase the heat recovery from the exhaust gases, and reduce the energy consumed to evaporate and heat liquid fuel droplets (spray) in the ICE cylinders.

Exhaust NO_x emissions are controlled using selective catalytic reduction (SCR). The flow rate of NH_3 required for the SCR process is determined based on the NO_x emission factor for diesel fuel, at a 1:1 ratio with NO on a molar basis. The liquid is drawn from RES–2, and then throttled to atmospheric pressure in the expansion valve. The resulting liquid-vapour mixture enters the exhaust recovery heat exchanger (HX–1) to be heated to a temperature within the considered range of 250–450°C.

System 3: Integrated Thermal DSU for H_2 Fuel Production from NH_3

Onboard hydrogen production from ammonia is introduced in System 3, based on the concepts described by Dincer and Zamfirescu in [7] for systems-integration approach to use exhaust and other waste heat sources to thermally crack ammonia into hydrogen and nitrogen gases, as described in the background section, and shown in Figure 4.3.

The system is fueled initially with selected ratio for the NH_3–ULSD mixture. A part of the NH_3 supply is pumped to heat exchanger HX–1, where it is heated by the ICE exhaust gases leaving the turbocharger (T1). The ammonia leaves as a superheated vapour, and is throttled to a lower pressure. The temperature is reduced by the process, therefore the NH_3 requires reheating before it can be sent to the decomposition and separation unit. A portion of the exhaust stream leaving the engine (ICE) is diverted from

the turbocharger, and is used to reheat the NH_3 to the required decomposition reactor temperature range (400–600°C). The high temperature NH_3 vapour is split and the required supply of rate for NO_x reduction is directed to the SCR. The temperature in this case is important to consider; if the temperature of the NH_3 stream is higher than 450°C, it should be cooled before entering the SCR to prevent formation of undesirable exhaust products. The remaining high temperature NH_3 vapour enters the decomposition reactor (DSU) where it is thermo-catalytically cracked into NH_3, H_2, and N_2 gases. It is not necessary to separate the streams in this option; the gas mixture is fed directly with diesel fuel into the ICE. The exhaust gas stream leaves HX–2 is reduced in pressure, and mixed with the main exhaust gases before passing through the SCR.

System 4: Thermal NH_3 Decomposition with N_2 Separation and Expansion

In the fourth approach, exhaust heat is used to thermally crack ammonia into hydrogen and nitrogen gases as described in System 3; however, as indicated in
, the nitrogen gas produced in the reaction is separated and expanded in a turbine, producing shaft work to supplement engine power demands.

Liquid ammonia is pumped through a heat exchanger (HX–1) to recover heat from the turbocharger exhaust, and then throttled to a lower pressure. The temperature of the reduced-pressure NH_3 stream is raised to the DSU operating temperature range by the ICE exhaust stream through heat exchanger HX–2, leaving as a superheated vapour. A fraction of the NH_3 vapour is supplied to the SCR prior to decomposition for NO_x reduction of exhaust gases. N_2 product gases are sent through the turbine T2 to provide useful work before being exhausted. The additional work produced by the N_2 turbine is evaluated in the Analysis and Results sections in terms of the change in enthalpy of the gas stream, and the isentropic efficiency of the turbine. The NH_3–H_2 gas mixture is fed with ULSD into the locomotive ICE. To fuel with gas and liquid fuels, the approach can be taken to inject the gas stream into the cylinder during compression, or to inject with the fuel blend using a specialized injector such as the dual injection systems described in the Literature Review section of this work.

System 5: Multistage Heat Recovery and Power Generation

The fifth system, shown in Figure 4.5, operates in a similar manner to System 4, but now introduces multistage expansion with reheat to increase the overall heat recovery effects by ammonia for the locomotive system. Liquid ammonia is pumped through heat exchanger HX–1 where it is superheated, and subsequently expanded in turbine T3. The gas is reheated in HX–2, and the required supply of NH_3 is directed to the SCR to reduce the NO_x emissions in the exhaust, with the remaining stream passing through the decomposition unit. The N_2 product gas mixture is expanded in turbine T2, and then exhausted to the surroundings. The NH_3–H_2 gas is compressed in C2, and sent with the ULSD stream for ICE injection.

System 6: Integrated Engine Cooling and Power Generation

The refrigeration effect of ammonia is used to indirectly cool the engine, by removing heat from the cooling water as it leaves the engine. As shown in Figure 4.6, liquid ammonia is drawn from the tank, and throttled in an expansion valve to a lower pressure and temperature. The result is a low temperature liquid-vapour mixture that can remove heat from the engine cooling water both by latent effect (by evaporation) and sensibly as it passes through HX–3. The resulting vapour is expanded in turbine T4, then passes through the turbocharger exhaust heat exchanger HX–1 for superheating, and expanded again in turbine T3. The stream is then reheated in the high temperature ICE–exhaust heat exchanger HX–2 to the decomposition reactor operating temperature. The required flow rate of NH_3 vapour is diverted to the SCR to reduce NO_x emissions, and the remaining NH_3 stream is partially decomposed in the DSU. N_2 is expanded in T2 and then exhausted. The NH_3–H_2 gas is compressed in C2 and injected into the ICE engine with the ULSD.

System 7: Integrated Compressed N_2 Gas Storage

In System 7 configuration, the nitrogen gas exiting the DSU is compressed and stored for production of expansion work on demand. In the configuration shown in Figure 4.7, NH_3

is drawn from the tank as a saturated liquid. The NH_3 passes through the heat exchanger HX–3, where it is evaporated before expansion in turbine T2. The stream is superheated in HX–1, and then expanded again in turbine T3. The stream is reheated in ICE exhaust heat exchanger (HX–2) and the resulting vapour is split into two streams. A small portion of the gas is diverted to the SCR (which is monitored such that the temperature at entry is less than 450 °C), and the majority of the vapour stream is then sent through the DSU for partial decomposition. The N_2 gas is separated from the gas stream, compressed in C4, and then stored in RES–7 to supply expansion work on-demand. The NH_3–H_2 stream is compressed prior to being sent to the ICE as a gaseous fuel to be combusted with the diesel fuel.

System 8: Indirect Engine Cooling (Heat Recovery) with Turbine Driven Fan Cooling

Additional engine cooling is integrated in the system configuration shown in Figure 4.8. The operation is similar the System 6, with the addition of a cooling fan powered by an ammonia turbine (T4) to increase the indirect cooling effect for the engine.

Ammonia is drawn from the tank, and throttled to an intermediate pressure, then directed to HX–3 where it provides some cooling for the engine coolant (water). The ammonia exits as a superheated vapour, and is expanded in a turbine (T4) coupled by rotor to a fan. The fan assists the radiator cooling system, but could be placed wherever needed. Following expansion in T4, the ammonia stream is re-superheated in HX–1, and expanded in T3 to produce shaft work. The low-pressure stream is again re-superheated (HX–2), and the stream is split into the SCR and DSU supply streams. N_2 gas is expanded in T2. NH_3–H_2 stream is compressed in C2 to be injected into the ICE engine with ULSD.

System 9: Integrated NH_3-Based Locomotive Cab Cooling

The configuration shown in Figure 4.9 includes the additional ammonia process of cab-cooling. Ammonia is throttled to an intermediate pressure level, with a low temperature

useful for cooling. The cold stream of ammonia is circulated through a chiller (CH), assumed to be filled with water. Chilled water is circulated in an air-cooling heat exchanger (HX–4) which allows the cooling to be on-demand for the operator, and can be controlled by a fan. The cool stream of ammonia leaves the chiller tank, and is used to provide cooling for the engine jacket water in HX–3. The warm ammonia is then superheated in HX–1, and expanded in T3, before being re-superheated (HX–2) and decomposed in the DSU. As in the previous system, a portion of the ammonia stream is diverted to the SCR to reduce engine NO_x. The gas mixture leaving the DSU is not separated, and instead is compressed (C2) and sent as a mixture with ULSD for combustion in the ICE.

The cooling system is assumed to have an overall COP of 2.0, which is the same assumption as other engine cooling processes for the locomotive. The temperature of the cold stream is kept above 0°C, to ensure that there is no ice formation in the water. Alternatively, the tank could hold brine or other mixtures which have lower freezing points to improve the cooling performance.

System 10: Exhaust Heat Recovery NH_3-RC and Integrated Power Generation

In the configuration shown in Figure 4.10, a heat engine operating as a Rankine cycle is integrated with the system, with the NH_3 fuel stream used as the working fluid cycle. The liquid NH_3 stream is pumped to the exhaust heat recovery exchanger HX–4, which serves as the boiler component for the NH_3–Rankine cycle (NH_3–RC) heat engine. Vapour produced in the heat recovery process (either saturated vapour, or superheated) is expanded in turbine T5 to produce shaft work, and is then condensed in HX-5 by transferring heat to the secondary NH_3 stream. The condensed NH_3 is then mixed with the ULSD stream and is fed into the ICE for combustion.

The secondary NH_3 stream is drawn from the tank and throttled to a lower pressure liquid-vapour mixture. The stream recovers heat in HX–5, and the vapour is expanded in T4 to produce work. The intermediate pressure NH_3 is reheated in HX–1, and then expanded to a lower pressure level in T3. The stream is reheated in HX–2, and the

required supply rate of NH_3 sent through the SCR for NO_x reduction. Following the decomposition process, N_2– gases are fed through the final expansion process in T2, and the H_2 stream is compressed to be injected into the ICE engine with ULSD. The remaining NH_3 gas is cooled, and pumped back to the storage tank.

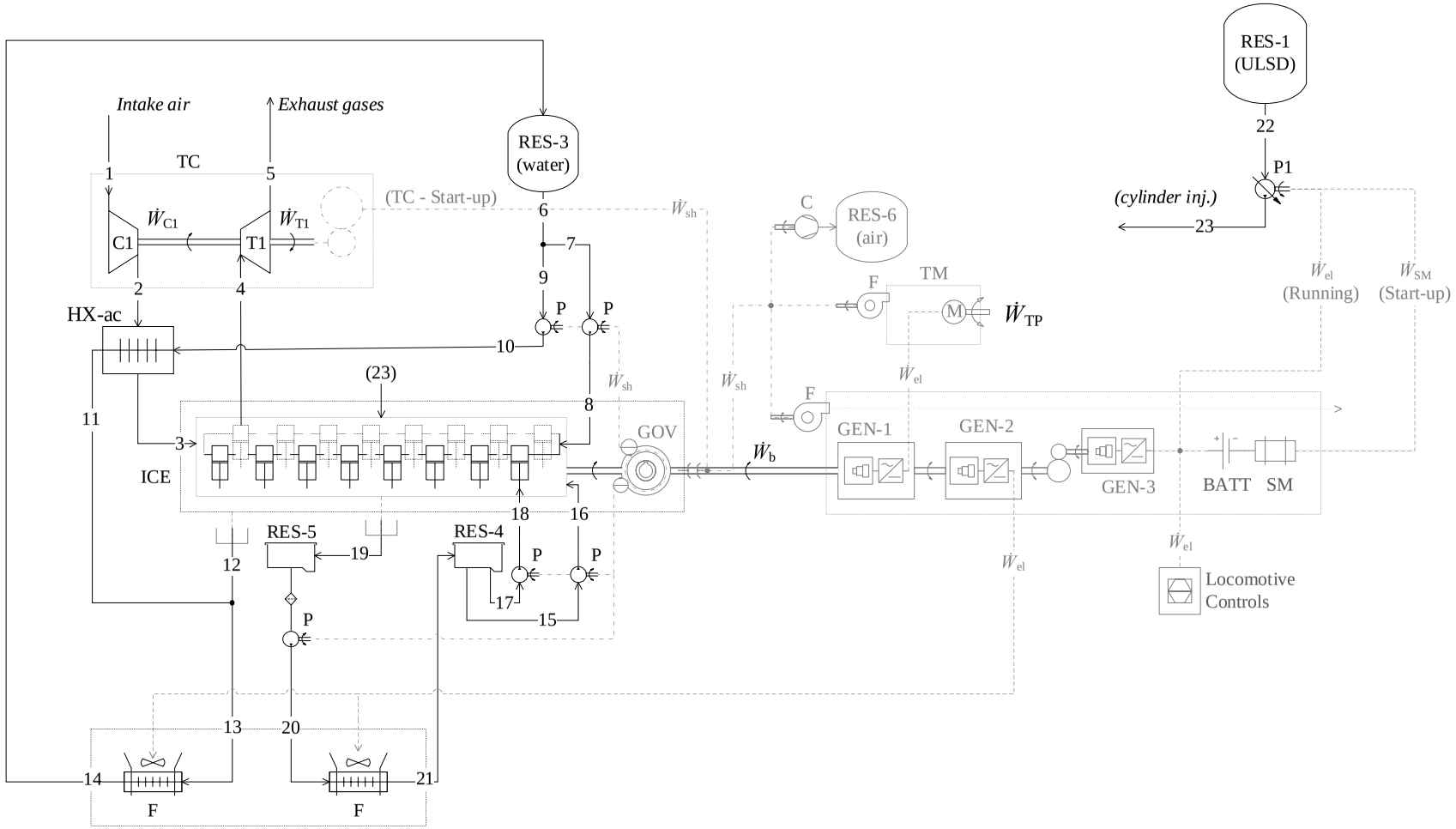

Figure 4.1: Baseline diesel–electric locomotive (System 1).

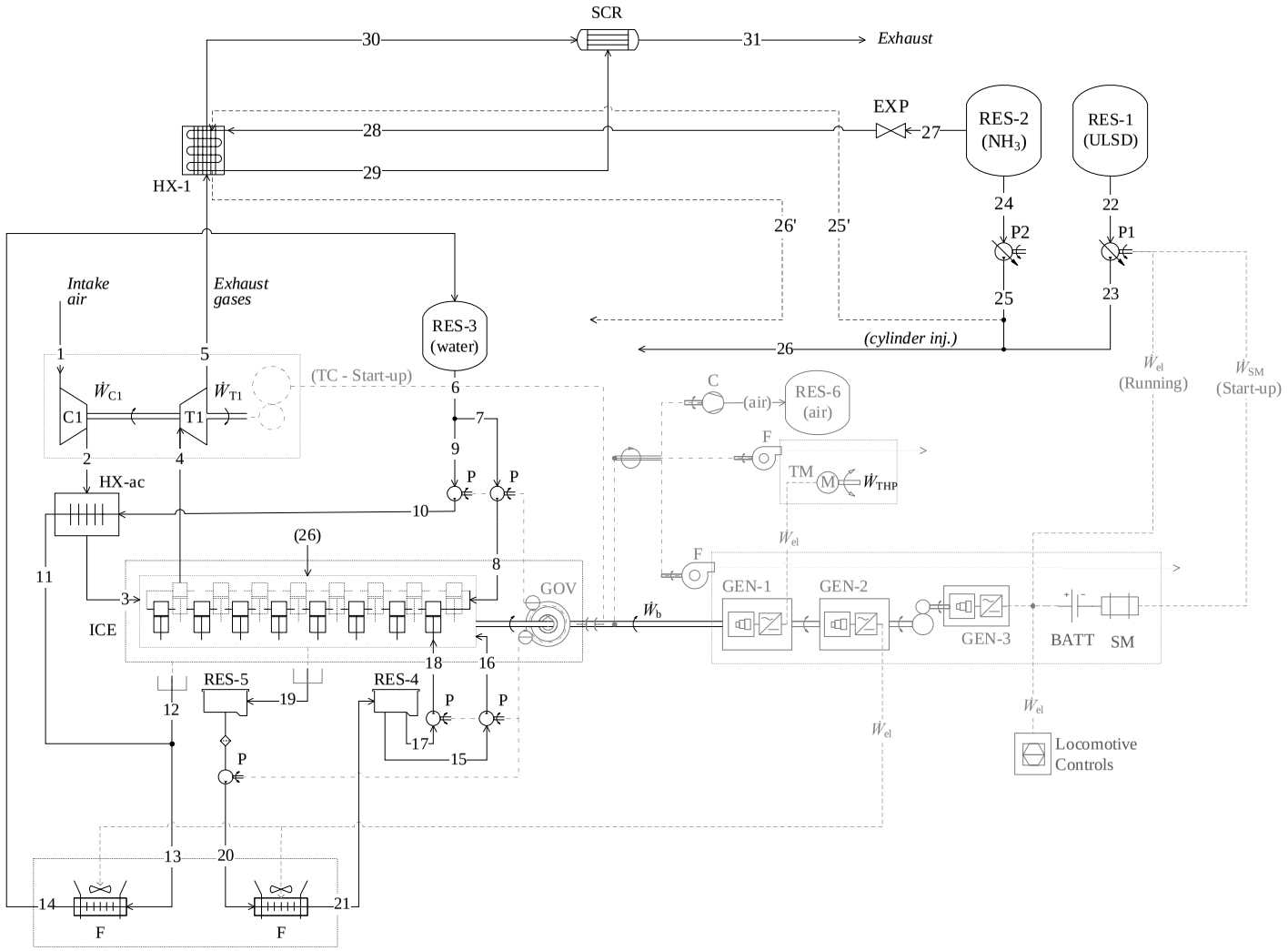

Figure 4.2: Diesel–NH_3 fueling with exhaust gas SCR (System 2).

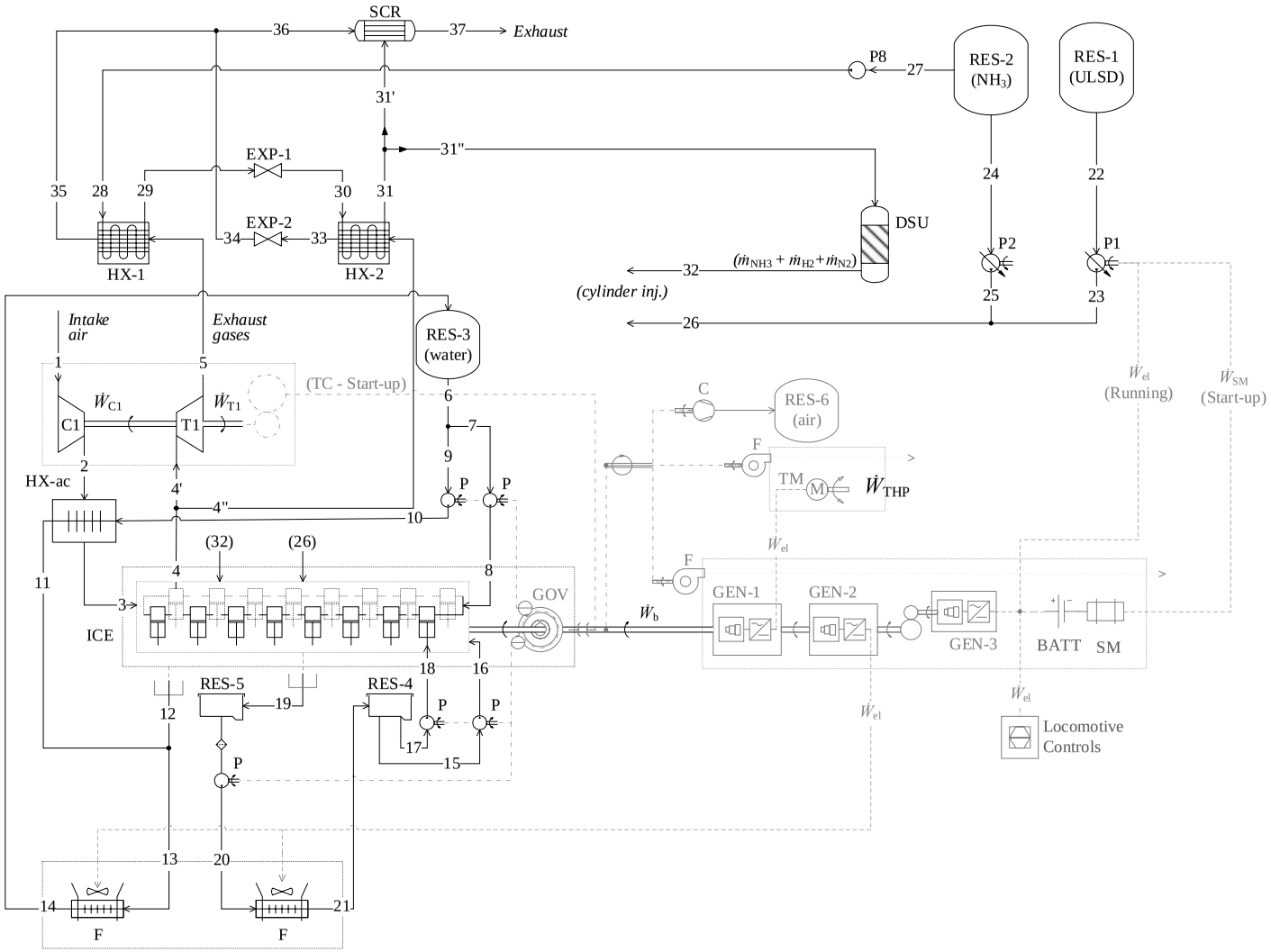

Figure 4.3: Integrated thermal DSU for H_2-fuel production from NH_3 (System 3).

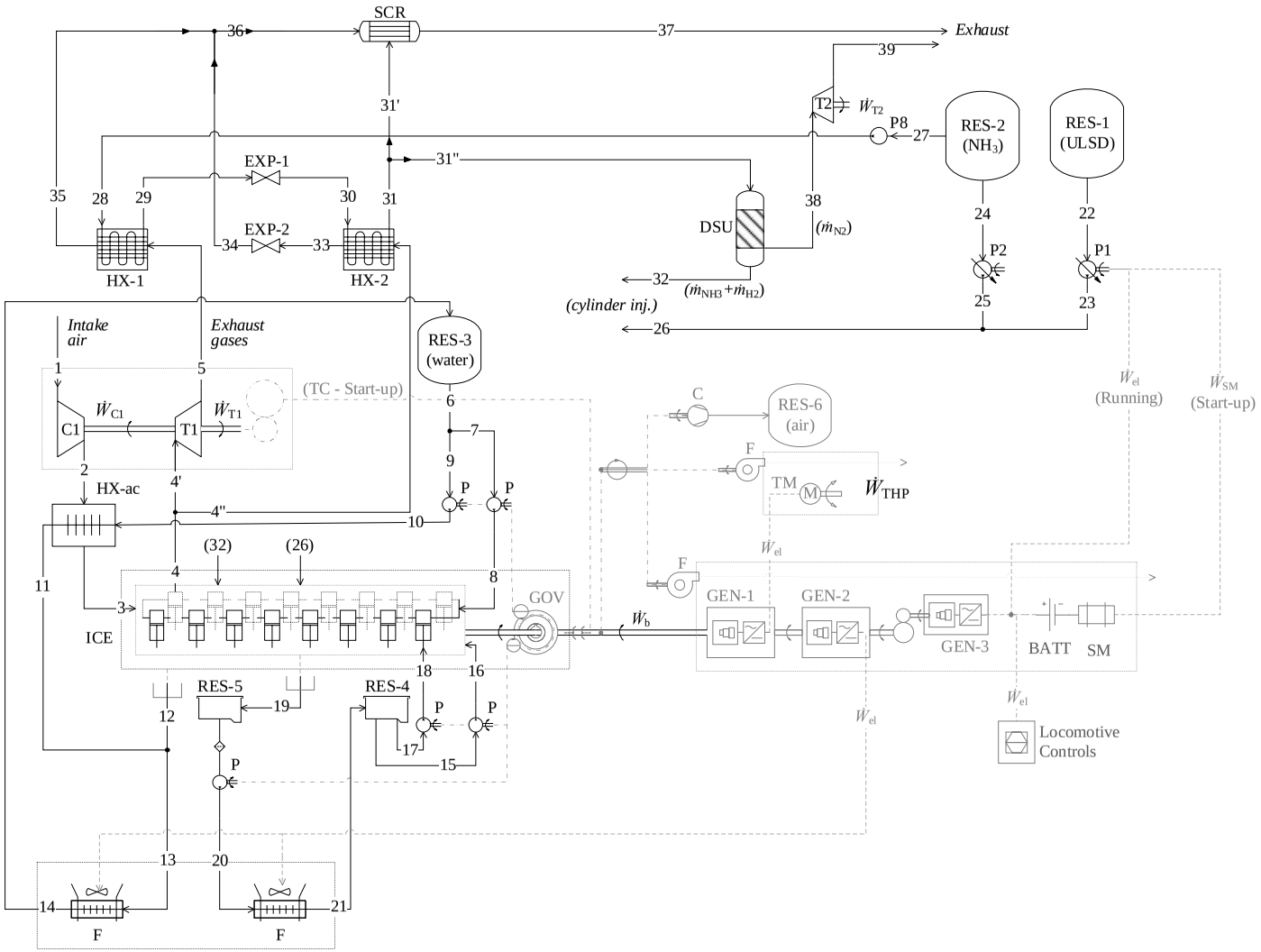

Figure 4.4: Thermal NH_3 DSU with N_2 separation and expansion (System 4).

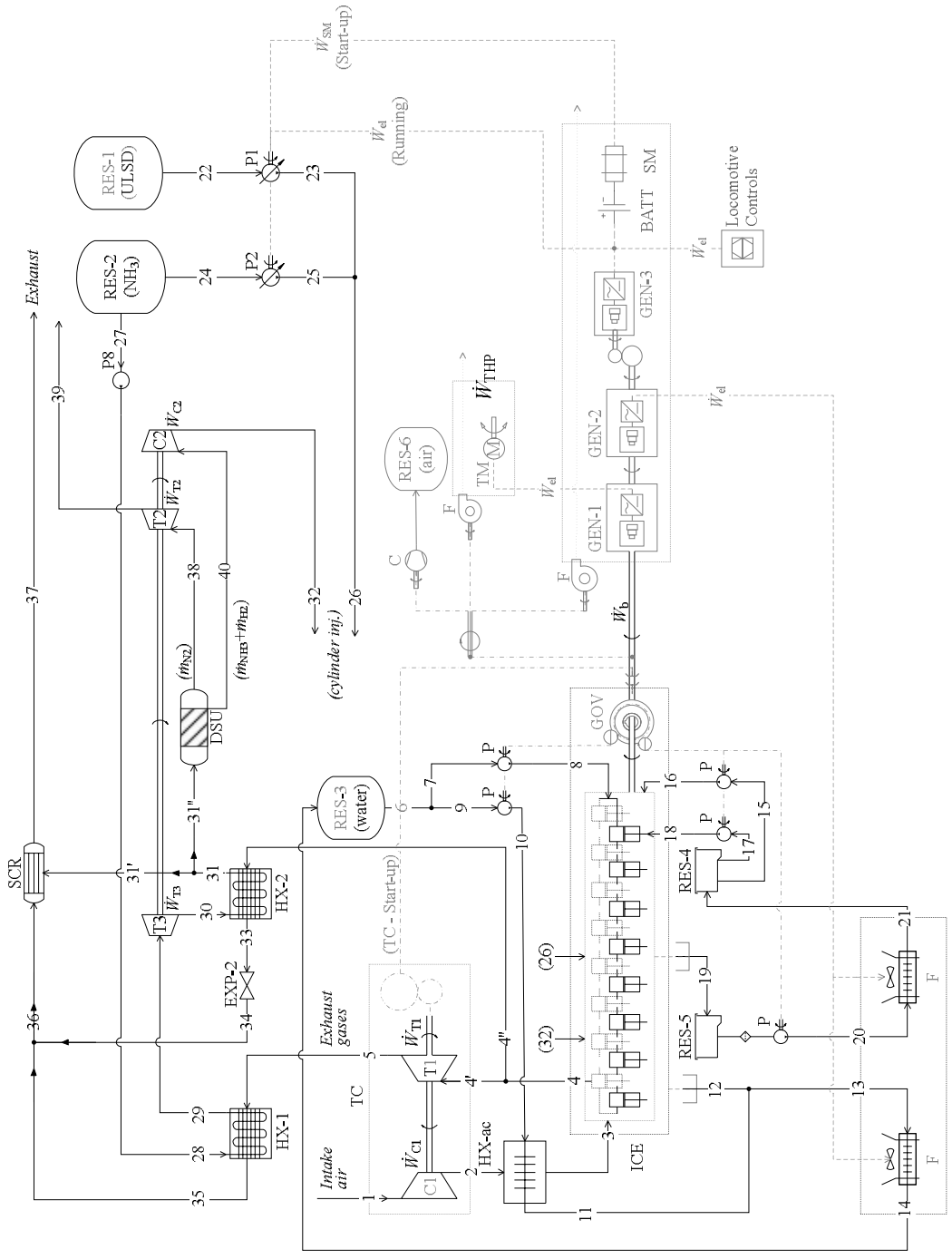

Figure 4.5: Multistage NH_3 heat recovery and expansion (System 5).

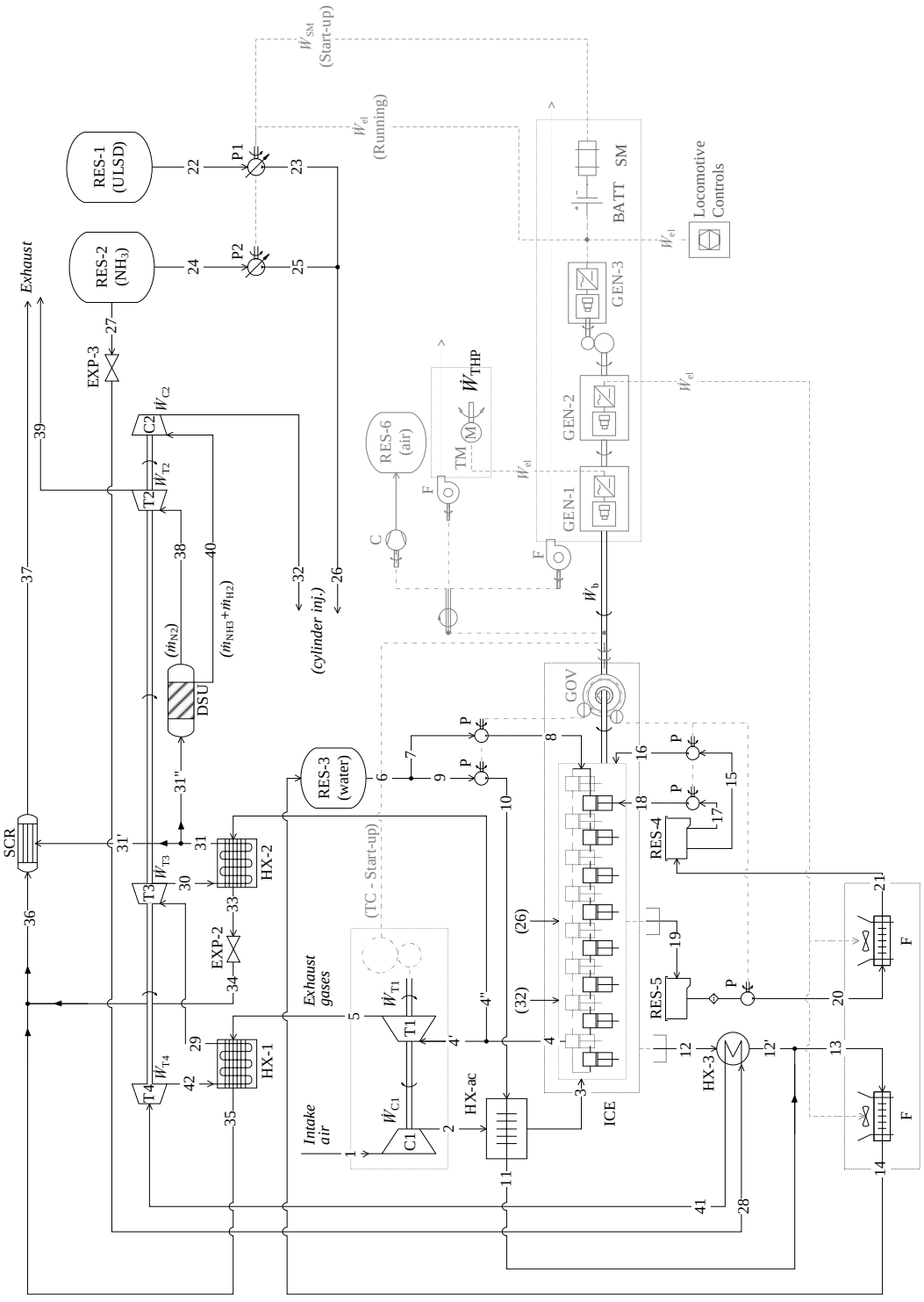

Figure 4.6: Integrated indirect engine cooling and power generation (System 6).

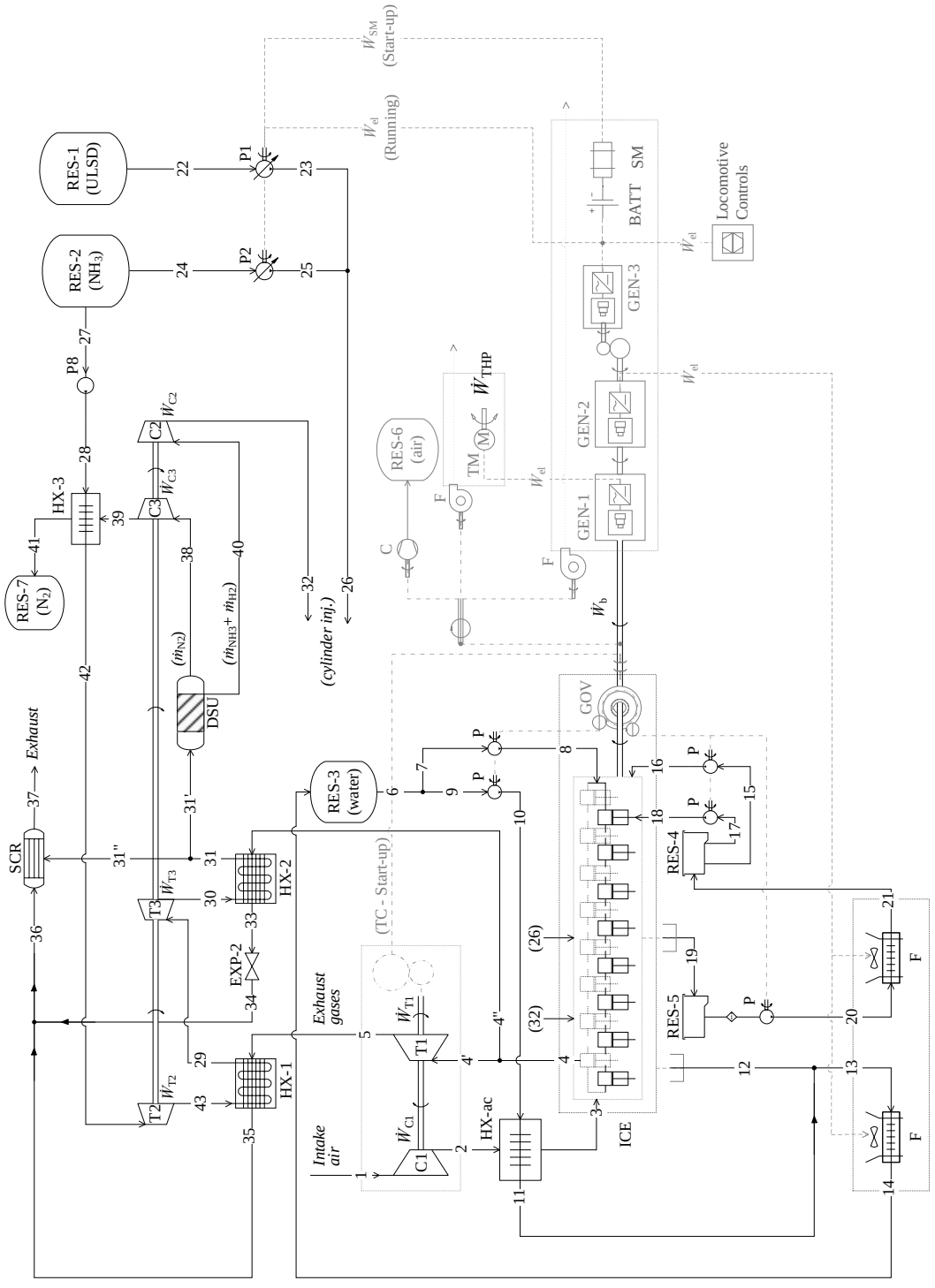

Figure 4.7: Compressed N_2 Storage (System 7).

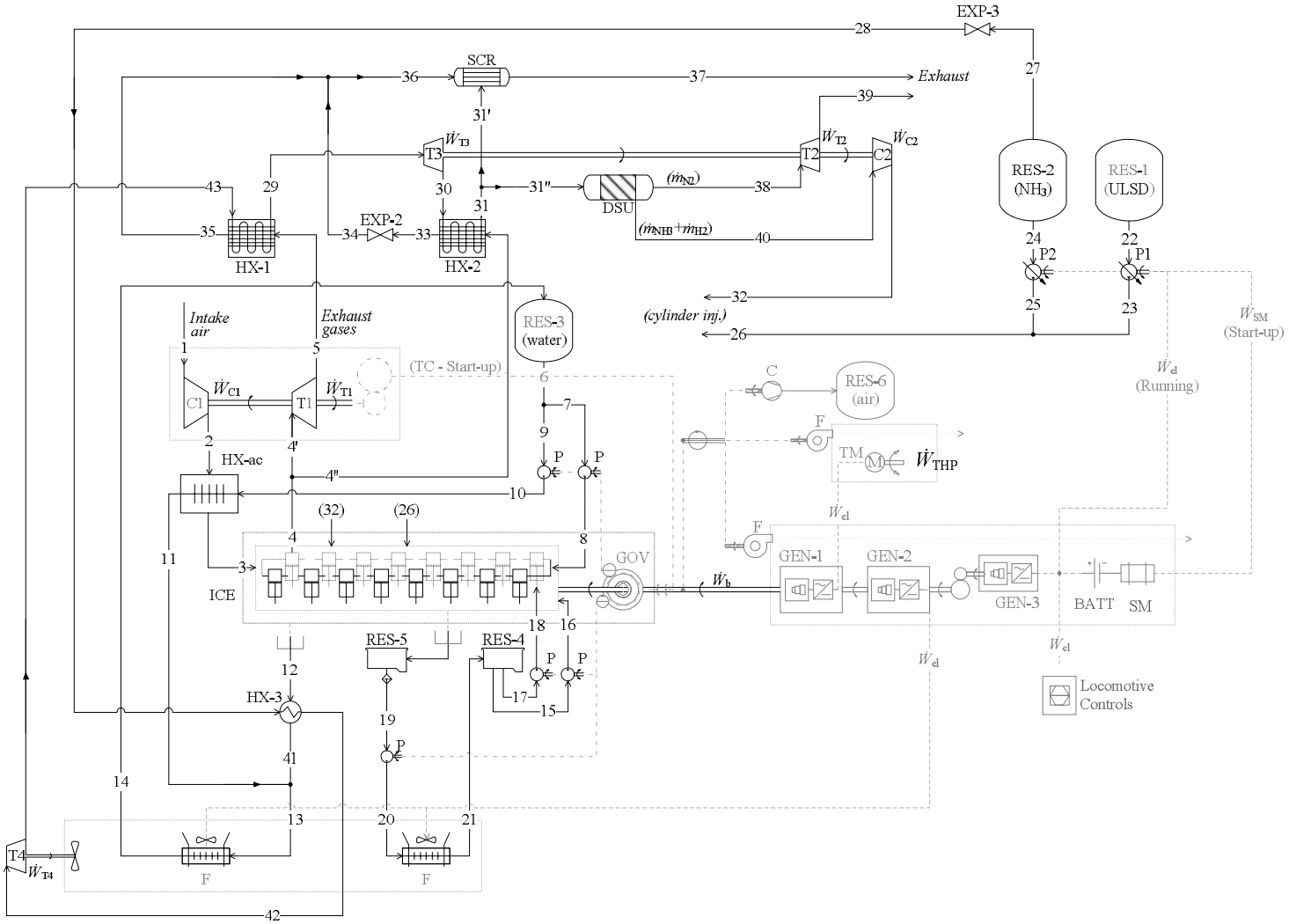

Figure 4.8: Indirect engine cooling by NH_3 heat recovery and turbine-driven fan (System 8).

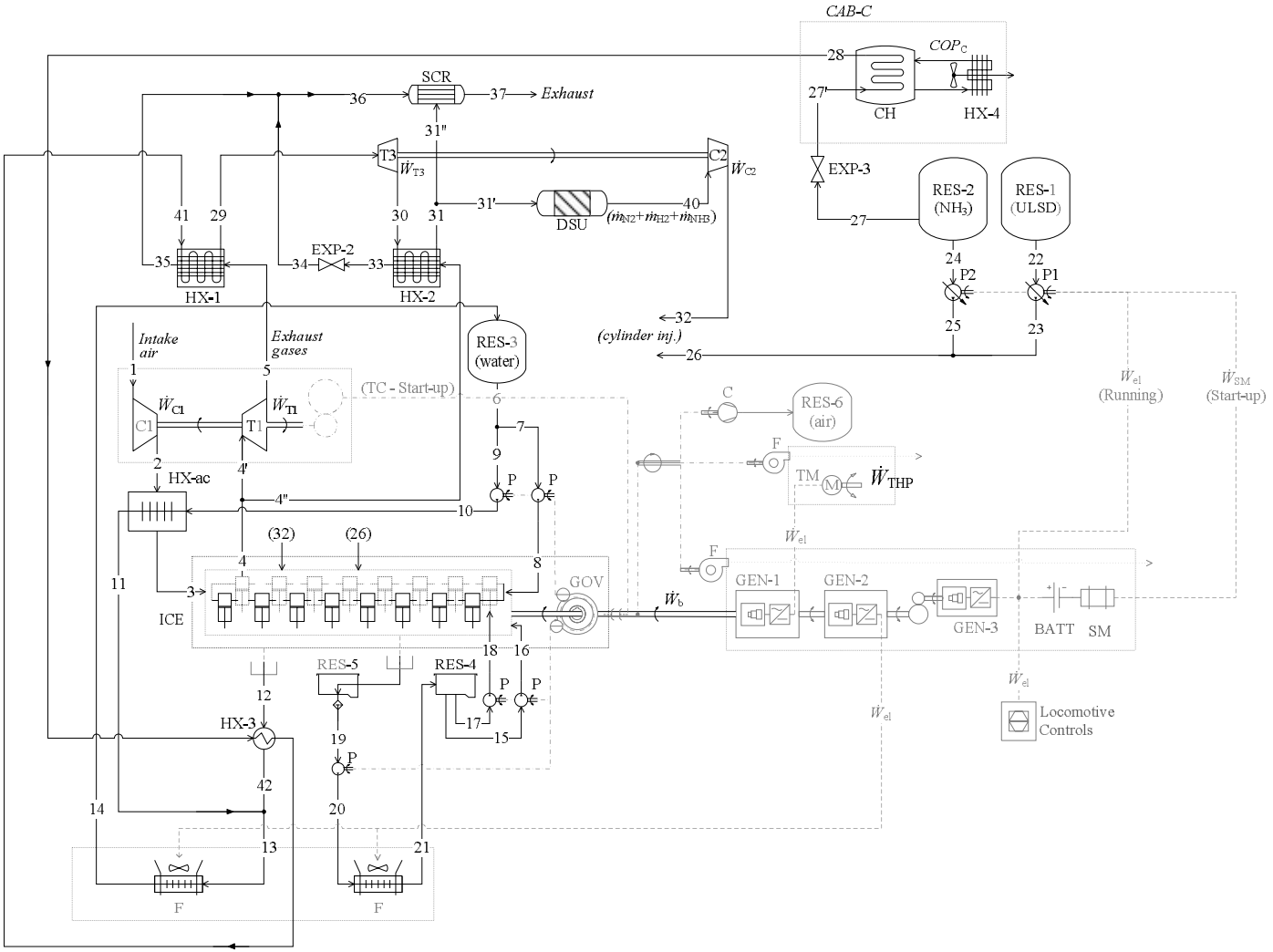

Figure 4.9: NH_3–based cab cooling (System 9).

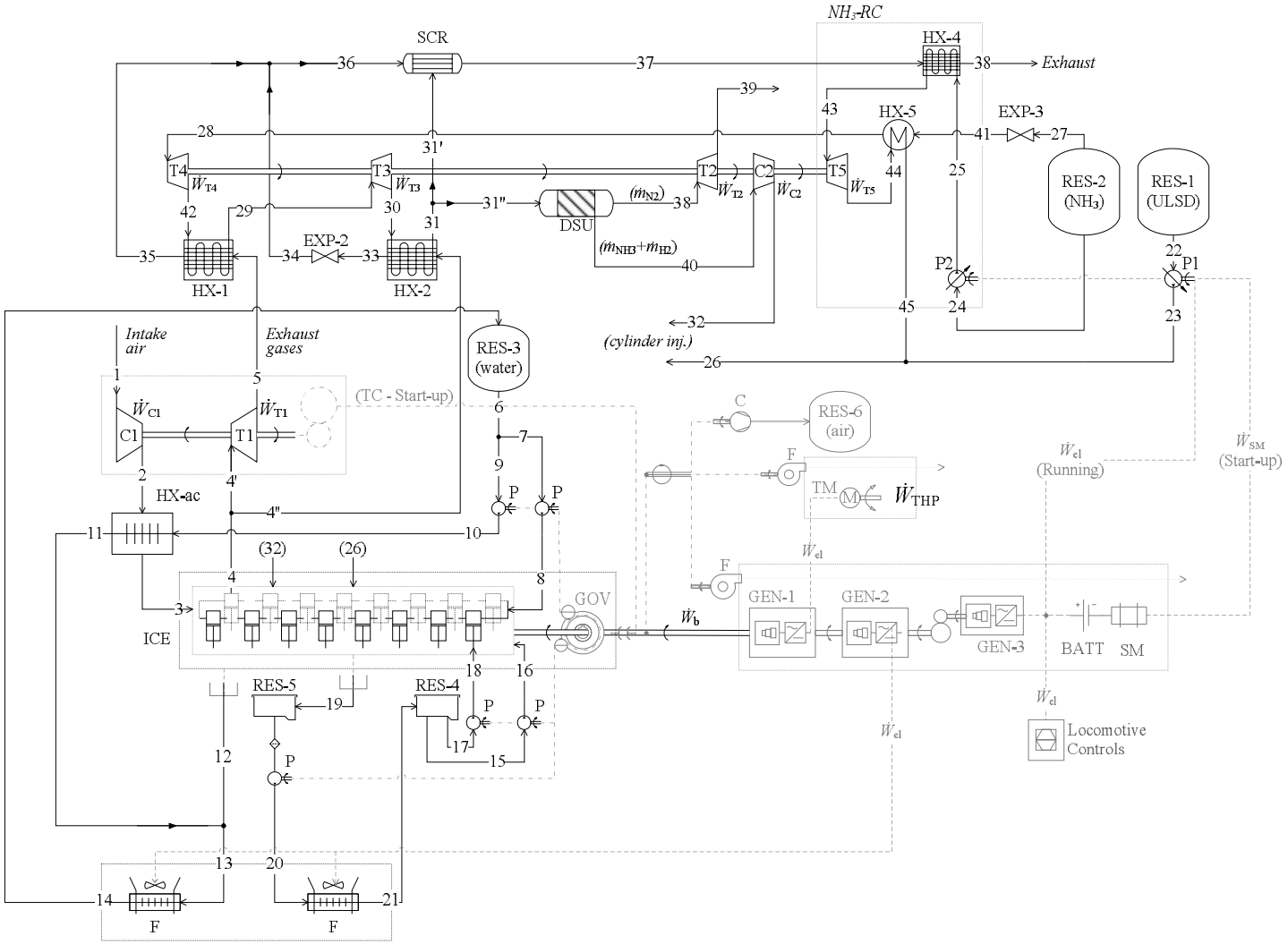

Figure 4.10: Exhaust recovery NH_3–Rankine cycle (System 10).

CHAPTER 5: ANALYSES

5.1 Energy and Exergy Analyses of Locomotive Prime Mover

5.1.1 Thermodynamic Analysis of Locomotive ICE

The locomotive prime mover is powered by a large two-stroke compression ignition (CI) diesel-fueled engine. Modern diesel CI engine cycles operate between upper and lower limits of the Otto and Diesel cycles according to the thermodynamic dual (limited pressure) cycle [54].

The ideal dual cycle, shown qualitatively in Figure 5.1, consists of four major processes: isentropic compression (1–2), heat addition (2–4A), isentropic expansion (4–5), and constant volume heat rejection (5–1). Heat addition occurs in two stages: constant volume (2–3A), and constant pressure (3A–4A).

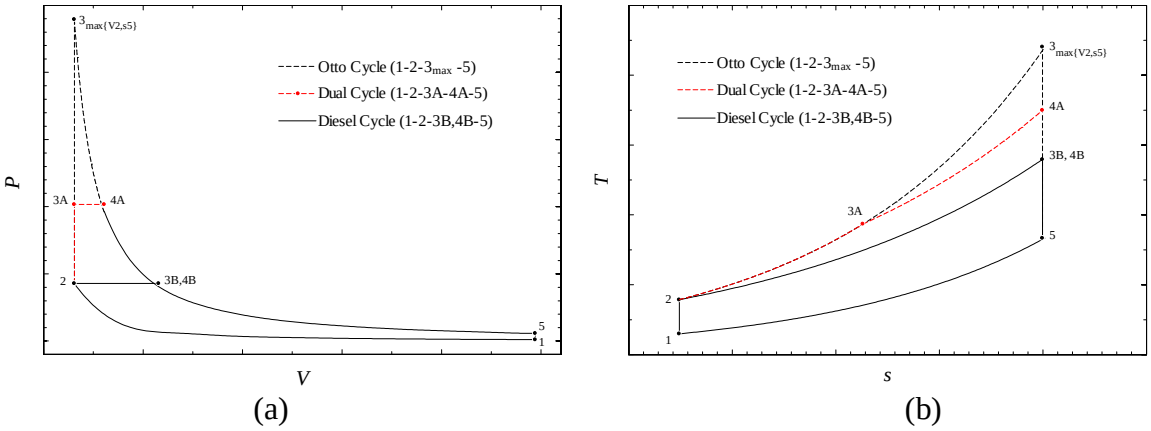

Figure 5.1: Air–standard qualitative (a) *P–V*, and *T–s* diagrams of engine cycles.

The cycle model is developed based on the known engine geometry and operating characteristics, such as, compression ratio (r), cylinder volumes (V_i), rated traction power, and maximum cylinder pressure ($P_{max} = P_3$). The equations describing the cycle processes are outlined in Table 5.1 for the ideal case with at a constant specific heat ratio, $k = 1.35$.

Table 5.1: Dual cycle thermodynamic relationships (k = constant).

State Points	Process	Equations
1—2	Isentropic compression	• $P_2 = P_1 r^k$ • $T_2 = T_1 r^{(k-1)}$
2 – 4	Heat addition at constant volume and constant pressure	• $\dot{Q}_{2-3} = \dot{m}_{\text{exh}} c_{\text{v}} (T_3 - T_2)$ (constant volume process, $V_2 = V_3$) • $\dot{Q}_{3-4} = \dot{m}_{\text{exh}} c_{\text{p}} (T_4 - T_3)$ (constant pressure process, $P_3 = P_4$) • $\dot{Q}_{\text{in}} = \dot{Q}_{2-3} + \dot{Q}_{3-4}$
4 – 5	Isentropic expansion	• $P_5 = P_4 \left(\frac{1}{r}\right)^k$ • $T_5 = T_4 \left(\frac{1}{r}\right)^{(k-1)}$
5 – 1	Heat rejection at constant volume	• $\dot{Q}_{5-1} = \dot{m}_{\text{exh}} c_{\text{v}} (T_5 - T_1)$

Source: [54]

Mass flow of air ($\dot{m}_{\text{a}}$) drawn into the intake manifold is determined based on engine geometry and rated operating conditions, for air composed of 21% oxygen and 79% nitrogen, by the equation:

$$\dot{m}_{\text{a}} = \eta_{\text{v}} \times \left[\frac{P_{\text{im}} \cdot V_{\text{D}} \cdot N_{\text{ICE}} \cdot (0.21 M_{\text{O2}} + 0.79 M_{\text{N2}})}{R_{\text{u}} \cdot T_{\text{im}}}\right] \tag{5.1}$$

where, T_{im} and P_{im} are the temperature and pressure after the turbocharger, V_{D} is the total volume displacement of the combustion engine, N_{ICE} is the rated engine speed iconverted to rev/s units, and the volumetric efficiency, η_{v}, assumed here to be 0.95.

Energy efficiency is defined for the locomotive ICE as the ratio of the useful power produced at rated conditions to the energy input, given by:

$$\eta_{\text{ICE}} = \frac{\dot{W}_{\text{TP}}}{\dot{Q}_{\text{in}}} \tag{5.2}$$

where $\dot{W}_{\text{TP}}$ is the locomotive traction power, and Q_{in} is the heat energy supplied by fuel. For the mixed fueling case, Q_{in} is the sum of the energy input for each fuel, calculated from the mass flow rate and lower heating value of each fuel according to:

$$\dot{Q}_{\text{in}} = \eta_{\text{c}} \cdot \sum(\dot{m}_{\text{f}} \cdot LHV_{\text{f}}) \tag{5.3}$$

where combustion is assumed to be complete ($\eta_{\text{c}} = 1.0$) for the general case. In the model, it is assumed that the summed total energy for the mixed-fuel cases is equivalent to the energy supplied by ULSD in the baseline case to produce the required traction power.

Exergy efficiency of the ICE is similarly defined as the ratio of useful power to the exergy content of the fuel input, given by,

$$\psi_{\text{ICE}} = \frac{\dot{W}_{\text{TP}}}{\dot{E}x_{\text{in}}} \tag{5.4}$$

where the exergy of the fuel input is given by $\dot{E}x_{\text{in}} = \sum\left[\dot{m}_i \cdot \left(ex_{\text{ph}} + ex_{\text{ch}}\right)_i\right]$, and ex_{ph} and ex_{ch} are the physical and chemical exergy values of the supplied fuel(s).

It is useful to define the overall the energy and exergy balances for the ICE in terms of heat and work duties and losses, since a portion of the heat energy losses from the engine represent potential performance gains if applied as process heating in the integrated ammonia systems. Engine cooling requirement is met by the water jacket cooling (Q_{wjc}) and aftercooler (Q_{ac}) systems, where cooling loads are related to the locomotive traction power by the equations:

$$\dot{Q}_{\text{wjc}} = HRR_{\text{wjc}} \cdot \dot{W}_{\text{TP}} \tag{5.5}$$

$$\dot{Q}_{\text{ac}} = HRR_{\text{ac}} \cdot \dot{W}_{\text{TP}} \tag{5.6}$$

where HRR_i terms refer to heat removal rates listed in Table 4.2, given by [51] for a similar locomotive unit and converted to kJ/kW·s units. Total heat removed for engine cooling is the sum of these, $Q_{\text{ec}} = Q_{\text{wjc}} + Q_{\text{ac}}$. The associated thermal exergy rate is evaluated using the general equation for exergy of heat, according to:

$$\dot{E}x_j^Q = \left(1 - \frac{T_o}{T_j}\right)\dot{Q}_j. \quad (5.7)$$

The energy and exergy balances for the ICE are the totals of the work and heat duties, and the system losses produced by the fuel energy supplied, defined by the equations:

$$\dot{Q}_{\text{in}} = \sum(\dot{m}\cdot h)_{\text{exh}} - \sum(\dot{m}\cdot h)_{\text{a}} + \dot{W}_{\text{TP}} + \dot{W}_{\text{acc}} + \dot{Q}_{\text{rec}} + \dot{Q}_{(\text{ac+wjc})} \quad (5.8)$$

$$\dot{E}x_{\text{in}} = \sum(\dot{m}ex)_{\text{exh}} - \sum(\dot{m}ex)_{\text{a}} + \dot{W}_{\text{TP}} + \dot{W}_{\text{acc}} + \dot{E}x_{\text{rec}}^Q + \dot{E}x_{(\text{ac+wjc})}^Q + \dot{E}x_{\text{loss}} + \dot{E}x_{\text{d}} \quad (5.9)$$

where accessory work, $\dot{W}_{\text{acc}}$, represents the power required for cooling and lubrication systems, and the energy loss term, $\dot{E}_{\text{loss}}$, represents heat loss due to friction, mixing heat transfer, and electromechanical losses associated with the conversion of shaft power to electricity, assuming generator conversion efficiency, η_{gen}, of 0.95.

Exergy destruction, $\dot{E}x_{\text{d}}$, is the loss from the engine that is not recovered. The primary sources of exergy destruction are compared using the exergy destruction ratio, given by:

$$ExDR = \frac{\dot{E}x_{\text{d},i}}{\dot{E}x_{\text{d,TOT}}} \quad (5.10)$$

The individual losses, $\dot{E}x_{\text{d,i}}$, include internal and external destructions, where the internal losses are irreversible, and a portion of the external losses may be recovered (i.e. exhaust gases at high temperature).

5.1.2 Modeling of locomotive combustion and emissions

Stoichiometric air-fuel ratios are given on a molar and mass basis for each fuel in Table 5.2, and are used to determine the mass flow rate of fuel, according to $AF_{\text{st}} = \dot{m}_{\text{a}}/\dot{m}_{\text{f.}}$. Carbon dioxide ($CO_2$) emissions produced by fuel combustion are evaluated based on

combustion analysis of the fuel, assuming complete combustion. The flow rate of the combustion product gas mixture is $\dot{m}_{exh} = \dot{m}_a + \dot{m}_f$. The actual combustion is assumed lean ($\varphi_{act} < 1$) to avoid unburned fuel and CO in exhaust products.

Table 5.2: Combustion properties of NH_3, ULSD, and H_2 fuels.

Specification	Ammonia	ULSD	Hydrogen
Molecular formula	NH_3	$C_{12}H_{23}$	H_2
Molecular weight, M_i (kg/kmol)	17.03	167.3	2.016
Stoichiometric air-fuel ratio (molar), a_{st} ($kmol_{air}/kmol_i$)	0.75	17.75	0.5
Stoichiometric air-fuel ratio (mass), AF_{st} (kg_{air}/kg_i)	6.05	14.57	34.2
Stoichiometric energy content (MJ/kg_{mix})	3.4	2.77	2.64
Ignition limits (%-vol. in air)	16-25	0.6-5.5	4-75
Adiabatic flame temperature (°C)	1850	1977	2000
Auto-ignition temperature (°C)	651	~ 225	571

Source: [59]

The stoichiometric reaction equations are given in Table 5.3 for each fuel. For mixed fueling of NH_3-ULSD and NH_3-ULSD-H_2, the equations are combined based on the fraction of fuel energy provided by NH_3 to maintain the required energy to produce the rated traction horsepower of the locomotive.

Table 5.3: Stoichiometric combustion reactions.

Fuel	Molecular Formula	Combustion Reaction
ULSD	$C_{12}H_{23}$	$C_{12}H_{23} + 17.75 \cdot (O_2 + 3.76 \cdot N_2) \rightarrow 12 \cdot CO_2 + 11.5 \cdot H_2O + 17.75 \cdot (3.76) \cdot N_2$
Ammonia	NH_3	$NH_3 + 0.75 \cdot (O_2 + 3.76 \cdot N_2) \rightarrow 1.5 \cdot H_2O + 3.32 \cdot N_2$
Hydrogen	H_2	$H_2 + 0.5 \cdot (O_2 + 3.76 \cdot N_2) \rightarrow H_2O + 0.5 \cdot (3.76) \cdot N_2$

The current GHG emission factors, listed in Table 5.4, are compared to combustion analysis results for CO_2 emissions based on the volume of diesel fuel consumed for the fuel mixture. Fuel feedstock is taken into consideration to assess the life cycle emissions of NH_3 and diesel, to assess the environmental impact associated with producing and consuming the fuels. The fuel and feedstock emissions are provided in Table 5.5 for NH_3 and ULSD, with natural gas and electricity from hydro as the feedstock energies for NH_3 production. It should be noted that this does not include CO_2 recovery, which can significantly reduce total emissions.

Table 5.4: Diesel fuel emission factors and global warming potential of GHG's (2010).

Gas Species	Emission Factor, EF_i (kg/L)	Global Warming Potential, GWP_i
Carbon Dioxide (CO_2)	2.66300	1
Methane (CH_4)	0.00015	21
Nitrous Oxide (N_2O)	0.00110	310
Carbon Dioxide Equivalent $CO_{2\ eq.}$	3.00715 [a]	--

a. Emission factor, $EF_{CO2\ eq.}=\Sigma(EF_i \cdot GWP_i)$
Source: [17]

Table 5.5: Fuel and feedstock related GHG emissions (kg $CO_{2,eq}$/L).

Fuel	**NH_3**	**Diesel fuel (ULSD)**
Feedstock	Natural gas	Crude oil
Production/Feedstock	1.0831	0.4227
Fuel Combustion	0	2.668
TOTAL	**1.0831**	**3.0908**

Source: [29]

5.1.3 Modeling of CAC emission reductions by selective catalytic reducer (SCR)

The CAC emissions from diesel fuel consumption are calculated using the current emission factors listed in Table 5.6, with the exception of sulfur dioxide (SO_2), which is determined from the sulfur content of diesel fuel by the equation:

$$EF_{SO2} = \rho_{ULSD} \cdot \left(\frac{M_{SO2}}{M_S}\right) \cdot S_{ppm} \times 10^{-6} \times f_{c,SO_2} \quad (5.11)$$

thus, for ULSD containing 15-ppm sulfur [19], liquid density ρ_{ULSD} = 850 kg/m^3, and an assumed conversion factor of $f_{c,SO2}$ = 0.98 (S $\rightarrow SO_2$) [50], the resulting emission factor $EF_{SO2} = 0.025\ g/L$.

Table 5.6: Diesel locomotive CAC emission factors.

Gas Species	Emission Factor, EF_i (kg/L)	
	Passenger	**Freight**
Particulate Matter (PM)	0.00118	0.00123
Hydrocarbon(s) (HC)	0.00223	0.00238
Nitrogen Oxides (NO_x)	0.05623	0.04923
Carbon Monoxide (CO)	0.00703	0.00706

Source: [17]

The CAC emission reduction by the SCR unit is modeled based on manufacturer data for a compact SCR installed in an operational EMD 12-710G3 diesel engine [51]. The emission reductions listed in Table 5.7 are provided by the manufacturer in terms of percent reduction from baseline locomotive operation without SCR. These reductions are applied to diesel combustion emissions, which are determined using current Tier 2 emission standards to indicate the improvement potential of utilizing SCR in locomotives in baseline operation.

Table 5.7: Compact SCR™ locomotive emission reduction (g/BHP·hr).

Duty-Cycle	Standard	HC	NO_x	PM	CO
Line Haul	Compact SCR™ reduction	> 90%	71%	61%	82%
Switch	Compact SCR™ reduction	> 90%	61%	57%	93%

Sources: [51]

The mass flow rate of NO_x is determined by the fraction of ULSD supplied, and the NO_x emission factor for current CAC emission limits, provided in Table 5.6. It is assumed that the molar ratio of supplied NH_3 to NO_x is 1:1, according to the main reaction:

$$4\,NH_3 + 4\,NO + 4\,O_2 \rightarrow 6\,H_2O + 4\,N_2 \tag{5.12}$$

Ammonia combustion is assumed to be complete; however, for the practical case where some NO_x results in the NH_3 combustion reaction, emissions may be easily controlled by adjusting the supply of NH_3 to the SCR, while also taking care to ensure that NH_3 slip does not exceed the EPA limit of 2–10 ppm NH_3 in the exhaust stream.

5.1.4 Modeling of Ammonia Decomposition

Hydrogen produced by thermo-catalytic decomposition of ammonia in the DSU is used as a combustion fuel to further reduce the diesel fuel consumption, and to assist the combustion of ammonia in the ICE. The decomposition occurs according to the reaction:

$$NH_3 \xrightarrow{\Delta h_d} \frac{3}{2}H_2 + \frac{1}{2}N_2 \quad (5.13)$$

where the heat of the endothermic reaction, Δh_d, is determined as a function of temperature using the Shomate equation given by the NIST Chemistry WebBook [60], for a temperature range of 300–800°C, following the methodology described by [3]. The decomposition may be written based on the dissociation fraction, x_d, describing the amount of each gas species in the product gas mixture by:

$$NH_3 \rightarrow \frac{3x_d}{2}H_2 + \frac{x_d}{2}N_2 + (1 - x_d)NH_3 \quad (5.14)$$

The heat required for the reaction is given by [53] in terms of the enthalpy change of ammonia to raise its temperature to the required level for decomposition, and the extent of the dissociation, given by:

$$\Delta h_{DSU}(T) = h_o(T) - h(T_o) + x_d \cdot \eta_d \cdot \Delta h_d(T) \quad (5.15)$$

where the efficiency of the decomposition process, η_d, is assumed to be 0.9 [3].

General operating characteristics for the decomposition unit considered for the proposed systems are given Table 5.8. To obtain the temperature necessary for the DSU reaction in the proposed systems, a portion of the exhaust stream is used to heat the ammonia to a temperature within the given range. The further integration of the NH_3 supply and N_2 product streams within the propulsion systems; such as, engine cooling (heat recovery) and expansion work, are described in the technology by [7], and applied to the various locomotive engine systems.

Table 5.8: DSU characteristics.

Chemical Reaction Equation	$NH_3 \rightarrow 1/2\ N_2 + 3/2\ H_2$
Standard Enthalpy of Reaction, ΔH_{NH3} (kJ/mol)	45.90
Operating Temperature, T_{DSU} (°C)	350–525

5.2 Analyses of Ammonia-Powered Locomotive Systems

5.2.1 Thermodynamic Analysis of Subsystem Components and Processes

Major components applied throughout the systems for both the existing and proposed locomotive propulsion processes include: compressors, turbines, heat exchangers, and pumps. Balance equations for these components are given in Table 5.9, based on mass, energy, entropy, and exergy of inlet and exit streams. The component efficiency is given in terms of the isentropic efficiency of work input/output components, and effectiveness of heat exchange processes.

Table 5.9: Mass, energy, entropy, and exergy balance equations of common components.

Component	Balance Equations[a]	Component Efficiency
Compressor	• $\dot{m}_i = \dot{m}_e$ • $\dot{m}_i h_i + \dot{W}_j = \dot{m}_e h_e$ • $\dot{m}_i s_i + \dot{S}_{\text{gen},j} = \dot{m}_e s_e$ • $\dot{m}_i ex_i + \dot{W}_j = \dot{m}_e ex_e + \dot{E}x_{\text{d},j}$	• $\eta_{\text{C,s}} = (h_{e,s} - h_i)/(h_e - h_i)$ • $h_{e,s} = h(P_e, s_i)$
Turbine	• $\dot{m}_i = \dot{m}_e$ • $\dot{m}_i h_i = \dot{m}_e h_e + \dot{W}_j$ • $\dot{m}_i s_i + \dot{S}_{\text{gen},j} = \dot{m}_e s_e$ • $\dot{m}_i ex_i = \dot{m}_e ex_e + \dot{W}_j + \dot{E}x_{\text{d},j}$	• $\eta_{\text{T,s}} = (h_i - h_e)/(h_i - h_{e,s})$ • $h_{e,s} = h(P_e, s_i)$
Pump	• $\dot{m}_i = \dot{m}_e$ • $\dot{m}_i h_i + \dot{W}_j = \dot{m}_e h_e$ • $\dot{m}_i s_i + \dot{S}_{\text{gen},j} = \dot{m}_e s_e$ • $\dot{m}_i ex_i + \dot{W}_j = \dot{m}_e ex_e + \dot{E}x_{\text{d},j}$	• $\eta_{\text{P,s}} = (h_{e,s} - h_i)/(h_e - h_i)$ • $h_{e,s} = h(P_e, s_i)$
Heat Exchanger	• $\sum \dot{m}_i = \sum \dot{m}_e$ • $\sum \dot{m}_i h_i = \sum \dot{m}_e h_e + \Delta\dot{Q}_j$ • $\sum \dot{m}_i s_i + \dot{S}_{\text{gen},j} = \sum \dot{m}_e s_e + \frac{\Delta\dot{Q}_j}{T_{\text{o}}}$ • $\sum \dot{m}_i ex_i = \sum \dot{m}_e ex_e + \dot{E}x_j^Q + \dot{E}x_{\text{d},j}$	• $\varepsilon_{\text{HX}} = \dot{Q}_{\text{useful}}/\dot{Q}_{\max}$ • $\dot{Q}_{\max} = (\dot{m}_i c_{\text{p},i})_{\min} \cdot (T_{\max} - T_{\min})$
Expansion valve	• $\dot{m}_i = \dot{m}_e$ • $h_i = h_e$ • $\dot{m}_i s_i + \dot{S}_{\text{gen},j} = \dot{m}_e s_e$ • $\dot{m}_i ex_i = \dot{m}_e ex_e + \dot{E}x_{\text{d},j}$	--

a. Balance equations refer to inlet (i) and exit (e) streams of j-component.

5.2.2 Energy and Exergy Efficiencies

To compare the performance of the ammonia-powered locomotive systems to the baseline performance, it is necessary to quantify performance gains from the additional work and heat recovery processes integrated for each configuration. Utilization efficiencies (η_u) are defined for the system(s) using on the general equation:

$$\eta_u = \frac{\dot{W}_{TP} + \dot{W}_{net} + \dot{Q}_{DSU} + \sum \dot{Q}_{useful}}{\dot{Q}_{in}} \tag{5.16}$$

where the net work, $\dot{W}_{net}$, includes the additional work produced/consumed by the integrated NH_3 system components (turbines, pumps, and compressors). For systems integrating H_2–production, the energy required to heat and decompose the NH_3 at the assumed dissocation temperature is calcuated based using $\Delta h_{DSU}(T)$, as described in Eq. 5.15, for the assumed dissociation fraction and NH_3 flow rate. and included in the utilization efficiency as a heat recovery. The general equation for the exergetic utilization efficiency of the systems is:

$$\psi_u = \frac{\dot{W}_{TP} + \dot{W}_{net} + \left(1 - \frac{T_0}{T_{DSU}}\right) \cdot \dot{Q}_{DSU} + \sum \dot{E}x^{Q}_{useful}}{\dot{E}x_{in}} \tag{5.17}$$

For integrated cooling systems that require work input (i.e., cab cooling in System 9), a coefficient of performance (COP_c) is applied to simplify calculation of the required work input ($\dot{W}_{in}$), given by:

$$COP_c = \frac{\dot{Q}_c}{\dot{W}_{in}} \tag{5.18}$$

where $\dot{W}_{in}$ represents pump and/or compressor duties to power cooling systems. An assumed COP_c value of 2.0 is applied, as suggested by [4] as a typical average for engine and air cooling systems.

5.2.3 Cost Analysis

To assess the economic feasibility of the ammonia-powered systems, additional equipment costs and total fuel cost are evaluated for each system. Base equipment cost data is collected from various sources for similar equipment where available, and an estimate of the present value purchase cost (C_P) is calculated according to:

$$C_P = C_0 \cdot \left(\frac{CE_P}{CE_0}\right) \cdot \left(\frac{S_P}{S_0}\right)^n \tag{5.19}$$

where C_0 is the reference (base) equipment cost, and the terms *CE* and *S* refer to the equipment cost index and size (capacity) for the base and present years. The historical and present *CE* index values of are obtained from [56]. The exponent *n* is an equipment-specific factor representing economy of scale, which is given a value of $n = 0.6$ for the cost comparison.

5.3 Sustainability Assessment

There are two major system frameworks to consider when assessing the overall sustainability of an ammonia powered locomotive – the locomotive prime mover, and the fuel product. These frameworks are depicted in Figure 5.2, indicating the major drivers affecting the performance of each system. While these frameworks may each be addressed separately, they are ultimately linked; since the sustainability of locomotive operation is affected by both the propulsion system efficiency, and the fuel/energy resource sustainability in terms of generated GHG and CAC emissions.

Impact factors are used to evaluate the results of the energy, exergy, environmental, and economic analyses, and assess the performance of the proposed systems in terms of overall sustainability and feasibility. These factors provide a method for performance comparison from various perspectives in order to make objective recommendations for system selection.

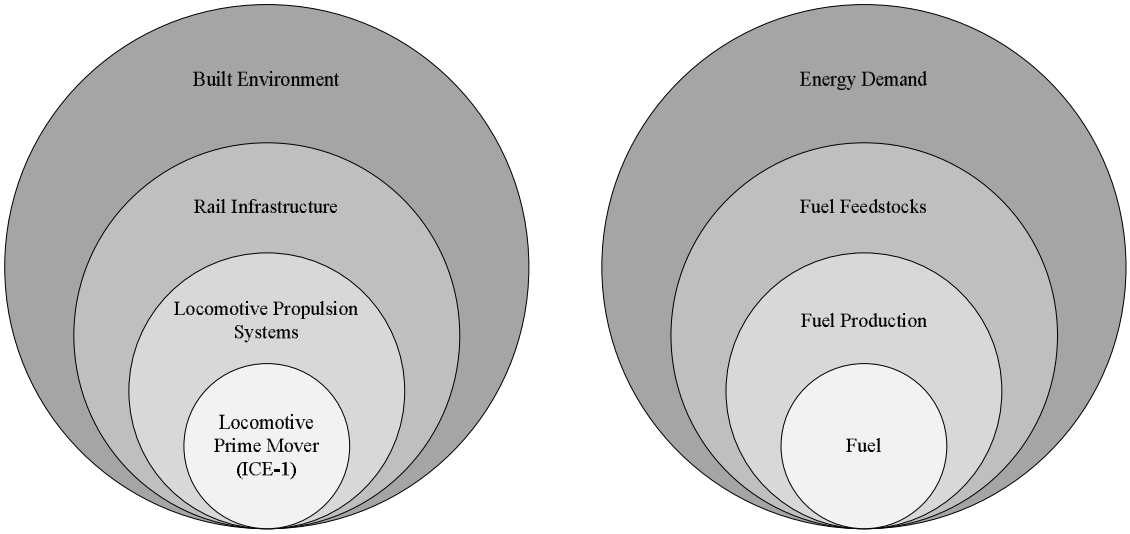

Figure 5.2: Framework (a) Locomotive Prime Mover, and (b) Fuel Product (adapted from [57])

Exergy efficiency is related to overall sustainability of each system by the Sustainability Index (*SI*), using the equation described in [58], according to:

$$SI = \frac{1}{1-\psi} \tag{5.20}$$

where the value of *SI* indicates how effectively a process or system utilizes the energy resource, with higher values indicating better sustainability. Taking the inverse of *SI* gives the Depletion Factor (D_P), which indicates the degree of environmental impact by the total exergy destruction of the system by the equation:

$$D_P = \frac{\dot{E}x_d}{\dot{E}x_f} \tag{5.21}$$

where higher values for D_p indicate that there are significant destructions within the system that may be reduced to improve performance of a system or compnent.

The environmental impact of alternative fueling on GHG emissions produced in fuel combustion is described by a Greenization Factor (*GF*), which indicates the degree of CO_2 reduction, given by:

$$GF = \frac{\dot{m}_{CO_2,ref} - \dot{m}_{CO_2,Sys_i}}{\dot{m}_{CO_2,ref}} \tag{5.22}$$

where the reference case is that of diesel-only combustion. Based on the assumption of equivalent total fuel energy input for the mixed fueling cases, the reduction in CO_2 is determined for each fuel blend. The Greenization Factor is a useful parameter for the comparison of the fuel blends with the base diesel case, and with respect to locomotive emissions reduction, may be considered in decision making and justification for the use of ammonia fueling.

For system comparison from a cost perspective, the estimated additional equipment costs and change in fuel cost are compared to the diesel baseline case for each system. For the fuel cost factor, the current price of diesel and ammonia is considered, and the change in cost is calculated by:

$$CF_{fuel} = 1 - \frac{C_{NH3,mixed}}{C_{ULSD}} \tag{5.23}$$

Regarding the equipment cost, the increased capital required for each of the systems is added to the base price of the locomotive, given by:

$$CF_{eq} = 1 - \frac{C_{new} + C_{ref}}{C_{ref}} \tag{5.24}$$

where C_{ref} is the present value of the locomotive considered, and C_{new} is the sum of the costs for the additional components.

CHAPTER 6: RESULTS AND DISCUSSION

6.1 Locomotive System Results

General Assumptions for Systems

The prime mover sizing details for the EMD locomotive engine used as the baseline system are given in Table 4.2, including the heat removal rate requirements for the cooling water circuits. These are used for each of the systems analyses, and are based on information from previous demonstration projects and manufacturer information for similar locomotives. The following assumptions are made in the analysis:

- Locomotive is assumed to be operating at rated conditions,
- All processes and systems operate at steady state,
- Component pressure losses are not considered,
- Additional turbines and compressor components have an isentropic efficiency of η_s = 0.75

6.1.1 Locomotive ICE Results

The thermodynamic cycle for the two-stroke compression ignition engine is shown in Figure 6.1 for the baseline case at rated locomotive operation, producing 2983 kW (4000 hp) of traction power after conversion to electric power in the generator with an assumed conversion efficiency of 0.95 [59]. The brake specific fuel consumption is calculated to be 0.255 kg/kW·h for the lean case (φ = 0.9), which is in agreement with other studies for the same locomotive engine [32,59,60]. Heat is partially recovered from the exhaust gases leaving the ICE by the turbocharger unit; intake air is compressed then cooled (in the aftercooler) prior to entering the engine intake manifold to increase the total mass flow rate of air into the engine.

The engine directly supplies shaft power to the engine cooling system components; including pumps for aftercooler and water jacket cooling circuits, and cooling fans for radiator cooling, and the useful work is the traction power of the locomotive.

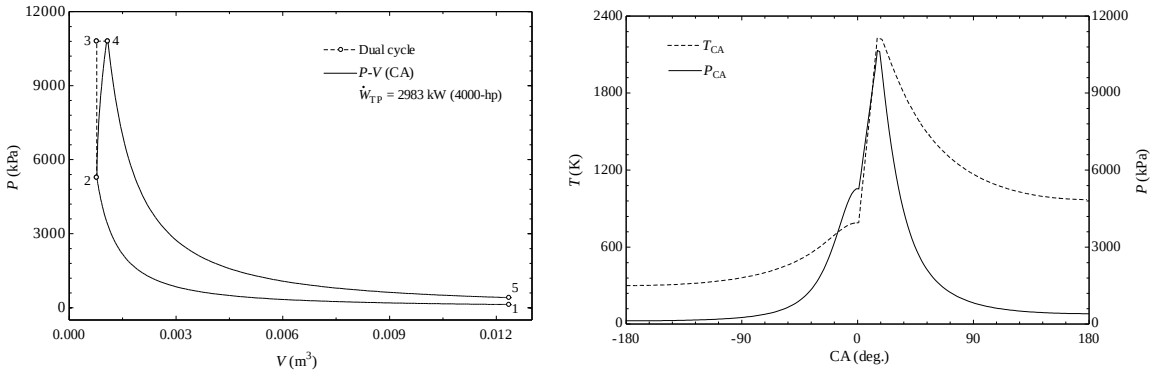

(a) (b)

Figure 6.1: Baseline ICE, (a) two-stroke dual cycle, and (b) cylinder temperature and pressure for one crankshaft revolution.

The energy balance is given in Figure 6.2, where the exhaust heat energy (Q_{exh}) is for the gases following TC heat recovery. The heat rejection from the engine is primarily associated with the aftercooler and water jacket cooling processes, and the exhaust gas stream, accounting for nearly two thirds of the total energy.

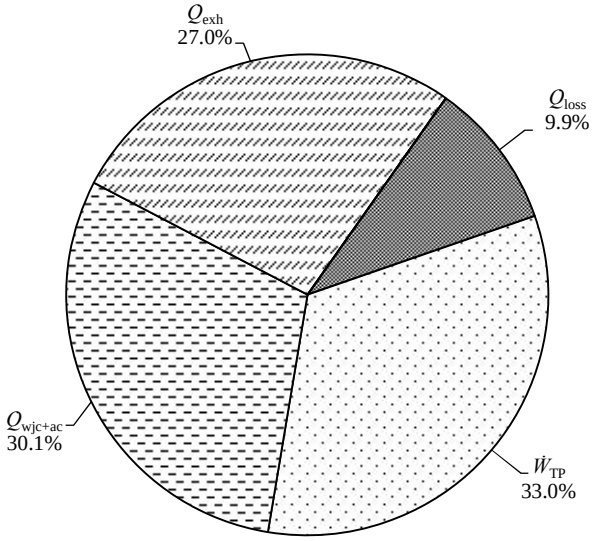

Figure 6.2: Energy balance of locomotive ICE (Q_{in} = 9050 kW).

To evaluate heat recovery options for the NH_3 systems, it is necessary to consider the quality of the heat source using exergy analysis. While the total energy of a given source (i.e. exhaust gas and coolant streams) may indicate a potential for recovery, its temperature is a limiting factor – particularly for mid- to low-temperature heat sources.

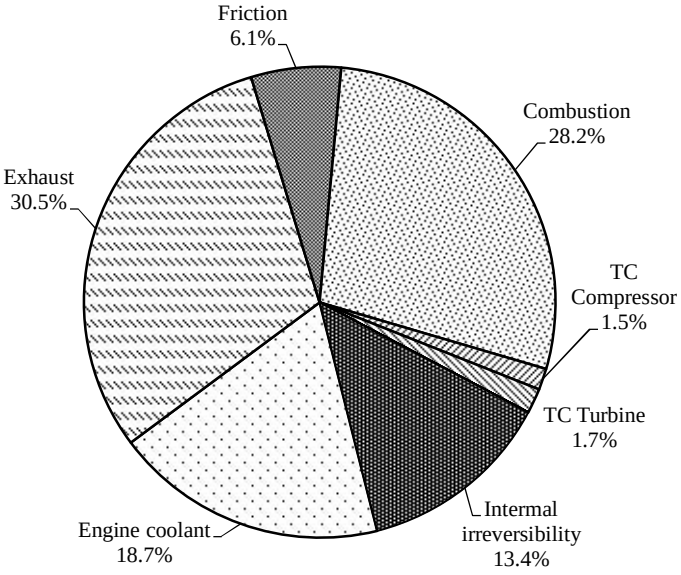

Figure 6.3: Exergy destruction ratios of internal and external losses for diesel ICE.

6.1.2 Ammonia-fueled locomotive emissions modeling results

Emission reductions achieved by co-fueling with NH_3 are plotted against the fraction of NH_3 fueling in the subsequent figures. GHG emissions are shown in Figure 6.4, considering the production related emissions for NH_3 production by natural gas with and without CO_2 capture. The results clearly indicate the impact of production CO_2 on the environmental advantage of NH_3, and support the use of renewable energy systems for the production of NH_3 fuel to provide carbon-free (or carbon-minimum) fuel.

Reductions for CAC emissions with and without SCR are shown in the Figure 6.5 to Figure 6.8. Tier 2, 3, and 4 emission limits—previously listed in Table 2.2—are included in the plots for comparison, and to give an indication of the benefit of investing in the alternative fuel and SCR technologies, since currently optional locomotive retrofits

and upgrades to reduce emissions will eventually become necessary as increasingly strict limits are imposed.

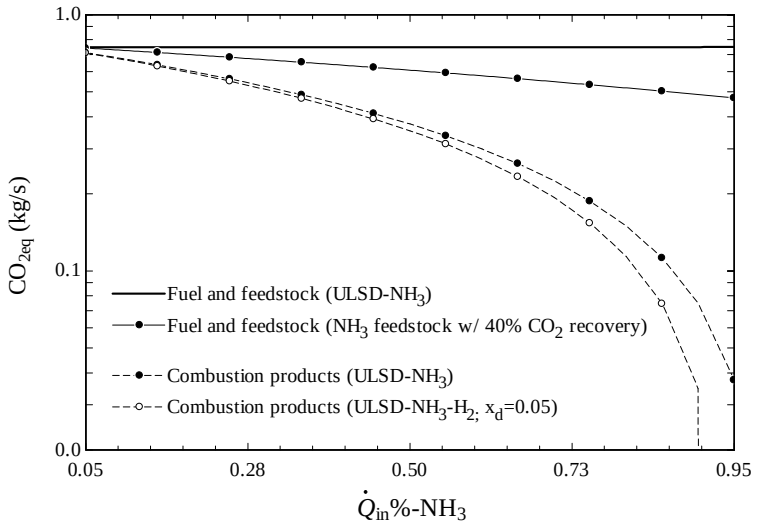

Figure 6.4: GHG's including fuel production (lifecycle) emissions and combustion-only for varying NH_3-ULSD fuel blends.

The level of NO_x emissions (Figure 6.5) are well below Tier 2 and Tier 3 limits, and even without SCR the emission reductions are achieved with approximately 50% of fuel input supplied by NH_3.

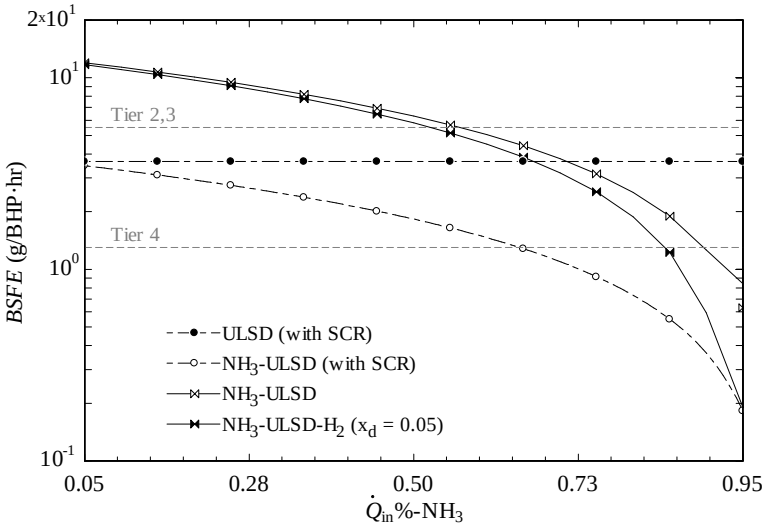

Figure 6.5: Brake specific NO_x emissions for varying NH_3 fuel-energy fraction.

Similar results are found for the PM emissions (Figure 6.6). The range of CO emissions indicates reduction below Tier 2, 3, and 4 limits for all of the fuel cases considered, with the maximum reduction achieved with NH_3-ULSD fueling and SCR.

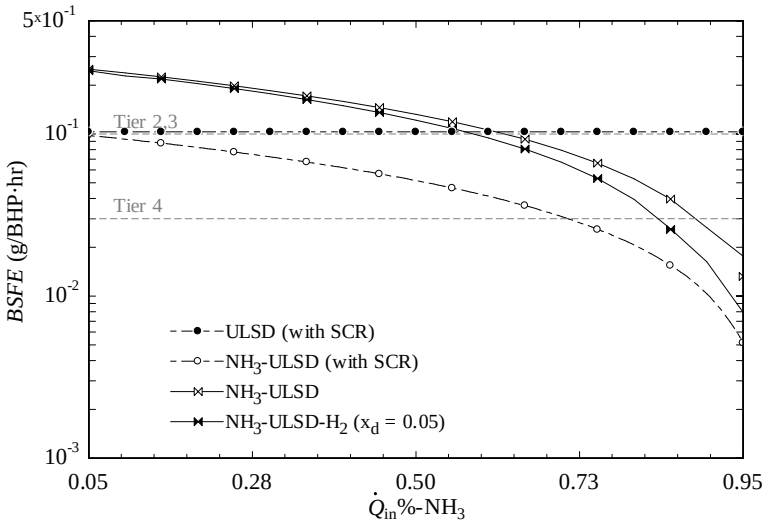

Figure 6.6: Brake specific PM emissions for varying NH_3 fuel-energy fraction.

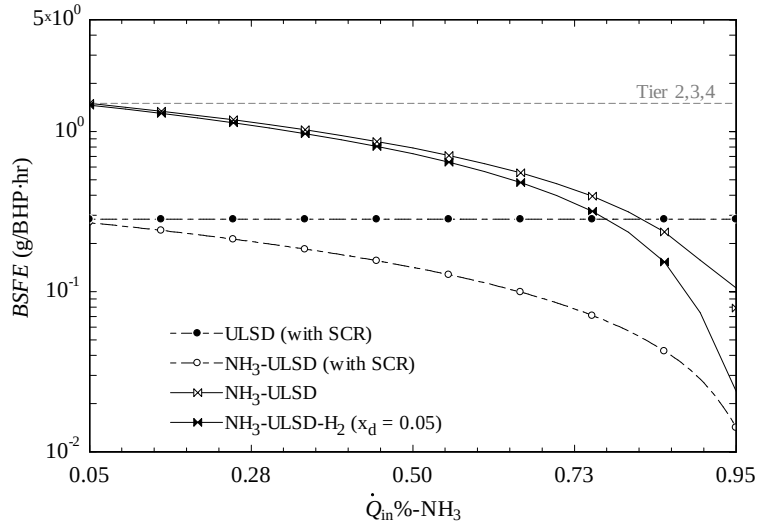

Figure 6.7: Brake specific CO emissions for varying NH_3 fuel-energy fraction.

HC emissions reductions are shown in Figure 6.8, showing emissions below Tier 2 and Tier 3 limits achieved with approximately 50% of fuel input supplied by NH_3 without the SCR unit, and approach Tier 4 limits for the mixed fuel case with SCR integration for the same NH_3 fuel energy fraction.

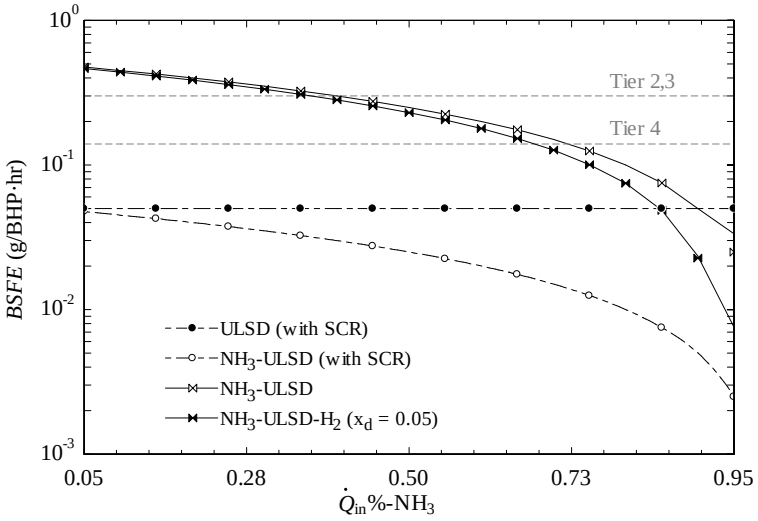

Figure 6.8: Brake specific HC emissions for varying NH_3 fuel-energy fraction.

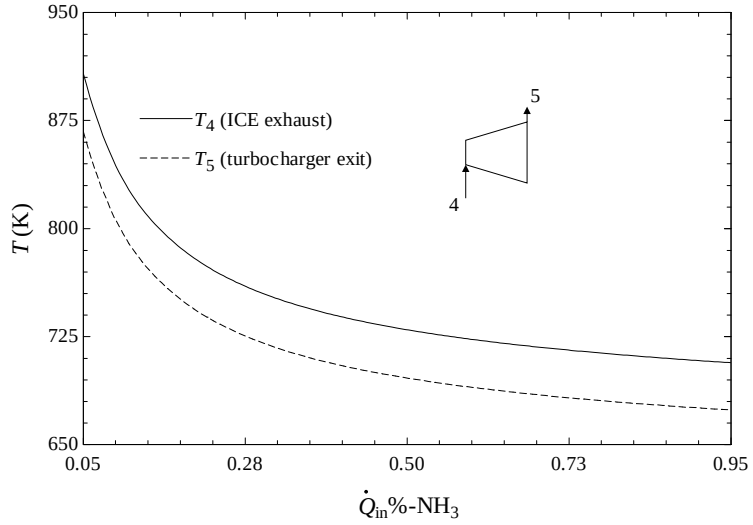

Figure 6.9: ICE and turbocharger exhaust temperatures for varying NH_3 fuel-energy fraction.

6.1.3 Alternative Locomotive System Results

Based on the emission reductions, and the exhaust temperature to maintain operation of the DSU and SCR units during rated locomotive operation, a fraction of 50% NH_3 fueling is assumed for the systems. The resulting fuel flow rates are listed in Table 6.1 for each fuel.

Table 6.1: Fuel mass flow rates ($Q_{in} = Q_{ULSD}$).

Fuel/Blend no.	System	%- Q_{in} NH_3	x_d	$\dot{m}_{ULSD}$	$\dot{m}_{NH3}$ [a]	$\dot{m}_{H2}$
				(kg/s)	(kg/s)	(kg/s)
1	1	100%-ULSD	0.0	0.212	--	--
2	2	50%-NH_3	0.0	0.106	0.241	--
3	3-10	50%-NH_3	0.05	0.0996	0.241	0.00225

a. Flow rate of NH_3 fuel only (does not include NH_3 supplied to the SCR).

System 2 Results: Ammonia-Diesel Fueling with NO_x Reduction (SCR)

The NH_3 processes for System 2 are shown in Figure 4.2, and include pressure reduction by throttling (state points 27–28) of the SCR-NH_3 supply to the operating pressure of the SCR unit, exhaust heat recovery to raise the temperature of NH_3 prior to injection into the SCR, and NH_3 fuel preheating prior to combustion. The expansion, and heat recovery processes are described in Section 4, and indicated in Figure 6.10 on a *T-s* diagram for ammonia. Liquid NH_3 is drawn from the tank at point 27 and throttled to atmospheric pressure at point 28. The liquid-vapour mixture is heated by exhaust gases in the exhaust recovery heat exchanger (HX-1) to the required temperature for the SCR at point 29.

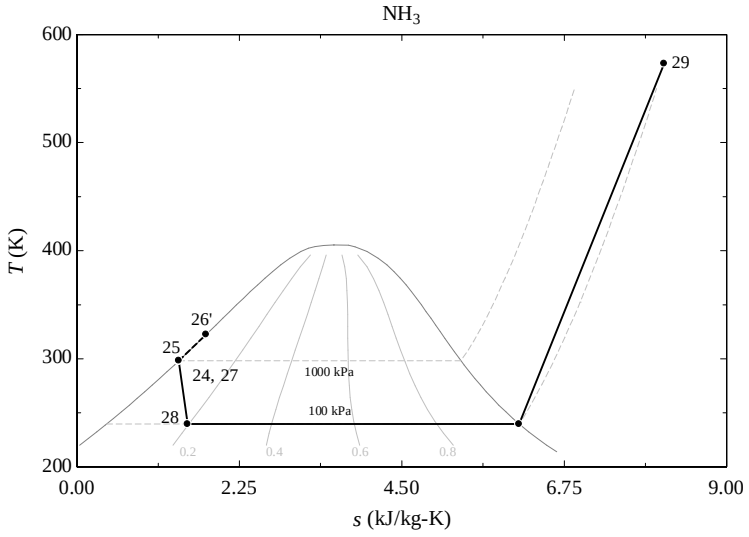

Figure 6.10: *T-s* diagram of NH_3 processes for System 2 (%-Q_{in} NH_3=50).

If dual-fuel injection technology for liquid-gas fueling is integrated, the level of preheating (and therefore, heat recovery) can be extended to saturated or superheated

conditions for the NH_3 fuel stream, with associated heat recoveries ranging from approximately 250–425 kW-thermal. Four scenarios are considered; SCR-NH_3 supply preheating (Scenario A), SCR-NH_3 + NH_3 fuel preheating to saturated liquid state (Scenario B), SCR-NH_3 + NH_3 fuel preheating to saturated vapour state (Scenario C), and SCR-NH_3 + NH_3 fuel preheating to superheated vapour state (Scenario D).

Table 6.2: System 2 NH_3-process results (%-$\dot{Q}_{in}$ NH_3=50).

Process		**System 2**
NH_3 fuel pump, $\dot{W}_{P2}$ (kW)		3.60
Exhaust heat recovery, $\dot{Q}_{rec,HX1}$ (kW)	SCR supply preheat (scenario A)	7.48
	SCR supply + liquid fuel preheat (scenario B)	122.6
	SCR supply + vapour fuel preheat (scenario C: saturated vapour)	262
	SCR supply + fuel preheat (scenario D: superheated)	437

For Case B, which does not require specialized fueling equipment for gas-liquid mixtures, the energy balance of the ICE is shown in Figure 6.11 for the heat recovery in HX-1. The exhaust energy is slightly lower than the baseline case due to lower exhaust temperature for the NH_3-ULSD fuel blend.

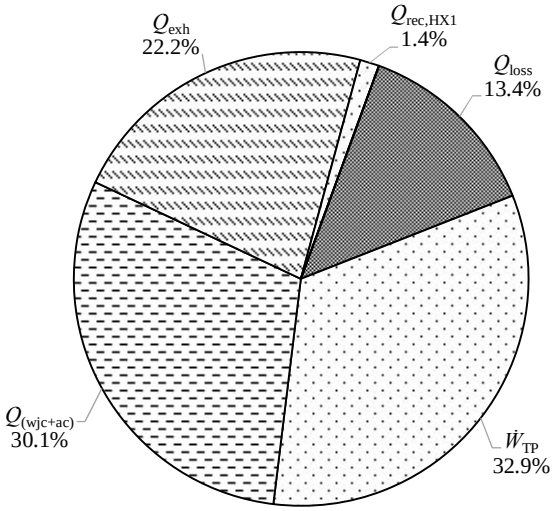

Figure 6.11: System 2 energy balance ($\dot{Q}_{in}$ = 9050 kW).

The exergy efficiency for System 2 is calculated to be 31.4%, and the exergy destructions are described in Figure 6.12 using the exergy destruction ratios for the major points of loss. There is a higher rate of exergy destroyed in combustion than in the diesel-

only case, due to the increased amount of energy required to burn NH_3, which has a lower flame speed and higher value for minimum ignition energy than diesel fuel. The internal (friction) losses are also higher, due to the higher volume flow of fuel than in the diesel case increasing the losses to fluid flow and pumping.

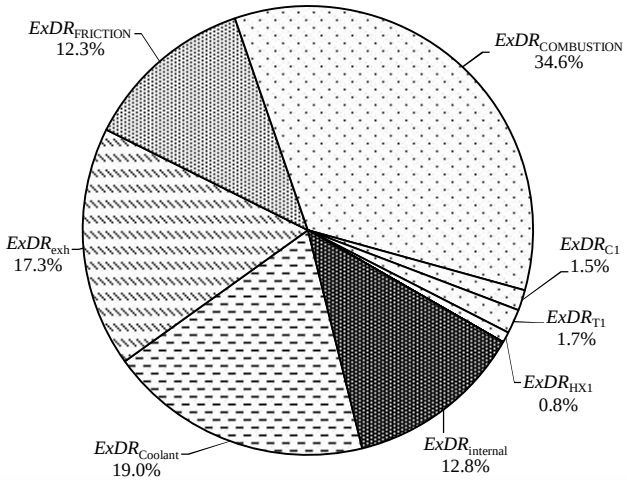

Figure 6.12: Exergy destruction ratios of internal and external losses for System 2.

If a wider range of NH_3 fueling is considered, fuel pre-heating in HX-1 is limited by the minimum exhaust temperature for SCR operating conditions (set to 300 °C). Superheating of the NH_3 gas is limited to temperatures below the autoignition temperature of NH_3. The energy and exergy efficiencies for four scenarios are shown in Figure 6.13 for a range of NH_3-ULSD fuel blends.

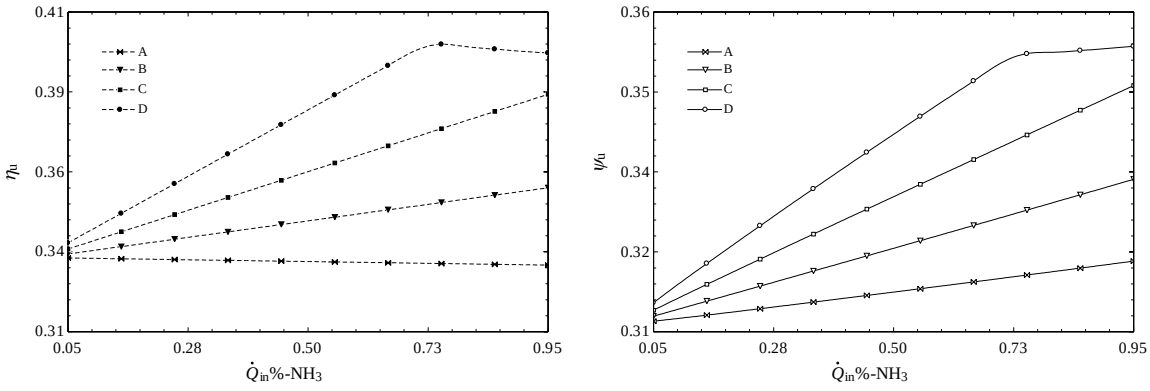

(a) (b)

Figure 6.13: (a) Energy and (b) exergy utilization efficiencies for Scenarios A-D.

Systems 3 and 4: Thermal NH_3 Decomposition with N_2 Separation and Expansion

System 3 introduces the thermal DSU, and an additional exhaust recovery heat exchanger (HX-2). The exhaust gas from the ICE is split into two streams, with a fraction directed to the turbine (T1) to maintain the required turbocharger operation, and the remaining fraction diverted to heat exchanger HX-2, to provide the final heating stage for the NH_3 stream. The total NH_3 fuel supply stream is sent through the heat exchangers to maximize the heat recovery. Figure 6.14(a) indicates the operations for Systems 3 and 4 integrated NH_3 processes. System 4 operates in a similar manner to System 3, but introduces the option of additional work production by expansion of the N_2 product stream, shown in Figure 6.14(b). Following decomposition, N_2 gas is expanded in turbine T1 to produce additional work ($\dot{W}_{T2}$). The DSU in this system is assumed to operate at 200 kPa, with the final pressure after the N_2-expansion process at atmospheric pressure.

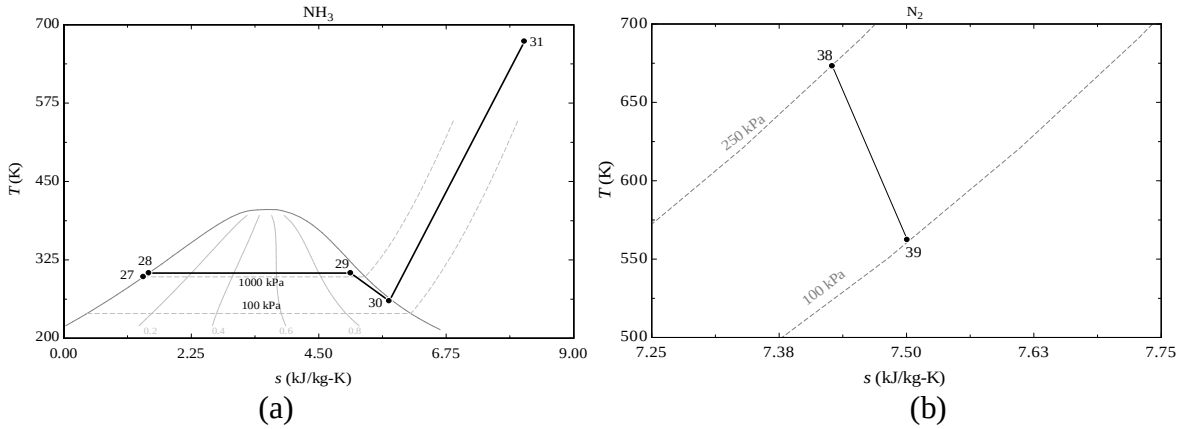

(a) (b)

Figure 6.14: *T-s* diagram of (a) Systems 3 and 4 NH_3 process heat, (b) System 4 N_2 expansion.

The results for heat recovery and additional work by the integrated processes of Systems 3 and 4 are given in Table 6.3. Heat recoveries from HX-1 and HX-2 are included in the value of Δh_{DSU}, calculated as described in Eq. 5.7, which represents the heat input required to raise the temperature of the NH_3 stream to the DSU operating temperature. Another consideration is the compression, ($\dot{W}_{C2}$) of the product gases from the DSU required for cylinder injection into the ICE. It is assumed that the gases are cooled to approximately 80°C prior to compression, to reduce the work requirement to

compress the gases leaving the DSU. Although this heat is not considered for recovery, it could be recovered to improve system efficiency.

Table 6.3: NH_3-process results (System 3 and System 4).

Process	System 3	System 4
NH_3 pump, $\dot{W}_{P8}$ (kW)	0.15	0.15
DSU heat recovery, Q_{DSU} (kW)	242	242
DSU product compression, $\dot{W}_{C2}$ (kW)	230	224
N_2 expansion work, $\dot{W}_{T2}$ (kW)	--	1.25

The modeled energy efficiency is 33.8% for System 3, and the energy balance is shown in Figure 6.15. Energy recovery from exhaust supplies heat for the DSU process, though a portion of energy is spent on the compression of the DSU products for injection into the ICE intake, which is assumed to take place at 2000 kPa [66].

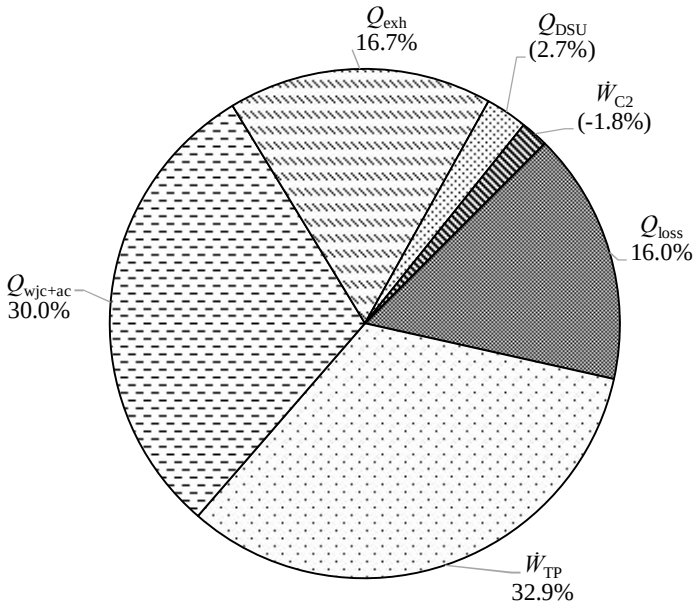

Figure 6.15: System 3 energy balance (Q_{in} = 9050 kW).

The System 3 exergy efficiency is calculated as 32.4%, with major exergy destructions in combustion and heat transfers in the exhaust and coolant streams, as well as NH_3 subsystem losses in the compression process for DSU products.

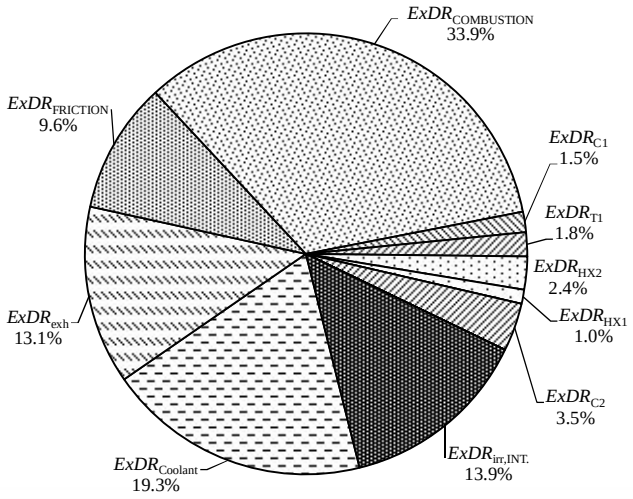

Figure 6.16: Exergy destruction ratios of internal and external losses for System 3.

The System 4 energy balance is shown in Figure 6.17, with energy efficiency determined to be 33.9%, with a very slight gain from the System 3 approach due to the additional turbine work.

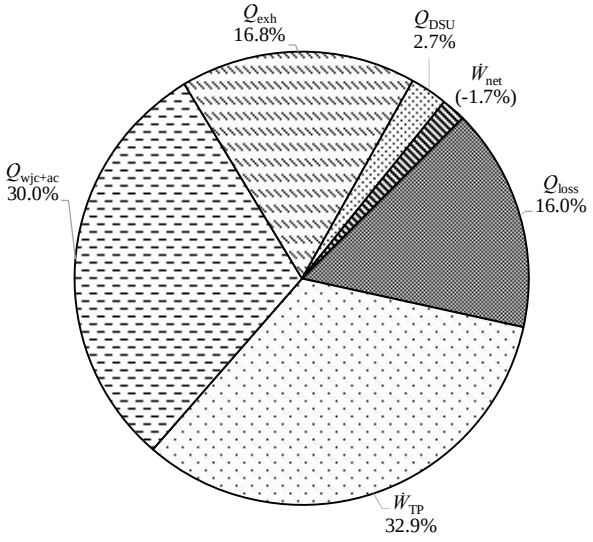

Figure 6.17: System 4 energy balance (Q_{in} = 9050 kW).

The exergy destruction for System 4 is calculated to be 32.6%, which is increased from System 3 due to the additional expansion process losses, indicating that the additional system irreversibility negates the benefit of the expansion work produced.

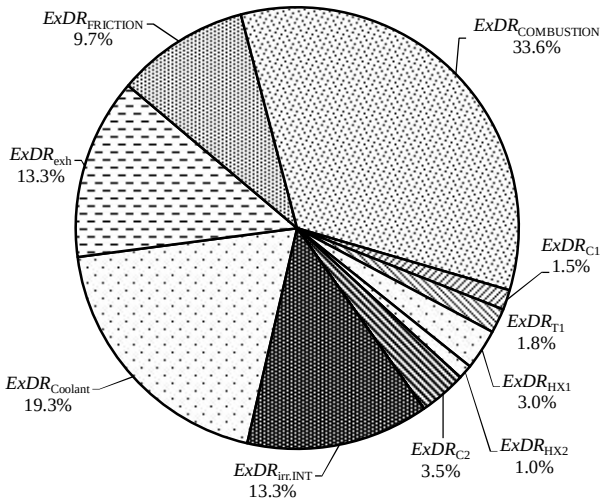

Figure 6.18: Exergy destruction ratios of internal and external losses for System 4.

Systems 5 and 6: Multistage NH_3 Heat Recovery with Power Generation

The ammonia processes for Systems 5 and 6 are indicated in Figure 6.19(a) and 6.19(b), respectively, and investigate the effect of multistage heat recovery, and multistage expansion processes on the performance of the system. The systems are shown in Figure 4.5 and Figure 4.6. The approach taken in System 5 uses a larger pressure ratio to increase the power produced by the turbine, recovering heat from exhaust gases from the turbocharger to superheat the ammonia stream. In the System 6 approach, low grade heat is recovered from the engine water jacket coolant (water) by reducing the pressure and temperature of the ammonia stream directed to the indirect engine cooling process, to produce a saturated vapour which can be superheated and expanded in multiple stages.

Table 6.4: NH_3-process results (System 5 and System 6).

Process	System 5	System 6
NH_3 pump, $\dot{W}_{P8}$ (kW)	2.22	--
DSU heat recovery, $\dot{Q}_{DSU}$ (kW)	242	242
DSU product compression, $\dot{W}_{C2}$ (kW)	159.8	190
N_2 expansion work, $\dot{W}_{T2}$ (kW)	2.01	0.792
NH_3 expansion work, $\dot{W}_{T3}$ (kW)	58.75	38.7
NH_3 expansion work (Sys. 6), $\dot{W}_{T4}$ (kW)	--	22.0

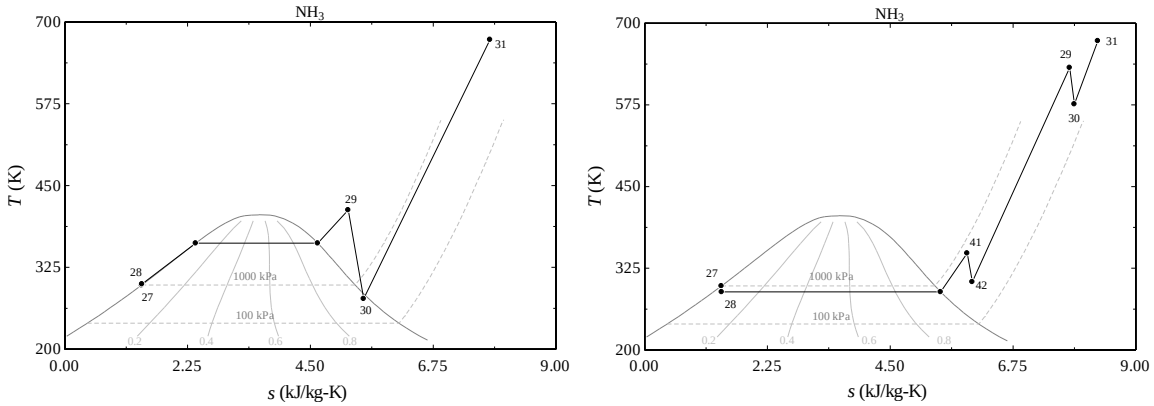

Figure 6.19: *T-s* diagram of NH_3 recovery processes for (a) System 5, and (b) System 6.

The energy balance for System 5 is shown in Figure 6.20, with a calculated energy efficiency of 35.5%. The increased power produced in the additional expansion processes reduces the impact of the compression requirements for the DSU product gases being sent to the engine intake.

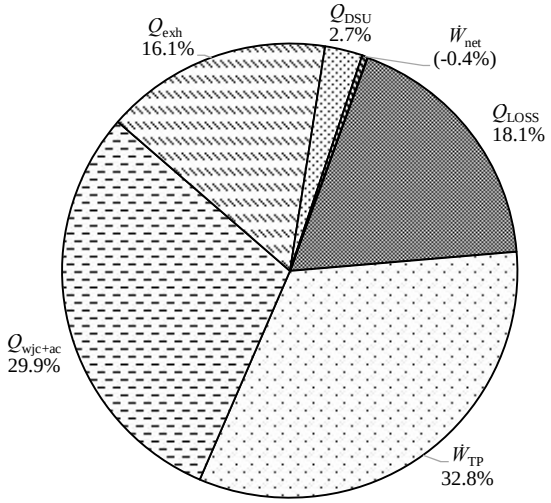

Figure 6.20: System 5 energy balance (Q_{in} = 9050 kW).

The exergy efficiency for System 5 is calculated to be 32.6, accounting for the losses that occur in the major ICE processes, as well as the additional NH_3 subsystems. The NH3 system losses are most significant in the compression of DSU products, as well as in the large heat exchangers, as shown in Figure 6.21.

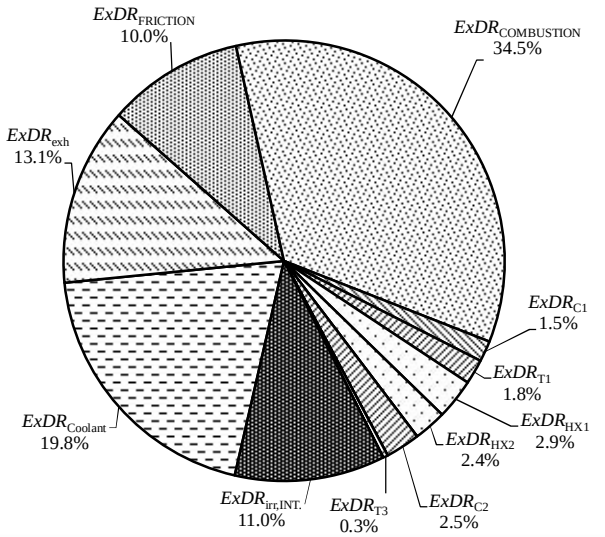

Figure 6.21: Exergy destruction ratios of internal and external losses for System 5.

Engine cooling (addressed in System 6) is a significant but necessary energy loss for the locomotive, and reducing the cooling load on the ICE by NH_3 indirect cooling can reduce the ICE power directed to water jacket and aftercooler processes. The energy balance for System 6 is shown in Figure 6.22, and the energy efficiency is determined to be 34.2%.

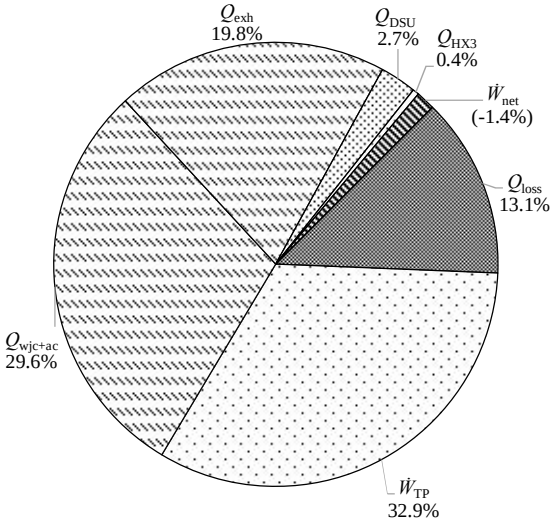

Figure 6.22: System 6 energy balance (Q_{in} = 9050 kW).

The exergy efficiency for System 6 is found to be 31.7%, with additional subsystem losses occurring in the second expansion process, due to turbine irreversibility and heat losses, indicated in Figure 6.22.

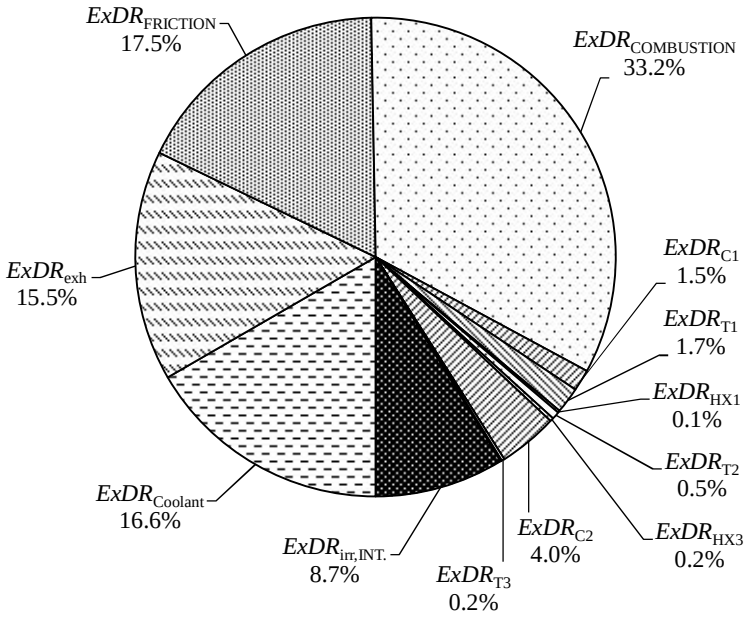

Figure 6.23: Exergy destruction ratios of internal and external losses for System 6.

System 7: Compressed N_2 Gas Storage

The system configuration considered in System 7, and shown in Figure 4.7, incorporates multistage NH_3 heat recovery and expansion, with the addition of compressed N_2 gas storage for on demand expansion work. The specific values for the work processes of the NH_3 subsystems are given in Table 6.5, and the NH_3 processes are indicated in a *T-s* diagram shown in Figure 6.24.

Table 6.5: NH_3-process results (System 7).

Process	System 7
NH_3 pump, $\dot{W}_{P8}$ (kW)	0.852
DSU heat recovery, Q_{DSU} (kW)	242
NH_3 expansion work, $\dot{W}_{T2}$ (kW)	35.5
NH_3 expansion work, $\dot{W}_{T3}$ (kW)	34.75
DSU product compression, $\dot{W}_{C2}$ (kW)	44.4
Compressed N_2 available work, $\dot{W}_{RES7}$ (kW)	1.104

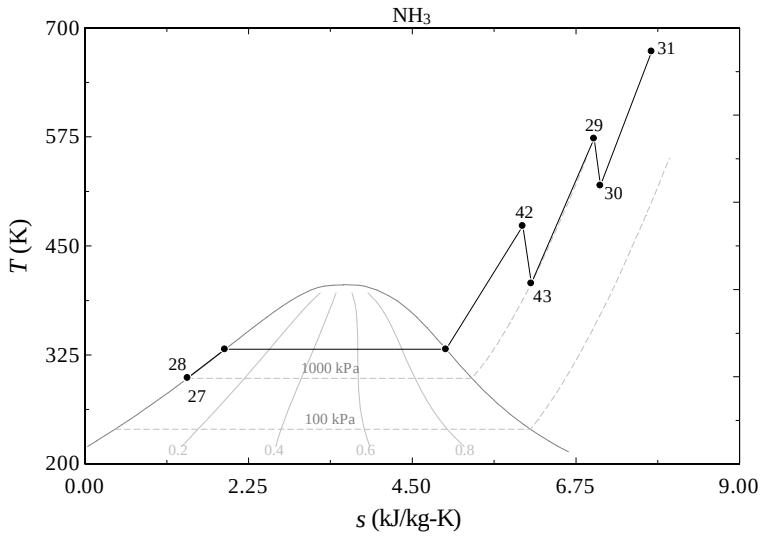

Figure 6.24: *T*-*s* diagram of NH_3 recovery processes (System 7).

The available expansion work is considered as the isothermal work (Pv^n = Constant; n=1), and an isentropic efficiency of 0.75. The compressed gas is stored at 500 kPa and atmospheric temperature. The heating of NH_3 for the first expansion in turbine T2 is obtained from the exhaust gases following the SCR process. The NH_3-H_2, and N_2 DSU product streams are cooled (not shown) before compression, and storage, respectively. The energy efficiency for System 7 is determined to be 35.9%, and the energy balance is indicated in Figure 6.25 for the ICE.

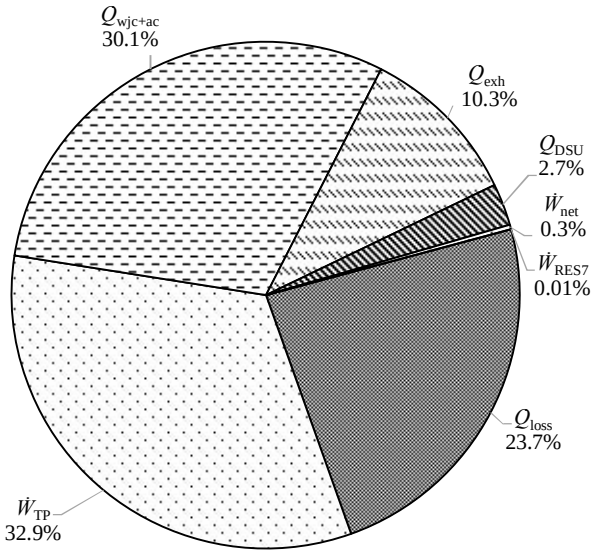

Figure 6.25: System 7 energy balance ($\dot{Q}_{in}$ = 9050 kW).

The exergy efficiency for System 7 is determined to be 33.2%, with the majority of NH_3 subsystem exergy destructions occurring in the heat exchange processes ratios are shown in Figure 6.27.

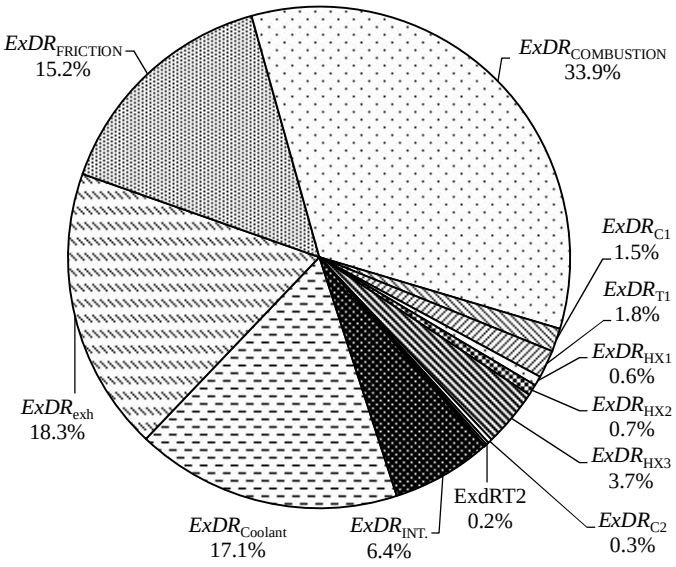

Figure 6.26: Exergy destruction ratios of internal and external losses for System 7.

System 8 and 9: Multistage Expansion and Cooling by NH_3

Systems 8 and 9 provide cooling for the locomotive, using a turbine-driven fan in System 8, and a chiller (cooled by ammonia) for cab-cooling in System 9. The systems are shown in Figure 4.8 and Figure 4.9. Ammonia processes are shown in Figure 6.27 (a) and (b) for the systems.

In System 8, indirect engine cooling superheats the ammonia in HX-3. The turbine is coupled by rotor to a fan that provides additional cooling to the radiator section, which further reduces the direct engine cooling by the ICE shaft work. System 9 provides cold storage, which is assumed to be applied to a cab air-conditioning unit at a COP of 2.0, but could be applied to engine cooling as well to potentially increase this effect. The system results for the useful work and heat products and the required work inputs are listed in Table 6.6 for each system.

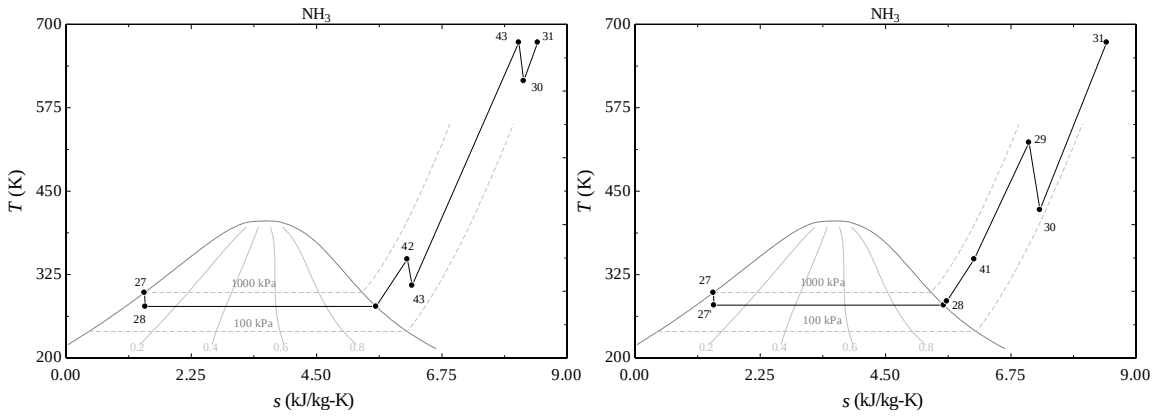

(a) (b)

Figure 6.27: *T-s* diagram of NH_3 cooling and work processes for (a) System 8, and (b) System 9.

Table 6.6: NH_3-process results (System 8 and System 9).

Process	System 8	System 9
NH_3 indirect ICE cooling[a], $Q_{ICE\text{-}c}$ (kW) (Sys. 8)	112	--
Locomotive cab cooling, $Q_{CAB\text{-}c}$ (kW) (Sys. 9)	--	294
Cab cooling work input, $\dot{W}_{CAB\text{-}c}$ (kW) (Sys. 9)	--	150
DSU heat recovery, Q_{DSU} (kW)	242	242
DSU product compression, $\dot{W}_{C2}$ (kW)	224	224
Expansion work, $\dot{W}_{T2} + \dot{W}_{T3}$ (kW)	41.7	0.318
NH_3 expansion work, $\dot{W}_{T3}$ (kW)	--	69.5

a. System 8 indirect cooling by turbine driven fan ($Q_{ICE\text{-}c} = COPc \cdot \dot{W}_{T4}$)

The energy balance for System 8 is shown in Figure 6.28, which has a calculated energy efficiency of 34.8%. The heat recovery from the exhaust gases and coolant streams is used to generate turbine work both by removing heat from the fluids, and by driving a fan to provide forced air cooling. The heat recovered in the high temperature heat exchangers at the exhaust is used to upgrade the temperature to the required DSU operating temperature.

The exergy efficiency for System 8 is determined to be 31.2%, with the DSU product compression and higher temperature heat exchangers having the largest destruction ratios for the NH_3 processes. The exergy destructions for the system are indicated in Figure 6.29.

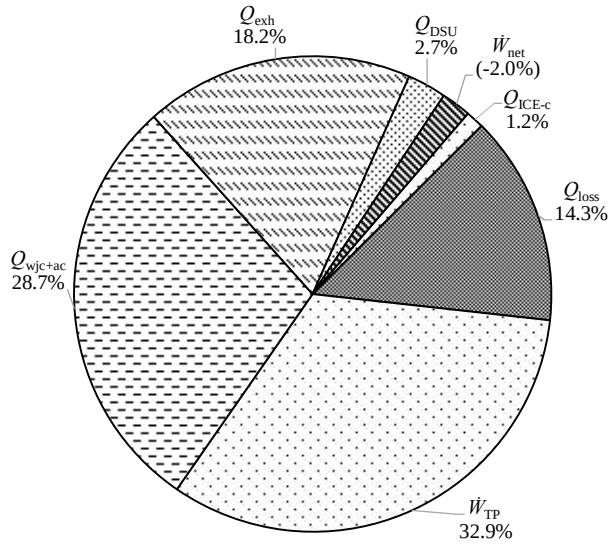

Figure 6.28: System 8 energy balance (Q_{in} = 9050 kW).

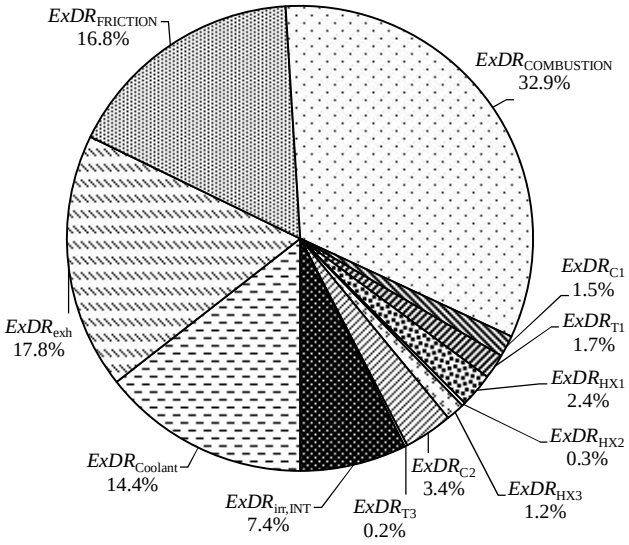

Figure 6.29: Exergy destruction ratios of internal and external losses for System 8.

The energy balance for System 9 is shown in Figure 6.30, which has an energy efficiency of 35.6%. The system includes a locomotive cab-cooling system using a chilled water tank to store cold-thermal energy produced by low-temperature NH_3 stream, which is throttled to lower pressure (and temperature) before entering the chiller tank. Liquid is circulated through a coil, and a fan blows forced air over it, producing the cooling effect in the cab. The exergy efficiency for System 9 is calculated to be 29.9%, with energy destructions described in Figure 6.31.

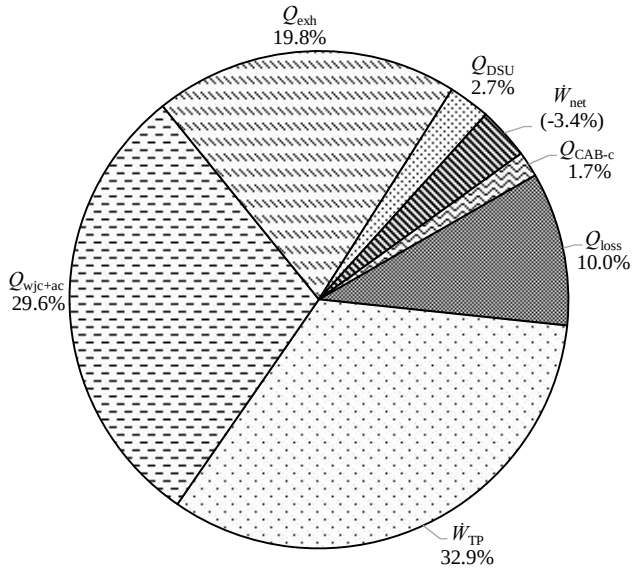

Figure 6.30: System 9 energy balance (Q_{in} = 9050 kW).

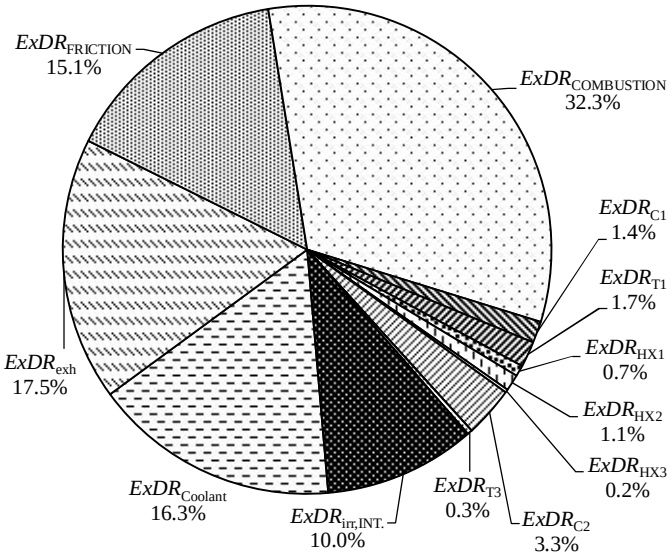

Figure 6.31: Exergy destruction ratios of internal and external losses for System 9.

System 10: Exhaust heat recovery NH_3-Rankine Cycle (NH_3-RC)

A cascaded approach is taken in the exhaust heat recovery arrangement proposed for System 10, with waste heat from the ammonia Rankine cycle (NH_3-RC) used as process heating. The NH_3-RC operates in the same way as an organic Rankine cycle (ORC), which uses organic working fluids. The thermodynamic processes for the NH_3-RC and

expansions are indicated in Table 6.7. The operating principles used in the NH_3-RC are simple; saturated liquid NH_3 is pumped to an upper pressure level of 5,000 kPa and then heated by exhaust waste heat to produce superheated vapour through a heat exchanger. The vapour is expanded in a turbine to produce shaft work. The low pressure stream at the outlet rejects heat in a condenser and is recirculated as the cycle continues. By integrating an NH_3 Rankine cycle, it is possible to take advantage of higher pressure ratios, increasing the additional work produced from recovered heat in the NH_3-RC, as well as multi-stage expansion and reheat of the secondary ammonia stream. The NH_3-RC 'boiler' uses exhaust waste heat after the SCR treatment, therefore the high grade exhaust heat in HX-1 and HX-2 is available for additional heat recovery and NH_3 expansion and decomposition processes.

The heat and work duties for the system are listed in Table 6.7. In the configuration shown in Figure 4.10, the condensed ammonia stream is sent to the engine as fuel, but it may also be used in a closed circuit for the NH_3-RC.

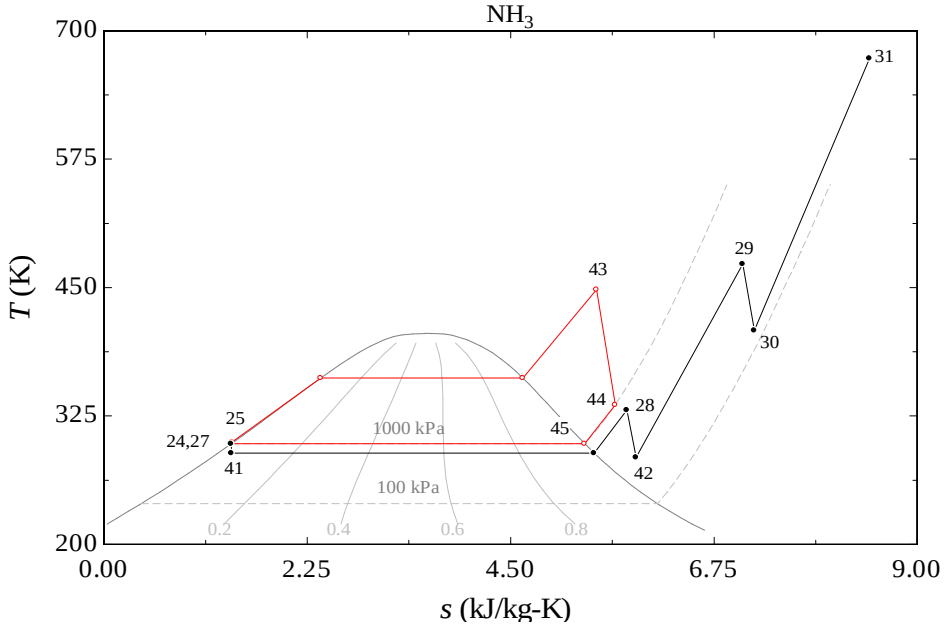

Figure 6.32: *T-s* diagram of NH_3 recovery processes and integrated NH_3-RC (System 10).

Table 6.7: NH_3-process results (System 10).

Process	System 10
NH_3-RC pump, $\dot{W}_{P2}$ (kW)	2.27
NH_3 additional fuel pump, $\dot{W}_{P}$ (kW) (not shown)	2.39
NH_3-DSU return pump, $\dot{W}_{P}$ (kW) (not shown)	0.415
DSU heat recovery, Q_{DSU} (kW)	242
DSU product compression, $\dot{W}_{C2}$ (kW)	18.5
N_2 expansion work, $\dot{W}_{T2}$ (kW)	0.311
NH_3 expansion work, $\dot{W}_{T3}$ (kW)	38.4
NH_3 expansion work, $\dot{W}_{T4}$ (kW)	22.5
NH_3-RC expansion work, $\dot{W}_{T5}$ (kW)	50.8

System 10 has a calculated energy efficiency of 36.7%, with the energy balance indicated in Figure 6.33. In this configuration, the heat recovery processes take advantage of the different temperature levels available in the ICE heat losses. The NH_3-RC recovers heat from the exhaust after the SCR unit, and the high temperature exhaust heat is used to produce expansion work by heating and re-heating the NH_3, and to raise the temperature of the NH_3 stream to the DSU temperature. The exergy efficiency is calculated to be 34.5 for System 10, with the exergy destruction ratios shown in Figure 6.34.

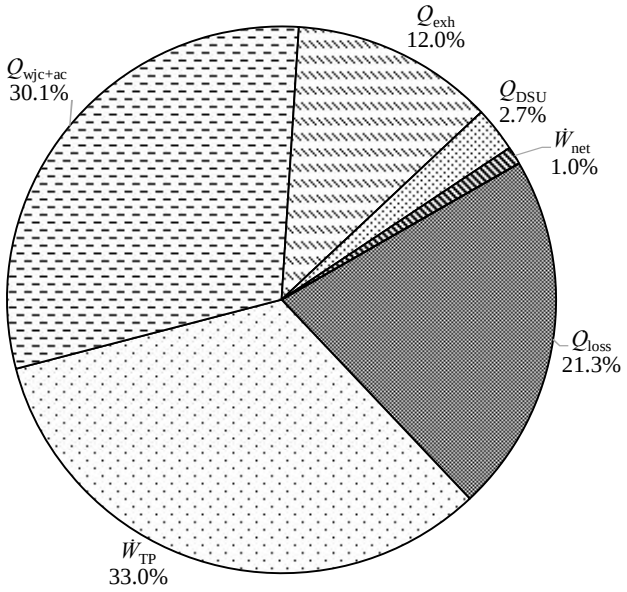

Figure 6.33: System 10 energy balance (Q_{in} = 9050 kW).

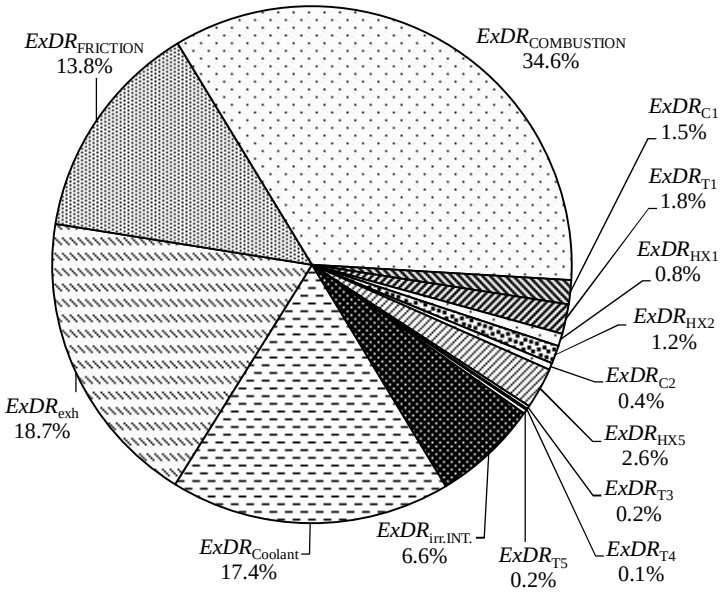

Figure 6.34: Exergy destruction ratios of internal and external losses for System 10.

6.2 Ammonia-Powered Locomotive Performance Results

6.2.1 Energy and Exergy Efficiency Results

The effect on system performance by the ammonia-powered processes is evaluated based on of the heat recovery of the ammonia, and additional work production determined in the system results. The results are shown in Figure 6.35, comparing the utilization energy and exergy efficiencies achieved for each system at rated operating conditions.

System 10 has excellent performance both energetically and exergetically, and offers flexible performance in terms of generating capacity, which can be increased by using a closed loop system instead of the flow-through scheme as described, which could help to provide additional power to the prime mover, or the head end power system. The systems are investigated in greater detail in the following subsection with respect to the emissions produced for the selected fuel blend, overall sustainability, and the associated costs.

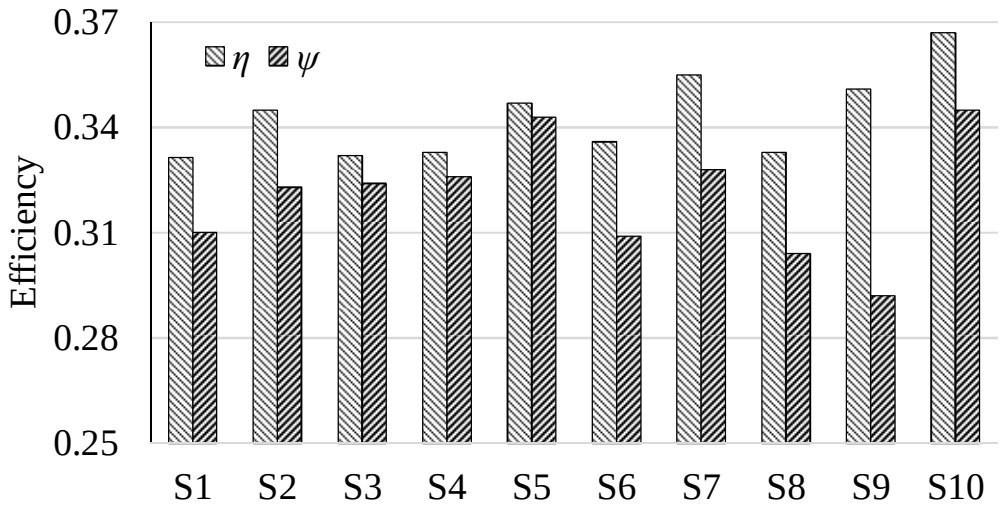

Figure 6.35: Energy and exergy efficiencies for Systems 1 – 10.

6.2.2 Environmental Impact Assessment Results

Figure 6.36 to Figure 6.40 indicate the emission levels for the assumed fuel blend, with 50% of fuel input from ammonia. The cases are shown for the CAC emissions which are reduced by diesel reduction, and by integration of the SCR unit.

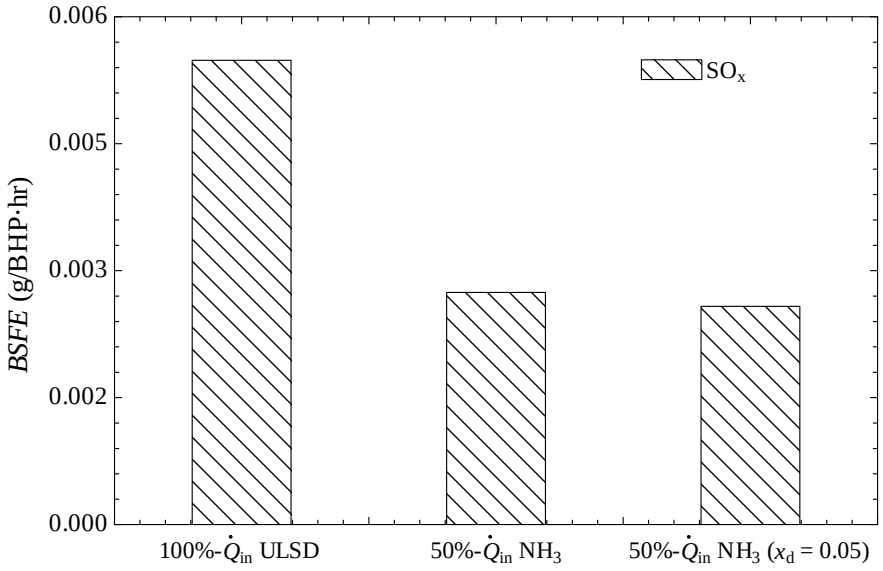

Figure 6.36: SO_x emissions for fuel blends.

Significant reductions for NO_x and HC emissions result with the SCR integration, with the lowest reductions observed for PM. Because ammonia contains no carbon, no soot is produced directly by NH_3 therefore, increasing the ammonia supply can help to further improve PM emissions.

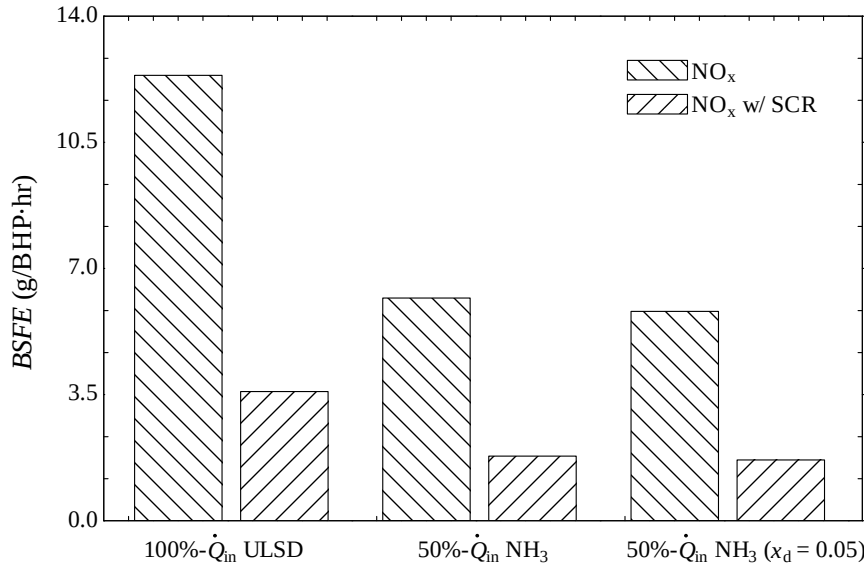

Figure 6.37: NO_x emissions, and SCR reduction for fuel blends.

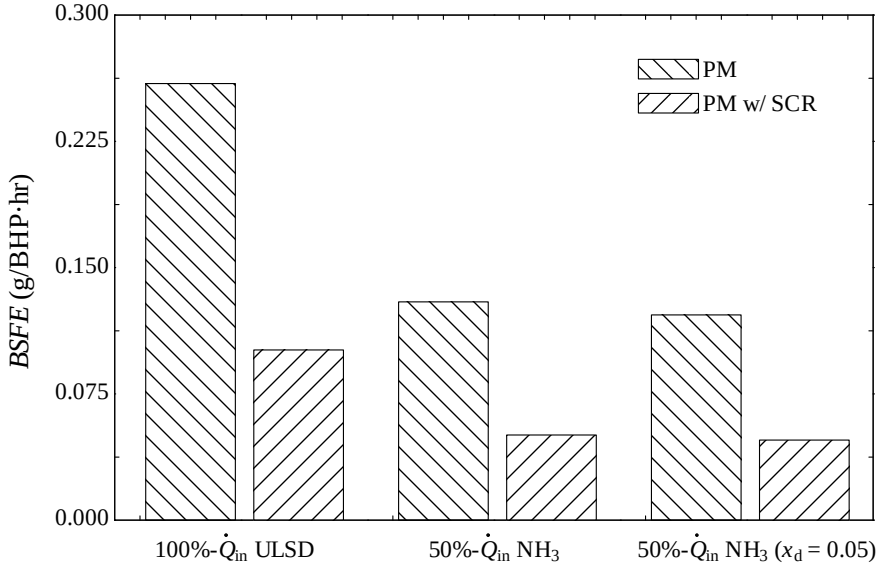

Figure 6.38: PM Emissions, and SCR reduction for fuel blends.

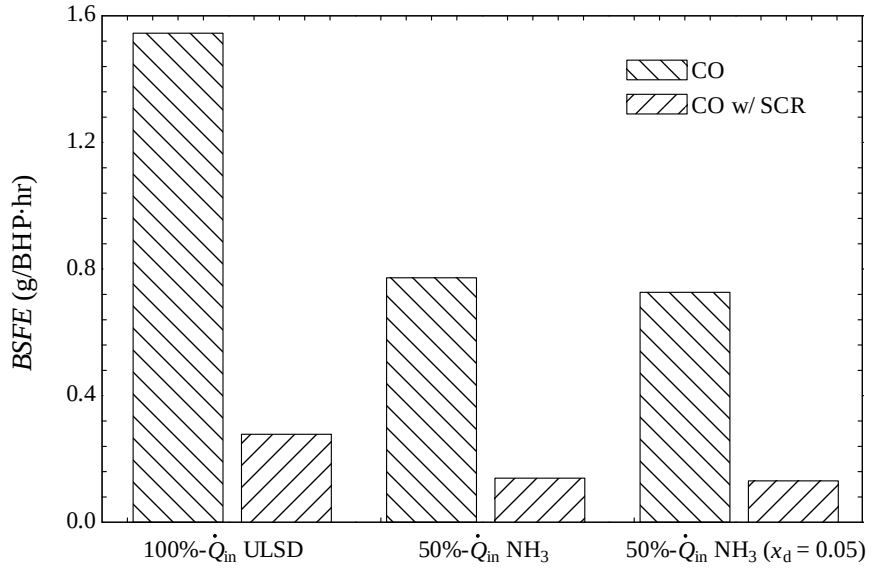

Figure 6.39: CO Emissions, and SCR reduction for fuel blends.

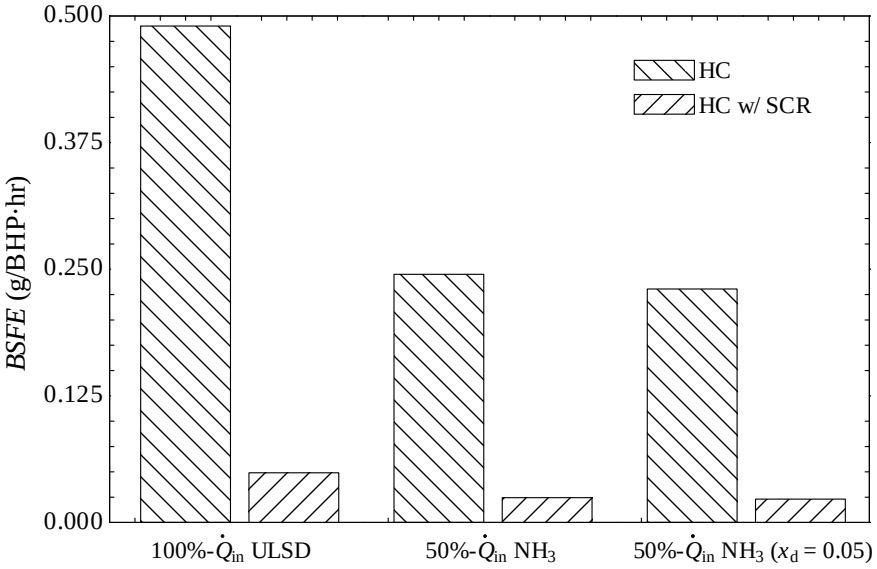

Figure 6.40: HC Emissions, and SCR reduction for fuel blends.

6.2.3 Cost Analysis Results

Estimated costs are outlined in Table 6.8 for additional equipment required for the proposed systems based on various cost data for similar equipment. The values are applied to each system to determine the increase in system cost in Canadian dollars ($CDN_{\$2013}$), with a cost index.

Table 6.8: Estimated capital costs of additional equipment.

Equipment Item	**Reference Cost Data**	
	C_0 **(USD$_{year}$)**	S_0
SCR system	150,000 $\$_{2003}$	2.0 MW_{TP}
NH_3 DSU	275 $\$_{2007}$	1.0 kW_{H2}
Dual-fuel conversion	250,000 $\$_{2003}$	(per unit)
NH_3 Pressure storage tank	1,450 $\$_{2006}$	1.0 m^3
Pump	400 $\$_{2006}$	1.0 kW
Gas compressor	25,000 $\$_{2006}$	100 kW
Gas compressor	2,000 $\$_{2006}$	2.25 kW
Power recovery turbine	10,000 $\$_{2006}$	40 kW
Air conditioning unit	60,000 $\$_{2006}$	700 kW_{th}
Exhaust recovery heat exchanger	55,000 $\$_{2007}$	300 kW_{th}
ORC unit	70,000 $\$_{2007}$	20 kW·h
Fan	8,250 $\$_{2006}$	60 kW·h

Sources: [59], [60], [61], [62], [63]

The estimated total costs for each system are listed in Table 6.9 based on the reference base costs, and component capacities for each of the systems. These estimates give a baseline for comparison, though a more rigorous system cost analysis should be conducted in subsequent design stages with greater detail.

Table 6.9: Estimated total capital costs of additional equipment for each System.

System	**CAD**
System 1’ (SCR only)	398.090
System 2	720,860
System 3	1,030,960
System 4	1,032,035
System 5	1,039,700
System 6	1,092,075
System 7	1,051,210
System 8	1,085,450
System 9	1,077,800
System 10	1,144,090

6.3 Sustainability Assessment Results

The Greenization factor for each fuel blend is given in in Figure 6.41, with constant factors resulting for Systems 3 to 10 based on the assigned fuel mixtures. The maximum reduction is calculated to be 53%, or a *GF* of 0.53.

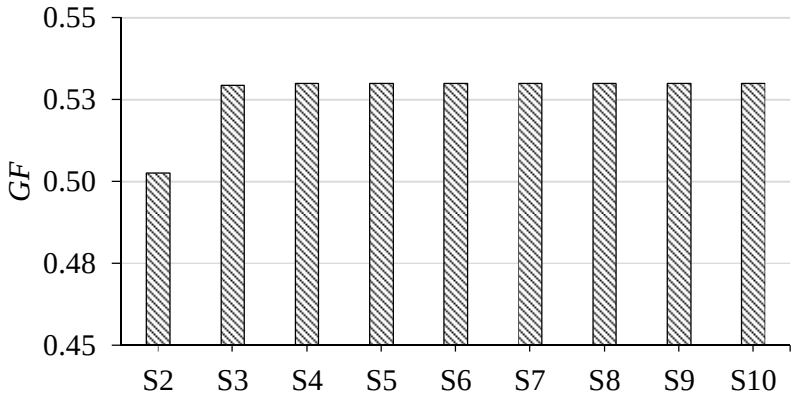

Figure 6.41: Greenization Factor (*GF*) for Systems 2 – 10 (S1 = 0).

The depletion factors are shown in Figure 6.42. These results give a clear indication of the performance in terms of the amount of exergy destroyed. From the results shown, Systems 8 and 9 have significant losses which make these less attractive as a potential option; however, because the energy is recovered from waste heat, these options still have value if the desired products are met – specifically, cabin air cooling, and supplementary engine cooling. Systems 5 and 10 have the lowest depletion factors, and make efficient use of the recovered energy.

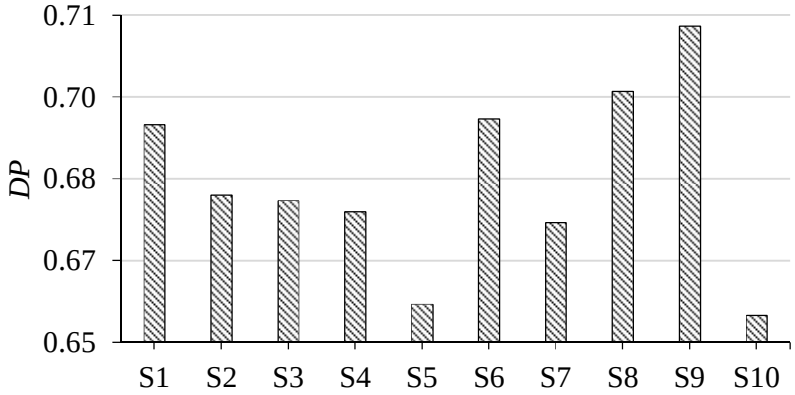

Figure 6.42: Depletion factor (D_P) for Systems 1 – 10.

The increase in total cost of the locomotive is evaluated based on capital cost estimates for the required system equipment for each configuration. The system S1' is the case of only SCR technology being implemented, with no additional ammonia processes. Overall, the majority of the systems are found to have capital cost increases between 10–15% from the base locomotive cost.

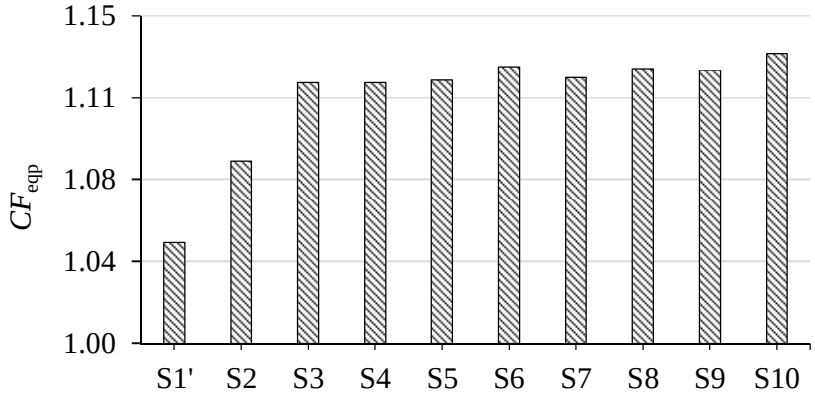

Figure 6.43: Relative cost increase for additional equipment.

6.4 Systems Comparison

To evaluate overall system performance considering all performance factors, the assessment results are compared using a target plot. Following the methodology by [64], the results for each impact factor are normalized to rank the systems highlight and the best case, which is identified in Figure 6.44 within the black outer circles. For the factors that concern the fuel mixture—*GF* and CF_f—the rankings show the associated systems grouped by either diesel only (System 1), NH_3-diesel (System 2), and NH_3-H_2-diesel (Systems 3-10). The plotted results show that System 10 performs the best in terms of its efficiency, and has the highest sustainability index, but also shows that these advantages come at the highest cost for additional equipment.

Different cases are considered in Figure 6.45 to present system comparisons with significance given to a particular performance factor. These prioritized factors represent decision making scenarios—for example, green initiatives, or cost savings in fuel—are highlighted by applying weight factors to the performance results.

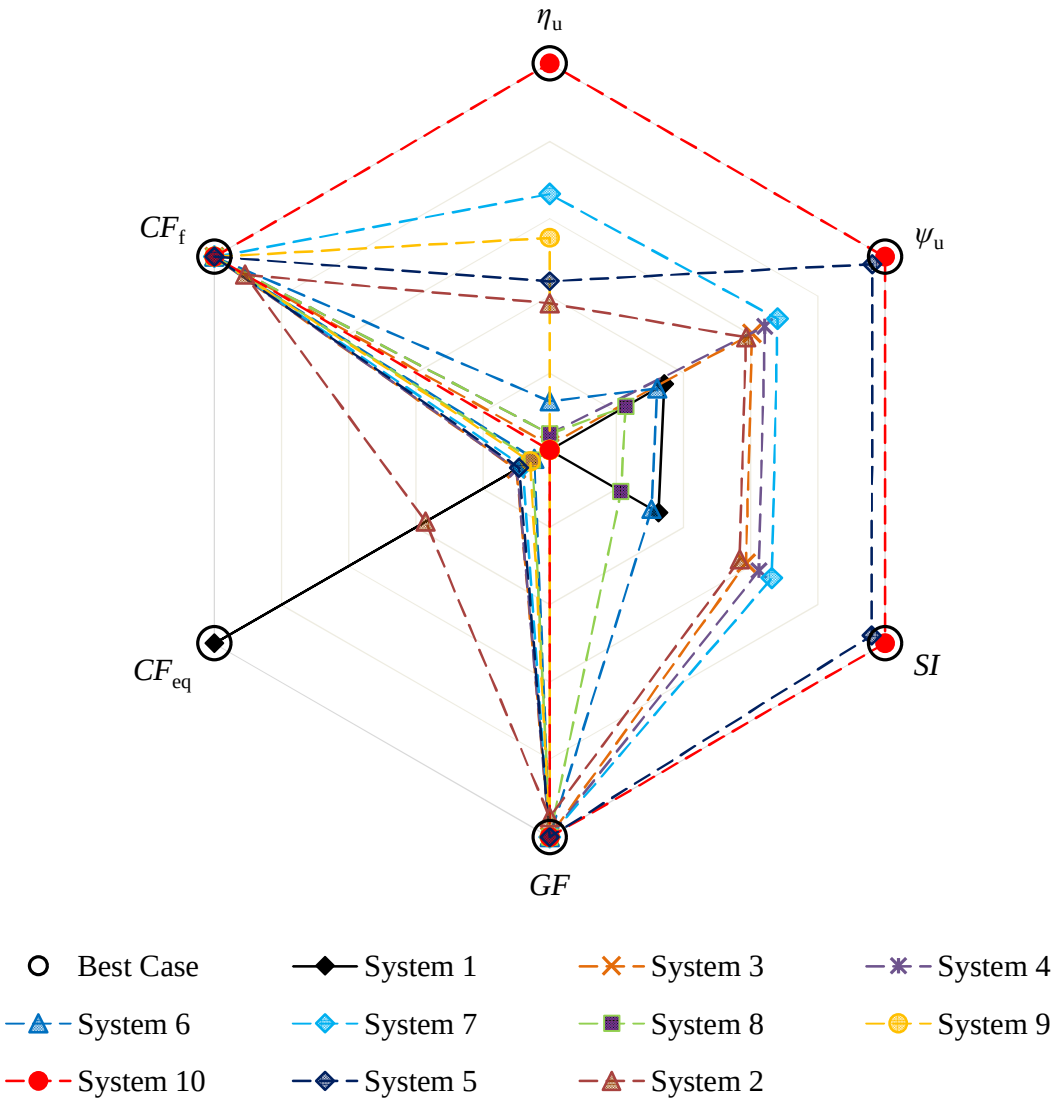

Figure 6.44: System comparison.

The weighted factor represents the priority consideration. In the first case shown in the figure, even weighting is given to each factor considered, including the Sustainability Index, fuel cost factor, equipment cost factor, Greenization Factor, and the energy and exergy efficiencies for each system. Cases 2—6 highlight the different factors as priority, to show the influence of that aspect of system performance within the overall assessment.

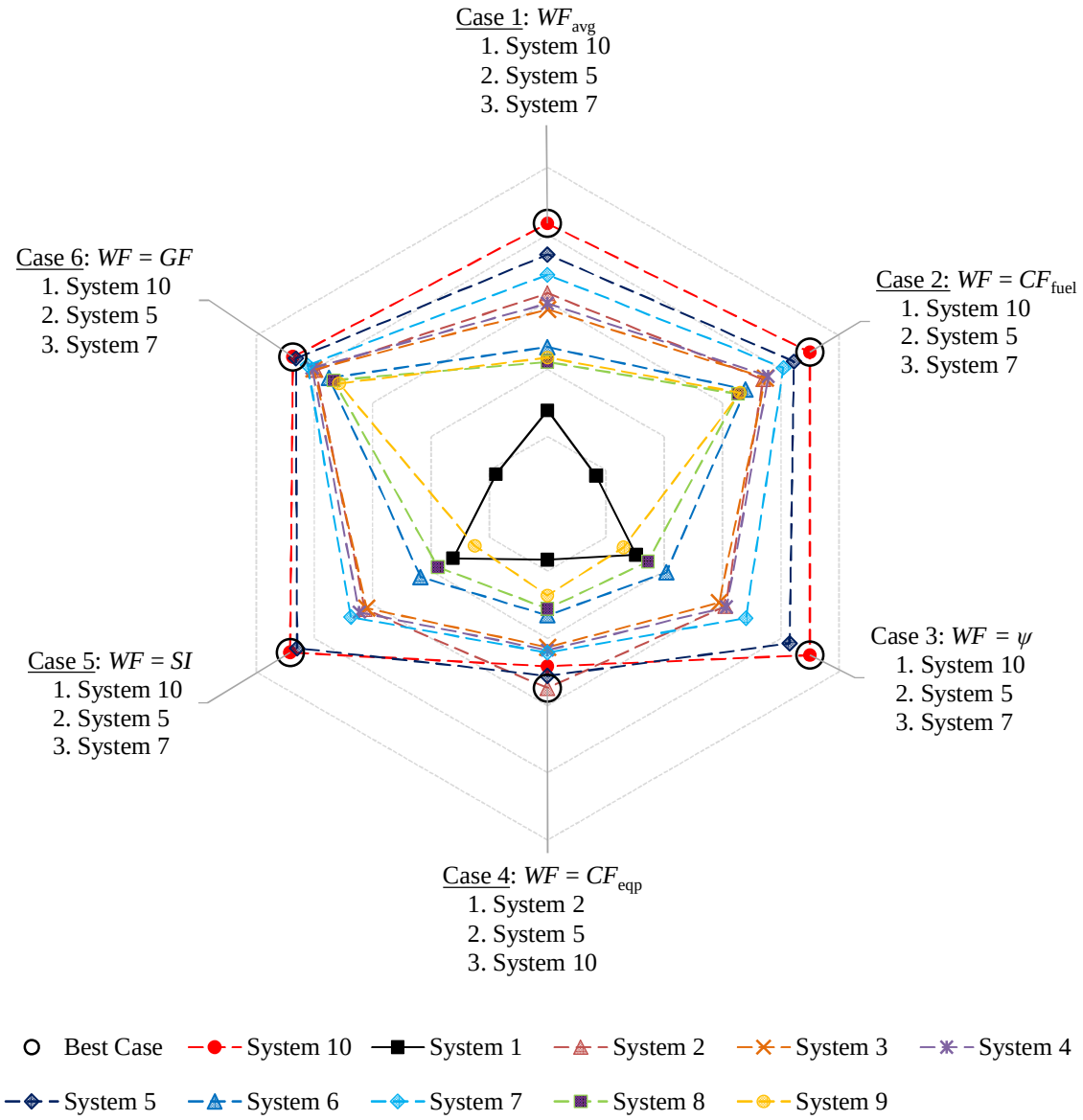

Figure 6.45: System comparison with weighted factors (Cases 1 – 6).

The results are summarized briefly in Table 6.10 for Systems 10, 5, and 7, which rank highest for their overall performance for the given comparison. These systems appear to be the best options, and are good candidates for further development and demonstration. While the systems are investigated based on the operating conditions of a specific locomotive, included components and subsystem processes are highly scalable, and may be optimized based on the operating conditions found in various locomotive engines.

Table 6.10: Summarized results for top three ranked systems.

	System 10	**System 5**	**System 7**
Description	• NH_3-RC • multistage heat recovery and expansions	• Multistage heat recovery and expansions	• Multistage heat recovery and N_2 compressed gas storage
Energy efficiency, η (%)	36.7	35.3	35.5
Exergy efficiency, ψ (%)	34.5	32.6	33.2
Sustainability Index, *SI*	1.53	1.52	1.49
Depletion Factor, D_p	0.655	0.657	0.672
Greenization Factor, *GF*	0.53	0.53	0.53
Estimated equipment cost, C_{eqp}, CAD_{2013}	$1,144,086.00	$1,039,700.00	$1,051,700.00

6.5 Commuter Transit Case Study: Ammonia Fueling for GTA GO Rail System

The GO Rail System is one of Canada's largest commuter rail networks, handling 185,000 passengers daily on weekdays, using 47 locomotives. The GO Rail Commuter fleet includes 65 Tier–2 emission compliant MP40PH–3C diesel-electric locomotives, capable of pulling/pushing 12 bi–level passenger coaches. The transit system operating details are given in Table 6.11. Ammonia fueling is considered for use in GO Rail operations, and the potential of the ammonia fueling is addressed for overall fuel cost, and environmental performance.

Table 6.11: GO Rail transit system details.

Passengers (weekday)	185,000
Number of Lines	7
Stations	63
Route Kilometres	450
Weekday train trips	203
Weekday train-sets in use	47
Locomotives (MP40PH-3C, Tier 2)	65
Bi-level passenger coaches	563 (162 seats)
Fuel capacity	8,410 L

Source: [10].

The duty cycle operation is given in Table 6.12 for commuter operation, with the daily operating time for Notch 1 (N1) and Dynamic Braking (DB) combined. Duty cycle average GHG emissions per passenger, and cost of fuel for weekday commuter operation of the GTA GO Rail Transit system are determined for the baseline diesel fueled case, and the considered ULSD-NH_3-H_2 fuel blend with 50-percent energy input by NH_3, and NH_3-decomposition of $x_d = 0.05$ to produce H_2 fuel.

Table 6.12: Commuter locomotive duty cycle.

Engine notch	**Low Idle**	**N1, DB**	**N2**	**N3**	**N4**	**N5**	**N6**	**N7**	**N8**
RPM	200	269	343	490	568	651	729	820	904
%-Daily Op. Time	59	6.1	2.3	2.2	2.1	1.3	1.2	1.8	24
Power (kW)	15	150	300	745	1044	1342	2480	2610	2983

Source: [73].

Fuel prices are assumed as 1.24 CDN$/L for diesel fuel, and price range for ammonia of 400–700 CDN$/tonne NH_3 (0.24–0.42 CDN$/L), accounting for the effect of significant price fluctuation of natural gas on ammonia cost. The results are given in Table 6.13 for ammonia co-fueling for in the rated notch position (Notch 8), which has exhaust emission temperatures high enough to maintain the system operation as described and the highest fuel consumption, and the remaining notch positions fueled by diesel fuel. The emissions per passenger do not include the emissions produced when the locomotive is in Low Idle and Idle (N1) notch positions, to better represent the commuter case when the locomotive is in transit.

Table 6.13: Duty cycle fuel consumption and fuel cost for GO Rail MP40 Locomotive.[a]

	100% ULSD	**50%-Qin NH_3 (x_d=0.05 H_2 prod.)**	
		ULSD	**NH_3**
Fuel mass consumed per duty cycle (kg)	2,857	1,693	2,625
Volume consumed per duty cycle (L)	3,360.00	1,992	4,353
Combustion GHG emissions (kg-CO_2)	8,950	5,305	--
GHG's per passenger (kg-CO_2/PAX)	2.05	1.14	
Fuel cost per duty cycle (CDN$)	~$4,166	$2,470	$1,050 – $1,838
Total fuel cost per duty cycle (CDN$)	$4,166	$3,520.00 – $4308	
CO_2-tax ($15/tonne-$CO_2$)	$134	$30	--
Total with imposed CO_2-tax (CDN$)	$4,300	$3,550 –$ 4,338	

a. ULSD-NH3-H2 blend used in Notch 8 only (Idle and Notch 1-7 use 100% ULSD)

The calculated results show that there is potential for significant economic benefit to using the fuel blend; with a 15% fuel cost reduction for fuel blending used in Notch 8 with the lower NH_3 price, but is not so competitive if the cost of natural gas spikes. Encouraging production of ammonia from renewable resources may help to lower the average cost by creating price competition with natural gas production, as well as improving the environmental performance of ammonia for the total lifecycle. Combustion GHG emissions are significantly reduced, with results indicating a 44% reduction in combustion CO_2 emissions per passenger.

CHAPTER 7: CONCLUSIONS AND RECOMMENDATIONS

7.1 Conclusions

This thesis has investigated the use of ammonia as a combustion fuel, heat transfer fluid, NO_x-reducing agent, hydrogen resource, and working fluid in a locomotive application. Ten systems are included in the comparative assessment, developed with long term sustainability and environmental impact reduction as the primary aim. While current methods to produce ammonia are associated with some GHG emissions, it may be produced from any renewable resource, and is able to provide significant cost and environmental impact reductions.

From the comparative assessment, the following conclusions are made with respect to the system performance:

- From a sustainability standpoint, System 10 has the best performance, followed by System 5 and System 7.
- In terms of emissions, the NH_3 Systems all perform well with significant reduction in GHG and CAC emissions by SCR reduction, and diesel fuel replacement by ammonia.
- With respect to cost performance, although the systems appear to have poor performance compared to the original system (without additional systems), this is due to capital costs. With the lower cost of ammonia, and renewable technologies becoming, more competitive, this will reduce operational costs over time.

7.2 Recommendations

With the reduction of large emission sources, and improvement of railway infrastructure, it is possible to make more reasonable estimations of the potential improvements by ammonia systems on rail performance. Advanced data logging and tracking techniques along with detailed modeling studies have a potential to present more insight to managing and reducing rail transportation emissions.

- Different methods of sustainable ammonia production should be investigated to reduce the lifecycle impact of ammonia fuel.
- Further research should be conducted on developing cheap and efficient fuel purification, cleaning, and storage systems.
- Advanced fuel technologies should be developed and investigated to optimize the mass and volume requirements, system efficiency, emissions, as well as, the system cost for onboard hydrogen production at different capacities from ammonia.
- System design improvement studies including weight and volume reduction should be conducted, to reduce the space demand in the locomotive.
- In addition to the aforementioned technical recommendations, further research should also be conducted on how to gain public awareness for ammonia.
- System scalability should be further investigated to provide solutions for light duty vehicles.

REFERENCES

[1] United Nations, "United Nations Framework Convention on Climate Change: Appendix I - Quantified economy-wide emissions targets for 2020," Jan. 2010. [Online]. Available: http://unfccc.int/meetings/copenhagen_dec_2009/items/5264.php. [Accessed 2013].

[2] Environment Canada, "Canada's Emissions Trends," Government of Canada, Ottawa, 2013.

[3] C. Zamfirescu and I. Dincer, "Ammonia as a green fuel and hydrogen source for vehicular applications.," *Fuel processing technology*, pp. 729-737, 2009.

[4] M. A. Midilli, I. Dincer and M. A. Rosen, "On hydrogen and hydrogen energy strategies I: current status and needs.," *Renewable ad Sustainable Energy Reviews,* vol. 9, no. 3, pp. 255-271, 2005.

[5] S. Dunn, "Hydrogen futures: toward a sustainable energy system.," *International Journal of Hydrogen Energy,* vol. 27, no. 3, pp. 235-264, 2002.

[6] A. Klerke, C. H. Christensen, J. K. Nørskov and T. Vegge, "Ammonia for hydrogen storage: challenges and opportunities.," *Journal of Materials Chemistry ,* vol. 18, no. 20, pp. 2304-2310, 2008.

[7] I. Dincer and C. Zamfirescu, "Methods and Apparatus for using Ammonia as a Sustainable Fuel, Refrigerant, and NOx Reduction Agent.". United States Patent Pub. No.: US 2011/0011354 A1, 19 February 2009.

[8] A. Taghizadeh and M. L. Payne, "Review of Natural Gas Fueled Locomotive Technology," Transport Canada, Ottawa, 1999.

[9] P. Eggleton, "Schema for demonstrating a natural gas-fueled railway operation," Transport Canada, 2002.

[10] GO Transit, "GOTransit.com - Quick Facts," 2013. [Online]. Available: <http://www.gotransit.com/public/en/docs/publications/quickfacts/Quick_Facts_Info_to_GO_EN.pdf>. [Accessed 2013].

[11] GO Transit, *GO Green Initiatives*, Toronto: gotransit.com, 2014.

[12] RAC, "Locomotive Emissions Monitoring Program 2011," Railway Association of Canada, Ottawa, 2014.

[13] GO Transit, "GOTransit.com - Maps," [Online]. Available: http://www.gotransit.com/timetables/en/schedules/sysmap.aspx. [Accessed 25 April 2013].

[14] Environment Canada, "Global Carbon Dioxide Emissions from Fuel Combustion," 2013. [Online]. Available: www.ec.gc.ca/indicateurs-indicators. [Accessed December 2013].

[15] Environment Canada, "Greenhouse Gas Emissions Data," 2013. [Online]. Available: http://www.ec.gc.ca/indicateurs-indicators. [Accessed 2014].

[16] Environment Canada, "National Inventory Report 1990-2012: Greenhouse Gas Sources and Sinks in Canada," 2014. [Online]. Available: http://ec.gc.ca/ges-ghg/default.asp?lang=En&n=68EE206C-1&offset=3&toc=show. [Accessed March 2014].

[17] RAC, "Locomotive Emissions Monitoring Program 2010," Railway Association of Canada, Ottawa, 2012.

[18] Railway Association of Canada, "2011-2015 Memorandum of Understanding Between Transport Canada and the Railway Association of Canada for Reducing Locomotive Emissions.," railcan.ca, Ottawa, 2013.

[19] www.epa.gov, "Locomotives -- Exhaust Emission Standards," 14 November 2012. [Online]. Available: http://www.epa.gov/otaq/standards/nonroad/locomotives.htm. [Accessed 15 November 2013].

[20] n.a., "Diesel Locomotive Technology," Railway Technical Web Pages, 2014. [Online]. Available: http://www.railway-technical.com/diesel.shtml. [Accessed April 2014].

[21] Elucidare, "Ammonia - New possibilities for hydrogen storage and transportation," Elucidare Ltd., 2008.

[22] A. J. Reiter and S.-C. Kong, "Combustion and emissions characteristics of compression-ignition engine using dual ammonia-diesel fuel.," *Fuel*, pp. 87-97, 2011.

[23] E. Bourbon, "Clean Cities Alternative Fuel Price Report: October 2013," U.S. Department of Energy, Washington, D.C., 2013.

[24] M. Appl, Ammonia - Principles and Industrial Practice, New York: Wiley-VCH, 1999.

[25] 3E Company, "MSDS Solutions," 2014. [Online]. Available: www.msds.com.

[Accessed April 2014].

[26] WHO, "Ambient (outddoor) air quality and health.," March 2014. [Online]. Available: www.who.int. [Accessed April 2014].

[27] Canadian Cancer Society, "Risk factors for lung cancer," 2014. [Online]. Available: www.cancer.ca. [Accessed 2014].

[28] "Canadian ammonia producers : benchmarking energy efficiency and carbon dioxide emissions," Canadian Industry Program for Energy Conservation., Ottawa, 2007.

[29] Elucidare Ltd., "Ammonia as a H2 Carrier," elucidare.co.uk, 2008.

[30] T. Weis, S.-P. Stensil and J. Harti, "Renewable is Doable: Affordable and flexible options for Ontario's long-term energy plan," Pembina Foundation, 2013.

[31] IETD, "Ammonia: Industrial Efficiency Technology & Measures," Industrial Efficiency and Technology Database, 2012. [Online]. Available: http://ietd.iipnetwork.org/content/ammonia#technology-resources. [Accessed April 2014].

[32] J. C. Ganley, J. H. Holbrook and D. E. McKinely, "NHThree, SSAS: NH3 Fuel Association," 15 October 2007. [Online]. Available: http://nh3fuelassociation.org/2013/01/01/nhthree-ssas/. [Accessed April 2014].

[33] M. L. Driscoll and J. D. Young, "Conversion of Burlington Northern Locomotive for Diesel Fuel / Natural Gas Operation," Canadian Institute of Guided Ground Transport, Kingston, Ottawa, 1985.

[34] Energy Conversions Inc., "Energy Conversions Inc.: Natural gas and dual fuel engine conversions related publications," 2010. [Online]. Available: http://www.energyconversions.com/pubs.htm. [Accessed 2013].

[35] CN, "CN tests natural gas/diesel fuel powered locomotives between Edmonton and Fort McMurray, Alta.", Edmonton: www.cn.ca, 2012.

[36] BNSF Railway Company, Union Pacific Railroad Company, Association of American Railroads and California Environmental Associates, "An Evaluation of Natural Gas-fueled Locomotives," California Environmental Protection Agency, California, 2007.

[37] MotivePower-Wabtec, "MPE-X Low Emissions Locomotives," 2007. [Online]. Available: http://www.motivepower-wabtec.com/locomotives/low-horsepower/mpex-low-emissions-locomotives.php. [Accessed 2013].

[38] S. G. Fritz, "Evaluation of Biodiesel Fuel in an EMD GP38-2 Locomotive.," National Renewable Energy Laboratory, Colorado, 2004.

[39] nssustainability.com, "Environmental Performance | Alternative Power Projects," Norfolk Southern Corp., Oct. 2013. [Online]. Available: http://nssustainability.com/2013_sustainability_report/environmental_performance/alternative_power_projects.html. [Accessed 2013].

[40] Y. Haseli, G. F. Naterer and I. Dincer, "Comparative assessment of greenhouse gas mitigation of hydrogen passenger trains," *International Journal of Hydrogen Energy*, vol. 33, pp. 1788-1796, 2008.

[41] Locomotive Technology Task Force, "Locomotive Vehicle/Technology Overview," Next Generation Equipment Commiittee, 2011.

[42] A. R. Miller, K. S. Hess, T. L. Erickson and J. L. Dippo, "Hydrogen fuel cell hybrid locomotives.". United States Patent US 8,117,969 B1, 21 Feb. 2012.

[43] D. Gibbs, "BNSF Patents and Demos Hybrid Fuel Cell Locomotive," 15 Oct. 2012. [Online]. Available: http://www.greenpatentblog.com/2012/10/15/bnsf-patents-and-demos-hybrid-fuel-cell-locomotive/. [Accessed 2013].

[44] A. S. Brown, "Battery Powered Locomotive Does the Job, but Quietly | Penn State University," 25 January 2012. [Online]. Available: news.psu.edu. [Accessed 2013].

[45] Westport Power Inc., "Westport: Combustion," www.westport.com, 2013. [Online]. Available: http://www.westport.com/is/core-technologies/combustion. [Accessed 2013].

[46] Sandia National Laboratories, "HCCI/SCCI Fundamentals - Combustion Research Facility," crf.sandia.gov, 2013. [Online]. Available: http://crf.sandia.gov/index.php/combustion-research-facility/engine-combustion/fuels/hcciscci-fundamentals. [Accessed 2013].

[47] Westport Power Inc., "Westport HDPI Technology," 2013. [Online]. Available: http://www.westport.com/is/core-technologies/hpdi. [Accessed Nov. 2013].

[48] "Westport: Monofuel Direct Injection," www.westport.com, [Online]. Available: http://www.westport.com/is/core-technologies/cng-di. [Accessed Dec. 2013].

[49] B. K. Yun and M. Y. Kim, "Modeling the selective catalytic reduction of NOx by ammonia over a Vanadia-based catalyst from heavy duty diesel exhaust gases," *Applied Thermal Engineering,* vol. 50, pp. 152 - 158, 2013.

[50] US EPA, "Air Pollution Control Technology Fact Sheet," 2003. [Online]. Available: www.ucsusa.org/assets. [Accessed 2013].

[51] EF & EE, "Compact SCR (TM) - Emission Control Technology for Diesel Engines," 2010. [Online]. Available: www.efee.com. [Accessed 2013].

[52] Manufacturers of Emission Controls Association, "Case studies of the use of exhaust emission controls on locomotives and large marine diesel engines.," meca.org, Washington, DC, 2009.

[53] I. Dincer and C. Zamfirescu, "Ammonia as a Potential Substance," in *Sustainable Energy Systems and Applications*, New York, Springer, 2012, pp. 203--232.

[54] V. Hacker and K. Kordesch, "Ammonia Crackers," in *Handbook of Fuel Cells - Fundamentals, Technology, and Applications*, vol. 3, W. Vielstich, A. Lamm and H. A. Gasteiger, Eds., Chichester, John Wiley & Sons, 2003, pp. 121-127.

[55] T. Graedel and B. Allenby, Industrial Ecology and Sustainable Engineering., Upper Saddle River, NJ: Prentice Hall, 2010.

[56] ECI, "System Information & Specifications EMD 645 Dual Fuel Conversion Systems," www.energyconversions.com, 2007. [Online]. Available: http://www.energyconversions.com/emdspec.htm. [Accessed 2013].

[57] GO Transit, "Quick Facts - GO Trains," January 2013. [Online]. Available: <http://www.gotransit.com/public/en/docs/publications/quickfacts/Quick_Facts_GO_Trains_EN.pdf>. [Accessed 25 April 2013].

[58] Motive Power-Wabtec, "MPXpress Specifications," Feb. 2008. [Online]. Available: www.motivepower-wabtec.com. [Accessed 2013].

[59] C. R. Ferguson and A. T. Kirkpatrick, Internal combustion engines: applied thermodynamics, 2nd ed., New York, NY: John Wiley & Sons, 2001.

[60] NIST , "Chemistry WebBook," National Institute of Standards and Technology, 2011. [Online]. Available: http://webbook.nist.gov/cgi/cbook.cgi?ID=C7664417&Units=SI&Mask=1#Thermo-Gas. [Accessed 2013].

[61] Chemical Engineering, "Plant Cost Index," 2013. [Online]. Available: http://www.che.com/pci/. [Accessed March 2014].

[62] T. Graedel and B. Allenby, "Sustainable Engineering in its systems context (Figure).," in *Industrial Ecology and Sustainable Engineering.*, Upper Saddle River, NJ, Prentice Hall, 2010.

[63] I. Dincer and C. Zamfirescu, Sustainable Energy Systems and Applications, Springer, 2012.

[64] C. Frey and B. Graver, "Measurement and Evaluation of Fuels and Technologies for Passenger Rail Service in North Carolina," North Carolina Department of Transportation, Raleigh, NC, 2012.

[65] R. Dunn, "Diesel Fuel Quality and Locomotive Emissions in Canada," Tansport Canada, Ottawa, 2001.

[66] G. Zacharakis-Jutz, "Performance characteristics of ammonia engines using direct injection strategies.," Iowa State University, 2013.

[67] R. Hattenbach, *Ammonia - The Key to U.S. Energy Independence,* Chemical Marketing Services, Inc., 2006.

[68] Genesis Engineering Inc. and Levelton Engineering Ltd., "Non-road diesel emission reduction study," Genesis Engineering Inc., Washington, 2003.

[69] J. R. Viguri Fuente, *Subject 7. Equipment Sizing and Costing,* Cantabria: UNIVERSITY OF CANTABRIA, 2011.

[70] T. Lipman and N. Shah, "Ammonia as an Alternative Energy Storage Medium for Hydrogen Fuel Cells: Scientific and Technical Review for Near-Term Stationary Power Demonstration Projects, Final Report," University of California, Berkeley, 2007.

[71] J. Jensen, *Waste Heat Applications: ORC vs Space Heating,* Anchorage, Alaska: Alaska Energy Authority, 2007.

[72] C. Acar and I. Dincer, "Comparative Environmental Impact Evaluation of Hydrogen Production Methods from Renewable and Nonrenewable Sources.," in *Causes, Impacts and Solutions to Global Warming.*, New York, Springer, 2013, pp. 493-514.

[73] Railway Association of Canada, "Locomotive Emissions Monitoring Program 2010," www.railcan.ca, Ottawa, 2012.

[74] Transport Canada, "Ch.8 - Rail Transportation," *Transportation in Canada 2011: Comprehensive Review,* 2011.

[75] J. R. Couper, W. R. Penney, J. R. Fair and S. M. Walas, "Chemical Process Equipment: Selection and Design," in *Chapter 21: Costs of Individual Equipment*, Oxford, Elsevier, 2005, pp. 719-728.

[76] Natural Resources Canada, "Energy Use Data Handbook: Handbook Tables | Office of Energy Efficiency," Dec. 2012. [Online]. Available: http://oee.nrcan.gc.ca/corporate/statistics/neud/dpa/handbook_tables.cfm?attr=0. [Accessed 2013].

[77] Linde Gas North America, "Liquefied Natural Gas Material Safety Data Sheet," 2011. [Online]. Available: www.lindecanada.com. [Accessed April 2014].